NASA Contractor Report 3026

Design and Fabrication of a Ring-Stiffened Graphite-Epoxy Corrugated Cylindrical Shell

Read Johnson, Jr.

CONTRACT NAS1-14547
AUGUST 1978

NASA

DISCLAIMER NOTICE

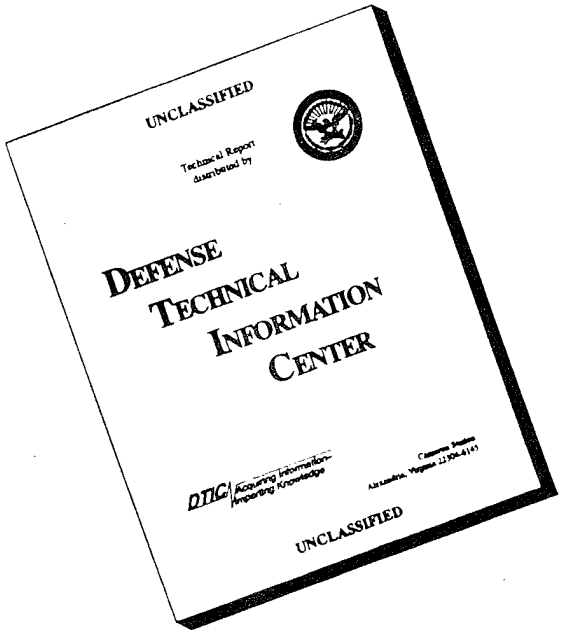

THIS DOCUMENT IS BEST QUALITY AVAILABLE. THE COPY FURNISHED TO DTIC CONTAINED A SIGNIFICANT NUMBER OF PAGES WHICH DO NOT REPRODUCE LEGIBLY.

NASA Contractor Report 3026

Design and Fabrication of a Ring-Stiffened Graphite-Epoxy Corrugated Cylindrical Shell

Read Johnson, Jr.
McDonnell Douglas Astronautics Company
Huntington Beach, California

Prepared for
Langley Research Center
under Contract NAS1-14547

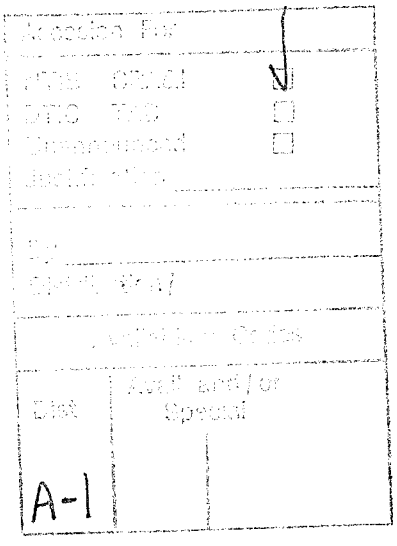

National Aeronautics
and Space Administration

**Scientific and Technical
Information Office**

1978

CONTENTS

Section 1
INTRODUCTION AND SUMMARY

The objectives of the program reported here are to advance lightweight composite shell design technology and evaluate appropriate design and analysis procedures for lightweight composite shells that must satisfy buckling requirements. To accomplish those objectives, the primary effort was to design and fabricate a graphite-epoxy cylindrical shell 3.05m (10 ft) in diameter by 3.05m (10 ft) long for evaluation in shell bending tests to be conducted by the Structures and Dynamics Division of the NASA Langely Research Center. Through such tests, the use of advanced composite materials will be evaluated for structural applications in future space missions such as those that involve spacecraft and structural assemblies to be used in geosynchronous missions. Spacecraft for such missions will require ultralightweight structures to achieve maximum payloads. Of equal importance is the requirement to provide designs that are cost-competitive with current structural approaches. For space structures that must resist buckling under compression or shell bending loads, composite materials offer an attractive approach for providing lightweight, low-cost structural components for future spacecraft. In recognition of the potential weight savings available through structural applications of graphite-epoxy materials, an earlier test program (Reference 1) was undertaken by the NASA to provide a technology base for flat, stiffened graphite-epoxy compression panels and to evaluate their effectiveness in reducing structural weight. The panels used in the earlier test program were designed using an advanced version of the analytical methods developed in Reference 2. Other tests were conducted with stiffened graphite-epoxy shear panels. The encouraging results achieved in prior efforts led to establishment of the current program to develop and evaluate appropriate design and analysis procedures for lightweight composite shells that must satisfy buckling requirements. The work conducted under this program is part of an overall effort by the NASA to evaluate advanced composite materials with which to achieve more efficient shell structures for application in future spacecraft.

The program described here was conducted over a total time span of 18 months, the test cylinder being delivered at the end of 18 months. In the initial portion of the program, the cylinder design was used as a basis to design and fabricate three types of subsize test panels; those panels were then tested in compression at the Langley Research Center to verify critical design features of the cylinder. During that portion of the program, tests were also conducted by MDAC to further define material properties, to verify the attachment joint that introduces the bending moment loads into the cylinder at each end, and to confirm the stiffness properties of the selected stiffening ring cross section. Eight subsize panels were fabricated and tested in compression, four panels being 0.61m (24 in.) long by 0.46m (18 in.) wide, two being 0.91m (36 in.) long and 0.46m (18 in.) wide, and the final two being 2.54m (100 in.) long and 0.94m (37 in.) wide. All test panels were designed with the full-size corrugation cross section of the shell wall. The 0.61m panels were used to evaluate local buckling of the corrugation elements, and the 0.91m panels were designed to evaluate the shell wall joint areas and the attachment joints at the cylinder ends. The 2.54m panels were tested in compression to determine the buckling characteristics of panels approximating the length of the cylinder and to evaluate the ring stiffener attachment to the corrugated wall. Tests of the 0.61m panels resulted in increasing the thickness of the corrugation crowns by one ply of material, a change that resulted in satisfactory local buckling behavior in the shell wall. No other changes were required as a result of the subsize panel tests. The fabricated shell wall panels had an average weight of 0.0156 kg/m^2 (0.37 lbm/ft^2), a weight that was computed to be approximately 23% lower than a comparable aluminum design.

Specific secondary objectives of the program included evaluations of weight, strength, production methods, and production costs of a lightweight graphite-epoxy cylindrical shell simulating the size and load-carrying ability of shell structures projected for future spacecraft. Weight, production methods, and production costs are evaluated herein; test results of the full-size cylinder will be reported separately in a NASA document.

The program was managed by Read Johnson, Jr., under the direction of Dr. J. F. Gabribotti, Chief Technology Engineer, Structures and Materials. Major contributions were made to the program by V. L. Freeman and J. K. Donahoe, of Non-Metallic Materials, Structures and Materials. Others who contributed significantly are M. H. Schneider, Jr. and S. J. Kong, of Structures, Structures and Materials, and Dr. C. D. Babcock, of the California Institute of Technology.

Use of commercial products or names of manufacturers in this report does not constitute official endorsement of such products or manufacturers, either expressed or implied, by the National Aeronautics and Space Administration.

Section 2
TEST CYLINDER DESIGN AND ANALYSIS

The cylindrical shell wall configuration was selected by NASA based upon extensive composite shell analysis efforts and correlation of composite flat panel test results with analytically predicted panel failures (Reference 1 and 2). Figure 1 summarizes the comparisons between aluminum and graphite-epoxy panels tested in compression and the theoretically predicted performmance by plotting the weight parameter W/AL as a function of the load parameter N_x/L. The lower weight achieved by graphite-epoxy panels at equivalent loadings for a given panel size is clearly shown in Figure 1.

A majority of the test panels described in Reference 1 were made from Thornel 300/5208 graphite-epoxy prepreg material, thus providing extensive data for that material. In addition, extensive coupon tests conducted by the Douglas Aircraft Company (DAC) provided a comprehensive material data base for T300/5208 tape material. For those reasons, T300/5208 was chosen as the material for the shell wall and stiffening rings.

The selected shell wall incorporates an open-corrugation design stiffened with external circumferential rings. While the basic shell wall corrugation dimensions and laminate orientations were determined from NASA studies and tests, the overall design approach and joint designs, the design of load-introduction rings at the shell ends, and attachment of the ring stiffeners to the shell wall were parts of the design effort conducted by MDAC. Similarly, the cross-sectional stiffness characteristics of the ring stiffeners were defined from NASA shell studies; however, the specific ring-stiffener cross section was designed by MDAC.

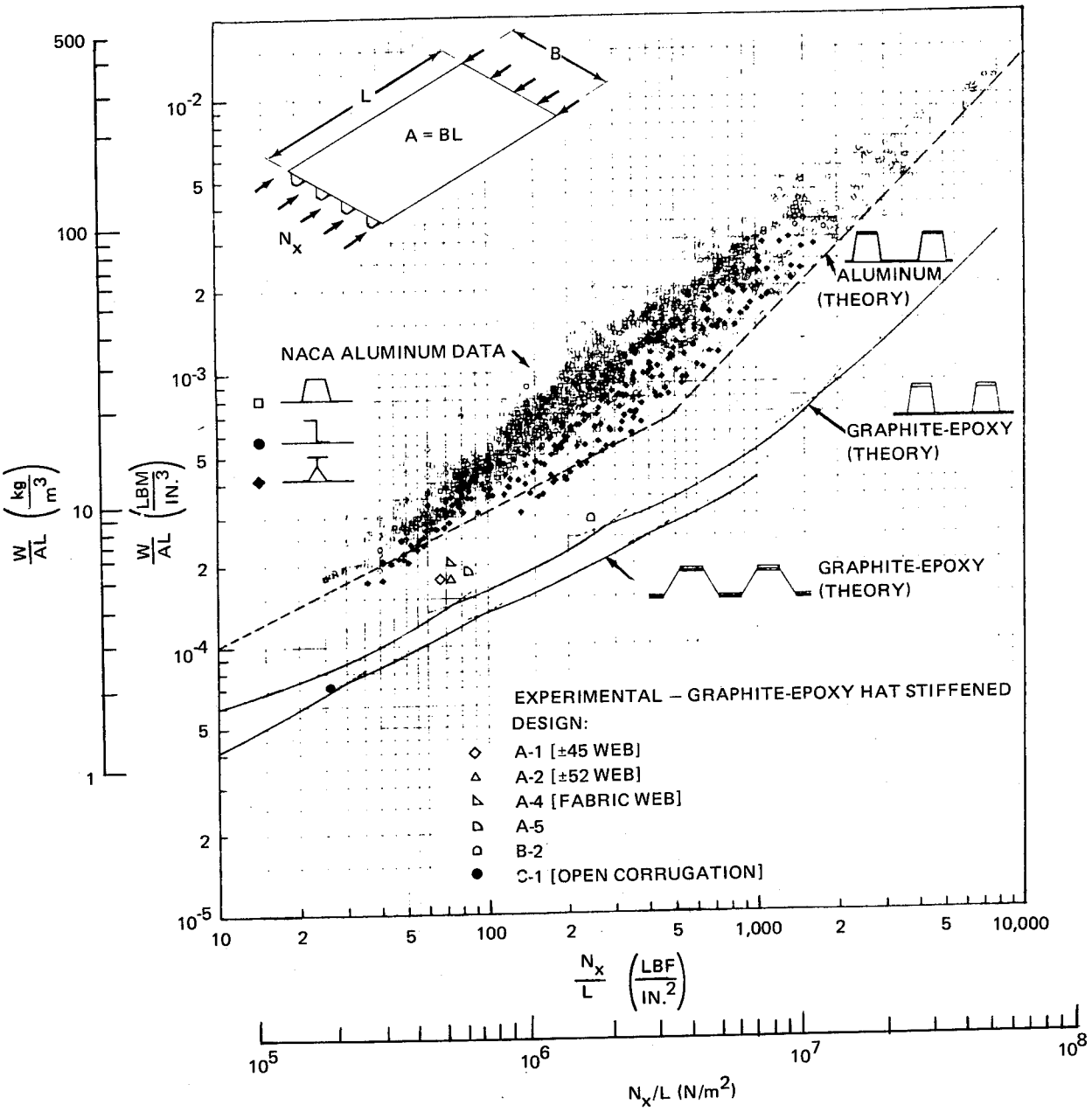

Figure 1. Comparison of Structural Efficiencies of Graphite-Epoxy and Aluminum Compression Panels

2.1 DESIGN APPROACH

The shell selected for this program was designed to sustain a pure bending moment of 1.150×10^6 N-m (10.18×10^6 in.-lb), resulting in a maximum load intensity in the shell wall of 1,576 N/cm (900 lb/in.). Preliminary shell analyses were conducted with the aid of computer codes to establish the corrugated wall geometry and define the required laminate construction. The principal computer programs used to establish the optimum wall configuration were BOSOR (Reference 3) and VIPASA (Reference 4), the former program being used to predict overall shell failure modes and the latter being used to predict local buckling modes as a function of load intensity and wall configuration. The BUCLAP program (Reference 5) was also used by MDAC as a further analytical method to evaluate local buckling of the shell wall elements. Shell design requirements, including dimensional tolerances, are summarized in Table 1. The shell configuration is shown in Figure 2.

The overall design of the shell with a 3.05m (10 ft) diameter consists of an open corrugated wall of 84 corrugations stiffened with four external rings spaced at 0.61m (24 in.) intervals. The total length of the cylindrical shell is 3.15m (124 in.), including the NASA-furnished steel loading rings, which serve as connecting interfaces with the test heads that apply the bending moment to the shell. The 84 open corrugations running the length of the cylinder have a pitch of 11.400 cm (4.488 in.) and a crown, or flat, width of 3.650 cm (1.437 in.). The basic material used for the cylinder wall and rings was Thornel 300/5208 graphite-epoxy prepeg, the material being obtained in a tape form 30.48 cm (12 in.) wide. The tape layup for the wall consists of four plies of symmetric ±45-deg fibers with five plies of zero-degree reinforcing longitudinals sandwiched in the center of the ± 45 plies at each crown. The zero plies at each crown provide maximum stiffness at the outer surfaces of the corrugation, thus giving the wall cross section a higher bending stiffness than could be achieved with a single sheet of isotropic material. The use of the zero plies in the cylinder wall is an excellent example of the selective stiffness and strength available in composite designs that are not readily available in metallic designs which use isotropic sheet materials.

The external stiffening rings have a closed hat cross section designed to be fabricated in two parts. The hat portion of the ring stiffener consists of

Table 1

TEST CYLINDER DESIGN REQUIREMENTS

Design Area	Design Requirement or Specification
Shell Wall and Ring-Stiffener Material	• Thornel 300/5208 graphite-epoxy prepreg tape
Shell Wall Design Load	$M = 1.150 \times 10^6$ N-m (10.18×10^6 in.-lb) Maximum wall load = $\pm$1,576 N/cm ($\pm$900 lb/in.) 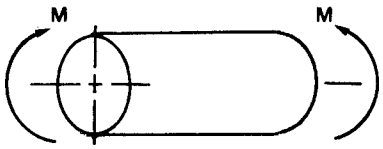
Ring-Stiffener Design Loads and Bending Stiffness Requirement	Required $EI_R = 69.7$ N-m^2 (2.43×10^4 lb-in.^{2}) **Detail A - Loads at Ring Attachment Points** 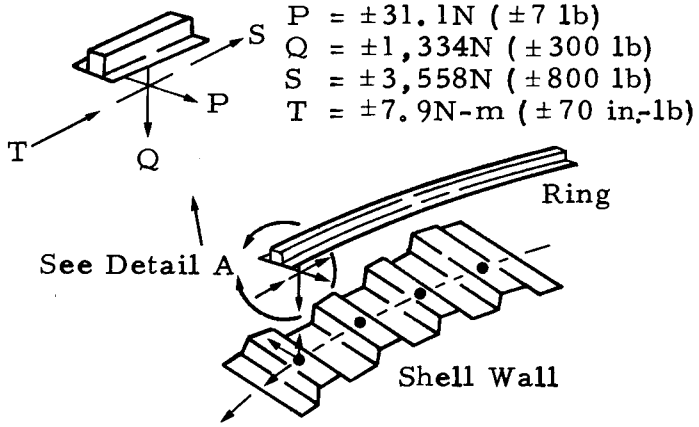
Dimensional and Weight Tolerances	• Shell wall local thickness shall not exceed $\pm$5% deviation from design value. • Ring inner radius: $\pm$0.25 cm ($\pm$0.10 in.) • Shell total weight: $\pm$5% of calculated value based on design dimensions and material property.

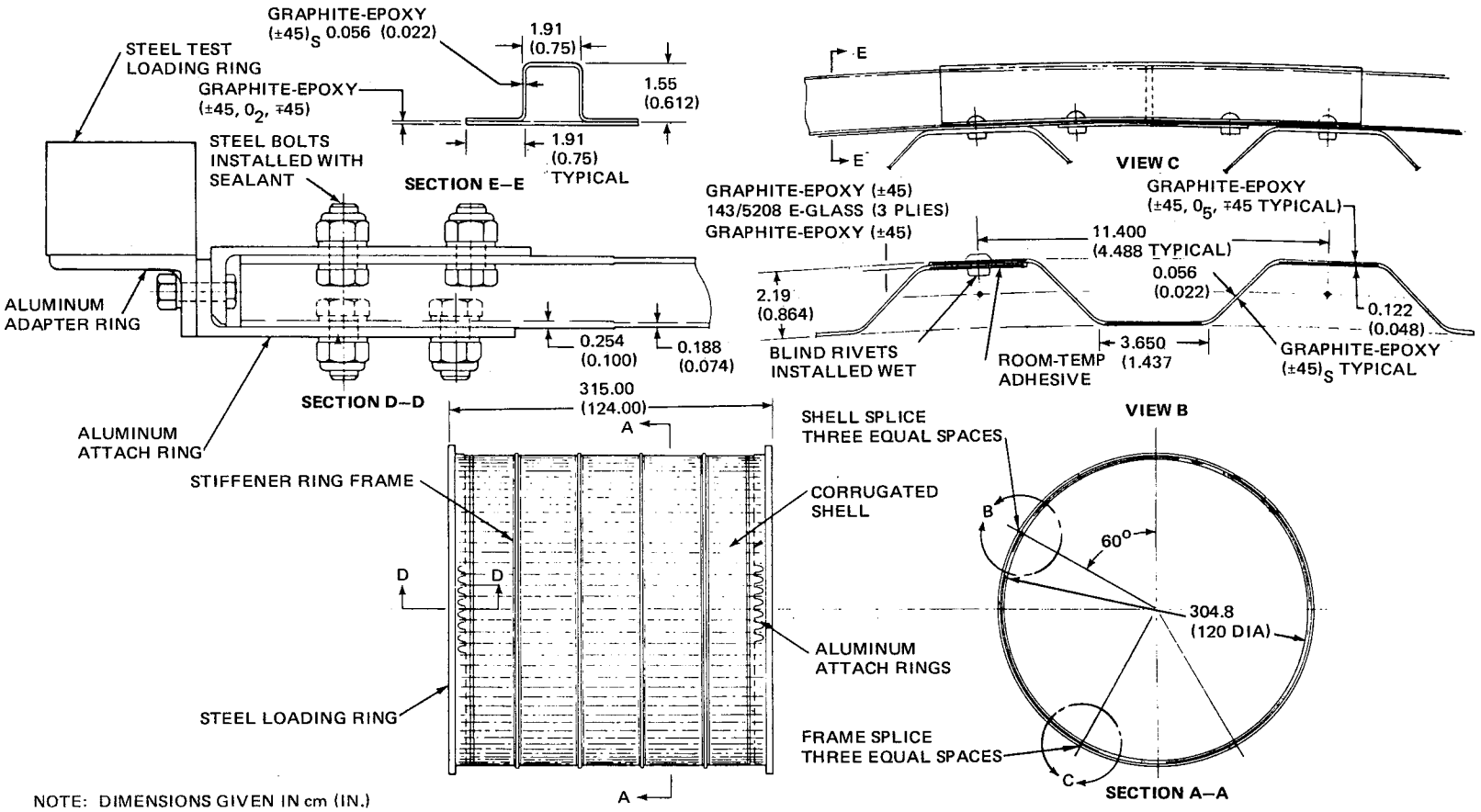

Figure 2. Configuration of 3.05m (10 Ft.) Diameter Graphite-Epoxy Corrugated Cylindrical Shell

four symmetric plies of ±45-deg fibers, while the separately made base strip consists of a $[\pm 45, 0_2, \mp 45]$ layup. After being cured, the two parts are adhesively bonded together. Aluminum adapter rings are located at each end of the shell to join the graphite-epoxy corrugated wall to the steel loading rings.

To simplify assembly of the shell and assure meeting the required fabrication tolerances (Table 1) on the cylinder diameter, the construction approach chosen was to make the shell wall in three segments, each segment being laid up and cured on a flat corrugated mold and subsequently wrapped to the correct cylindrical shape on assembly. The flexibility of the thin corrugations, combined with the relatively large cylinder radius, permitted the use of such an approach and thus reduced the tooling costs for the initial layup and curing steps in manufacturing the wall segments. The three longitudinal seams where the panels were joined to each other permitted circumferential adjustments of the panels during assembly which, in turn, allowed achievement of a ±0.254-cm (±0.10 in.) radius tolerance in the finished cylinder. For the same basic reasons, the four external stiffening rings were each made up of three 120-deg segments joined with a splice cap where the segments meet. Segmenting the rings permitted minor adjustments on assembly, thereby providing an accurate mating of the rings with the shell wall.

Initial design of the shell was based upon an established material property data base for various tape laminate constructions. Basic material property data for T300/5208 monolayer (undirectional) tape construction are presented in Tables 2, 3, and 4. Test data were also available for multidirectional laminate constructions, but none of the laminate orientations in the data base were identical to those designed for the crown areas of the shell wall panels. The latter layup $[\pm 45, 0_5, \mp 45]$, was not included in the existing test data, and thus additional test data were generated as required during initial test phases of the program. A summary of the material coupon test data generated in this program is presented in Section 2.4.3. Strength, elastic modulus, Poisson's ratio, density, and laminate thickness characteristics were available from the data base for typical laminate orientations of T300/5208 material.

Table 2

TENSILE, COMPRESSION, AND SHEAR STRENGTH DESIGN ALLOWABLES FOR T300/5208 TAPE MONOLAYERS

Note: Values normalized to constant ply thickness of 0.014 cm (0.0055 in.)

Design Allowable	Temperature	Stress N/m^2 ($lb/in.^2$)		
		Average	"A" Value*	"B" Value**
F_L (Tension)	Room	1.539×10^9 (223,270)	9.138×10^8 (132,544)	1.171×10^9 (169,805)
F_L (Compression)		1.393×10^9 (202,000)	7.267×10^8 (105,414)	9.998×10^8 (145,023)
F_T (Tension)		4.231×10^7 (6,137)	2.926×10^7 (4,244)	3.461×10^7 (5,021)
F_T (Compression)		1.475×10^8 (21,400)	6.880×10^7 (9.980)	1.011×10^8 (14,670)
F_{LT} (Shear)		9.534×10^7 (13,830)	8.069×10^7 (11,704)	8.671×10^7 (12,577)
Shear (Short Beam)	Room	1.303×10^8 (18,900)	–	–
F_L (Tension)	-53.9°C (-65°F)	1.404×10^9 (203,716)	8.342×10^8 (121,000)	1.069×10^9 (155,000)
F_L (Compression)		1.566×10^9 (227,083)	8.135×10^8 (118,000)	1.124×10^9 (163,000)
F_T (Tension)		$3,316 \times 10^7$ (4,810)	2.289×10^7 (3,320)	2.709×10^7 (3,930)
F_T (Compression)		1.682×10^8 (24,400)	7.859×10^7 (11,400)	1.151×10^8 (16,700)
F_{LT} (Shear)		9.493×10^7 (13,770)	7.997×10^7 (11,600)	8.618×10^7 (12,500)
Shear (Short Beam)	-53.9°C (-65°F)	1.564×10^8 (22,700)	–	–
F_L (Tension)	121.1°C (250°F)	1.523×10^9 (220,883)	9.031×10^8 (131,000)	1.158×10^9 (168,000)
F_L (Compression)		1.087×10^9 (157,633)	5.667×10^8 (82,200)	7.790×10^8 (113,000)
F_T (Tension)		2.499×10^7 (3,625)	1.724×10^7 (2,500)	2.041×10^7 (2,960)
F_T (Compression)		1.433×10^8 (20,780)	6.680×10^7 (9,690)	9.789×10^7 (14,200)

Table 2 (Concluded)

TENSILE, COMPRESSION, AND SHEAR STRENGTH DESIGN ALLOWABLES FOR T300/5208 TAPE MONOLAYERS

(Note: Values normalized to constant ply thickness of 0.014 cm (0.0055 in.)

Design Allowable	Temperature	Stress N/m^2 ($lb/in.^2$)		
		Average	"A" Value*	"B" Value**
F_{LT} (Shear)	121.1 C (250 F)	6.308×10^7 (9,150)	5.336×10^7 (7,740)	5.736×10^7 (8,320)
Shear (Short Beam)	121.1°C (250°F)	7.997×10^7 (11,600)	–	–

*"A" value: A statistical value where 99% or greater of the samples will achieve such a strength with a 95% confidence level.

*"B" value: A statistical value where 90% or greater of the samples will achieve such a strength with a 95% confidence level.

Table 3

DESIGN VALUES FOR ELASTIC MODULUS

Note: (1) Values normalized to constant ply thickness = 0.014 cm (0.0055 in.)
(2) T300/5208 monolayer construction.

Temperature	Modulus N/m^2 ($lb/in.^2$)				
	Tension E_L	Compression E_L	Tension E_T	Compression E_T	Shear G_{LT}
Room	14.68×10^{10} (21.3×10^6)	13.10×10^{10} (19.0×10^6)	1.09×10^{10} (1.58×10^6	1.30×10^{10} (1.89×10^6)	0.64×10^{10} (0.93×10^6)
-53.9°C (-65°F)	14.89×10^{10} (21.6×10^6)	14.27×10^{10} 20.7×10^6)	1.21×10^{10} (1.76×10^6)	1.22×10^{10} (1.77×10^6)	0.81×10^6 (1.17×10^6)
121.1°C (250°F)	15.03×10^{10} (21.8×10^6)	9.38×10^{10} (13.6×10^6)	0.75×10^{10} (1.09×10^6)	0.79×10^{10} (1.15×10^6)	0.56×10^{10} (0.84×10^6)

Table 4

DESIGN VALUES OF FAILURE STRAIN AND POISSON'S RATIO
(T300/5208 monolayer construction)

Temperature	Failure Strain			Poisson's Ratio, μ_{LT}	
	Zero-Deg Direction		90-Deg Direction		
	Tension	Compression	Tension	Tension	Compression
Room	0.011	0.0086	0.0036	0.377	0.380
-53.9°C (-65°F)	0.0093	0.0078	0.0021	0.386	0.373
121.1°C (250°F)	0.0099	0.0097	0.0032	0.379	0.400

Subelement panel tests, described in Section 3, produced only one modification to the original shell wall design. Four plies of reinforcing zero-degree plies were originally used in the corrugation crowns, that number being increased to five plies after initial compression tests with the first two 0.61m long panels. Thickness measurements of the first two test panels showed the average cured ply thickness to be lower than the average thickness derived from the data base, thus resulting in local buckling at lower load intensities than the design goal of 1,576 N/cm. The five plies of longitudinals resulted in a computed cylinder weight increase of approximately 5% when compared to the original design. No other changes were required in the original cylinder design.

The overall design approach thus used a shell wall made of three flat panels that were formed to the required cylindrical shape on assembly and joined at three longitudinal seams. Similarly, the four ring stiffeners were each made in three segments and joined with splice caps during assembly. The selected approach was chosen to simplify fabrication, lower costs, and permit achievement of required cylinder tolerances.

2.2 SHELL BUCKLING ANALYSIS AND RING-STIFFENER DESIGN

A primary objective of the design effort was to achieve a test cylinder that would fail in general instability buckling. To achieve this goal, the corrugated shell wall configuration was designed to provide adequate margins of

safety in local element buckling and shell buckling between rings. Simultaneously, the spacing and stiffness characteristics of the stiffening rings were adjusted to allow a minimum design margin in the general instability buckling mode of failure.

Results of analytical failure predictions, summarized in Figure 3, show the effects of variations in ring bending stiffness on the load intensity that causes general instability failure in the shell. Load intensities that cause local buckling of corrugation elements and buckling between rings are unaffected by ring stiffness and are therefore shown as constant values. As shown in Figure 3, the load causing failure by general instability increases with increasing ring stiffness until another failure mode becomes critical. The design ring bending stiffness parameter, EI_R, was chosen as 69.7 N-m^2 (2.43 x 10^4 lb-$in.^2$) to meet the design load intensity of 1,576 N/cm with a small margin of safety. A closed hat section (Figure 2) was selected for the ring-stiffener cross section to provide adequate torsional stiffness as well as the desired bending stiffness.

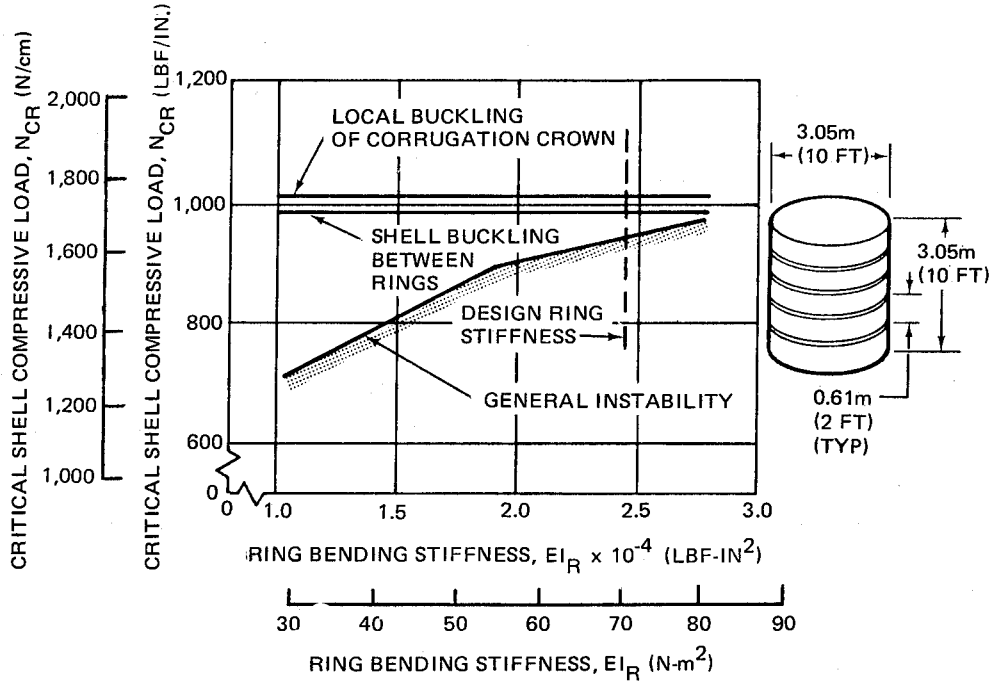

Figure 3. Summary of Critical Shell Compressive Load as a Function of Ring Bending Stiffness

Primary criteria for sizing the intermediate ring stiffeners were: (1) the bending stiffness of the ring cross section would meet the value of EI_R determined in NASA preliminary studies, and (2) the extensional and torsional stiffness characteristics would meet or exceed the preliminary study values.

Ring stiffness properties defined in preliminary analyses were:

$$EI_R = 69.7 \text{ N-m}^2 \ (2.43 \times 10^4 \text{ lb-in.}^2)$$

$$EA_R = 19.4 \times 10^5 \text{ N} \ (4.37 \times 10^5 \text{ lb})$$

$$GJ_R = 44.5 \text{ N-m}^2 \ (1.55 \times 10^4 \text{ lb-in.}^2)$$

The selected design for the intermediate ring stiffeners, shown in Figure 4, consists of a hat section adhesively bonded to a base plate. The closed section is required to meet the torsional stiffness requirements defined in preliminary design studies.

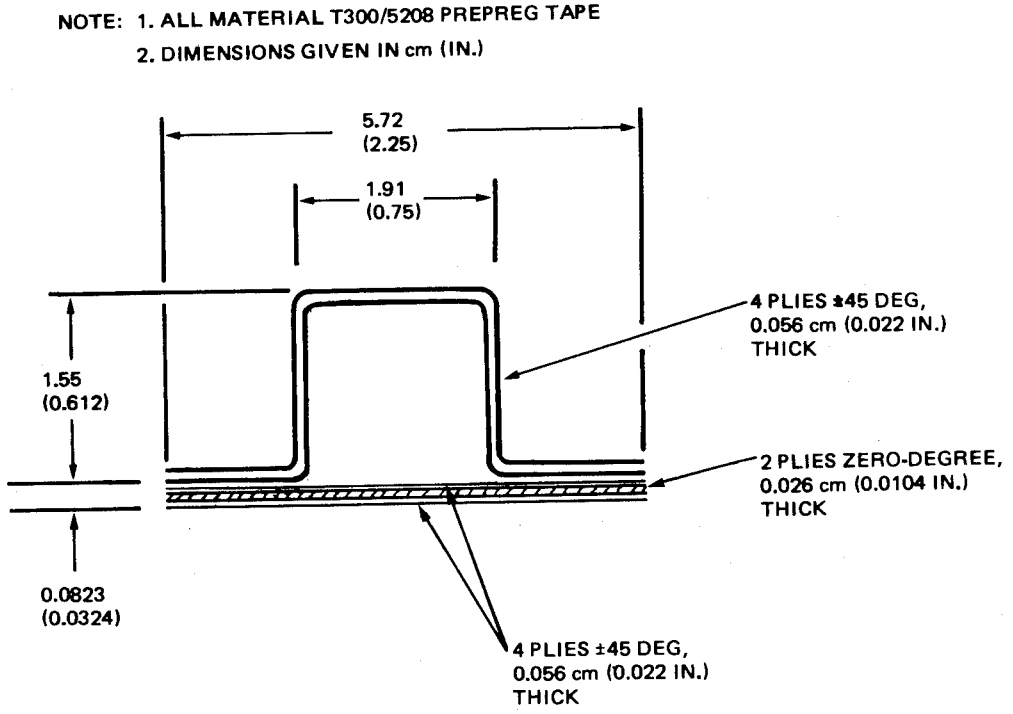

Figure 4. Ring-Stiffener Cross Section

Also, the ring stiffeners were designed to meet the attachment loads as shown in Table 1. Other criteria considered in designing the ring stiffeners were: (1) the design would minimize the possibility of warping or the introduction of severe residual strains during cure, and (2) the design would lend itself to ease of fabrication with low cost and minimum weight. Positive margins of safety were computed for all design load conditions for the ring stiffeners, and those calculations were subsequently substantiated in tests of the 2.54m (100 in.) panels.

The use of clips to attach the rings to the inner corrugation crowns was considered in initial design studies. However, previous tests (Reference 6) have shown such attachments do not increase the cylinder's resistance to general instability buckling. Thus, ring-to-shell attachment clips posed the disadvantages of increased weight and cost without providing any significant increase in shell strength. For those reasons, the simple attachment of the stiffening rings at points where the rings mate with the external corrugation crowns was chosen.

2.3 DETAILED DESIGN OF SHELL

Special design attention was required for joints in three areas of the cylinder. The first such area, attachment of the cylinder ends to the steel test rings, required a joint with sufficient strength to satisfactorily introduce the loads into the shell wall and sufficient stiffness to prevent local buckling of the graphite-epoxy corrugated shell from stress concentrations near the attachment areas. A bolted joint design (Figure 2) was selected that used three aluminum rings made from stretch-formed extruded angles. Each ring was made in three 120-deg segments which were joined together on assembly. The two rings that mated with the corrugated wall had scalloped fingers to pick up the corrugation crowns with two shear bolts at each crown position. The scalloped fingers on the aluminum rings permitted access to the bolts from both sides of the joint because the inner and outer corrugation crowns form an alternating pattern around the circumference of the wall. Stepped graphite-epoxy doublers reinforced the corrugation crowns near the shell ends to provide added stiffness and to give adequate strength at the bolt

attachment area. The attachment design featured close-tolerance bolts of 0.953-cm (0.375 in.) diameter, placed in attachment holes that were match-drilled and reamed on assembly.

A second area requiring special design attention was found in the longitudinal joints along the length of the shell wall where the three corrugated panels were joined to form the completed cylindrical shell. The joint area was required to have adequate strength and also elongation (EA) stiffness characteristics equal to the basic wall, so that buckling characteristics of the wall remained constant. An overlapping joint was designed in which two crowns were overlapped, adhesively bonded, and riveted with blind rivets. To maintain stiffness equal to other corrugation crowns, the five plies of reinforcing T300/5208 zero-degree strips were replaced with three 143/5208 glass cloth strips having significantly lower modulus. Thus, the thicker area at the overlapping joint was offset by low-modulus reinforcing strips to maintain constant EA characteristics.

Criteria for sizing the splice were (1) the extensional stiffness of the splice would not exceed the value for the shell wall but would match the stiffness of the shell wall as closely as possible, (2) the riveted connections would not result in local interfastener buckling, (3) the splice method would not affect the straightness of the shell wall, and (4) local buckling of the spliced segment would equal or exceed that for the shell wall.

Several combinations of materials and plies were considered in the preliminary design, and the selected combination was one that replaced the five T300/5200 zero-degree plies with three plies of E-glass longitudinals (see Figure 5). The splice area extensional stiffness obtained with such a design was one that most nearly matched the basic shell wall extensional stiffness.

Because local buckling is a function of both local stiffness and local wall thickness, the local buckling allowable in the splice area was significantly higher than that of the basic corrugation crown due to the approximately equal stiffness characteristics combined with the greater thickness in the splice area.

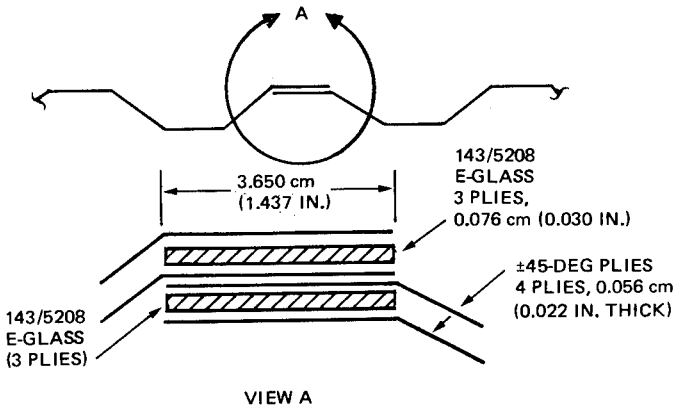

Figure 5. Shell Wall Longitudinal Splice Design

A third area requiring special attention was the attachment of the external stiffening rings to the shell wall. Design loads for the ring attachments were developed based on computed buckling patterns of the shell. The ring attachment was designed to use blind rivets and an adhesive bond at each position where the rings cross the external crown areas; the design was subsequently proven satisfactory in compression tests of two 2.54m (100 in.) test panels.

From initial design studies, the weight of the basic corrugated shell wall was computed to be 0.0143 kg/m^2 (0.34 lbm/ft^2). With allowance for joints and ring stiffeners, the shell wall weight was estimated as 0.0156 kg/m^2 (0.37 lbm/ft^2). To compare those weights with shell wall weights of aluminum cylindrical shells, Figure 6 was plotted to show the weight parameter, W/AR, as a function of the shell load intensity parameter, N_x/R. For the shell loading of interest (1576 N/cm) and a shell radius of 1.524m (60 in.), the graphite-epoxy corrugated shell shows a weight saving of approximately 23% over a similar aluminum shell.

2.4 DESIGN DEVELOPMENT TESTS

Development tests were conducted with sample parts or coupons for three purposes: (1) to verify the design characteristics of the attachment area at the cylinder ends, (2) to confirm the stiffness characteristics of the stiffening ring design, and (3) to determine the tensile, flexure, and compression characteristics of samples made with the same layup as that used in the corrugation crown areas.

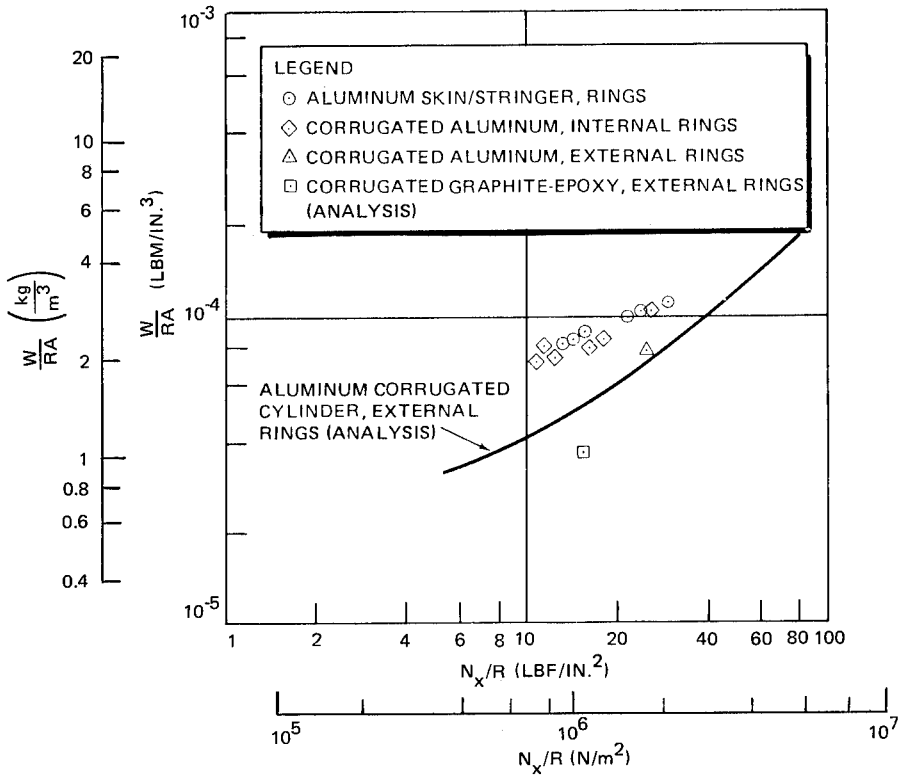

Figure 6. Structural Efficiencies of Cylindrical Shells in Compression

2.4.1 Cylinder End Attachment Tests

A typical bolted joint sample used in tests to evaluate the attachment of the adapter rings to the cylinder ends is shown in Figure 7. The maximum design load required to be introduced at each corrugation crown is 8,985N (2,020 lbf), based on a maximum bending load intensity of 1,576 N/cm (900 lbf/in) along the circumference of the cylinder and a crown spacing of 5.70 cm. Three bolted joint samples with four zero-degree reinforcing plies were initially tested in tension, two having both bolts in place at each end and one having one bolt removed at one end of the sample. Test results, presented in Table 5, show the reinforced corrugation samples sustained tension loads of 2.291×10^4N (5,150 lbf) and 2.202×10^4N (4,950 lbf) when both bolts were used. With only one bolt acting, the load at failure was 1.913×10^4N (4,300 lbf). Thus, more than twice the design load of 8,985 N was carried with only one bolt acting, indicating a substantial margin of safety. Two additional samples were tested after changing from four to five reinforcing plies in the crowns.

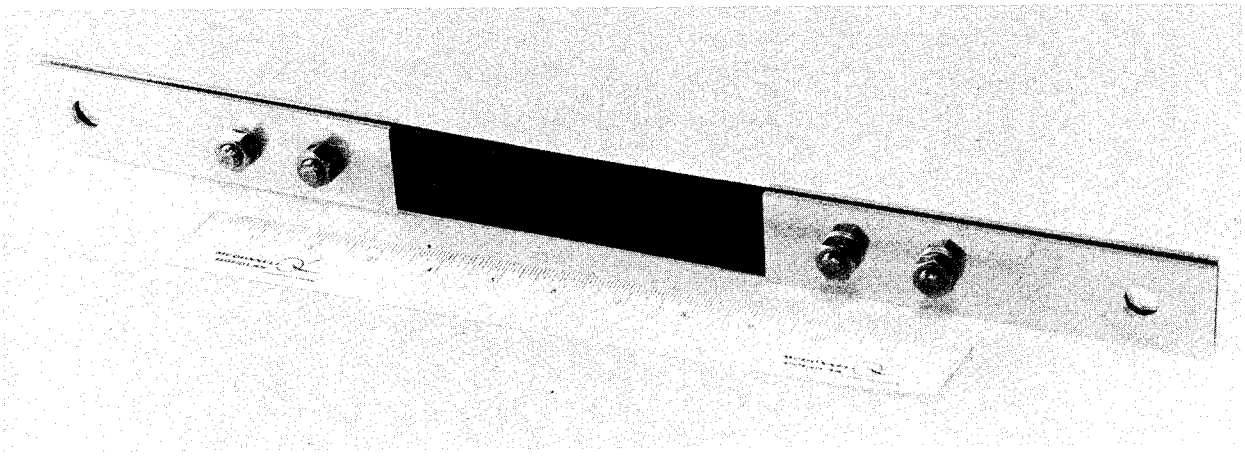

Figure 7. Bolted Joint Test Sample Simulating Shell End Attachment

With the additional reinforcing ply, the fourth and fifth test samples failed at 2.313×10^4N (5,200 lbf) and 2.580×10^4N (5,800 lbf), respectively. Thus, a high margin of safety in tension loading was demonstrated by the bolted joint samples simulating the adapter ring attachment to the cylinder wall.

Figures 8 and 9 show typical failures in the bolted joint samples. Figure 8 shows the failure in sample 1 (Table 5) in which tensile failure of the reinforced graphite-epoxy area at the inner bolt hole was the mode of failure. The bearing stress failure of sample 2 (Table 5) is shown in Figure 9, where the sample was tested with only the outer bolt in place at one end of the sample.

2.4.2 Ring-Stiffener Tests

Ring-stiffener tests were conducted to evaluate ring bending stiffness as a function of stiffener depth. Such tests were deemed necessary because of the significant change in cylinder general instability failure load that occurs with changes in the ring-stiffener bending stiffness, EI_R (Figure 3). Four simulated ring-stiffener segments of three different depths were fabricated for

Table 5

BOLTED JOINT TEST RESULTS

Test Sample	Failure Location and Type	Failure Load	Failure Stress
No. 1 (All bolts in position)	Inner Bolt Hole, Tension Failure 	22,910 N (5,150 lb)	3.23×10^8 N/m^2* (46,900 psi)
No. 2 (One bolt removed)	Outer Bolt Hole, Bearing Failure 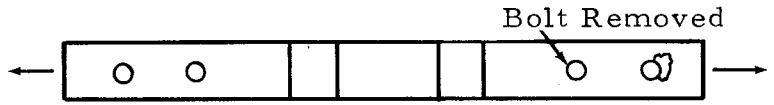	19,130N (4,300 lb)	7.67×10^8 N/m^2 (111,200 psi)
No. 3 (All bolts in position)	Center Area, Tension Failure at End of Doublers 	22,020N (4,950 lb)	5.52×19^8 N/m^2 (80,000 psi)
No. 4 (All bolts in position)	Tensile Shear Failure at Bolt Holes 	23,130N (5,200 lb)	0.652×10^8 N/m^2 (9,455 psi) (shear)
No. 5 (All bolts in Position)	Tensile Shear Failure at Bolt Holes 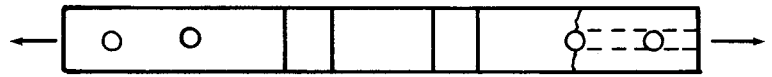	25,800N (5,800 lb)	0.727×10^8 N/m^2 (10,545 psi) (shear)

*Net area stress at bolt hole.

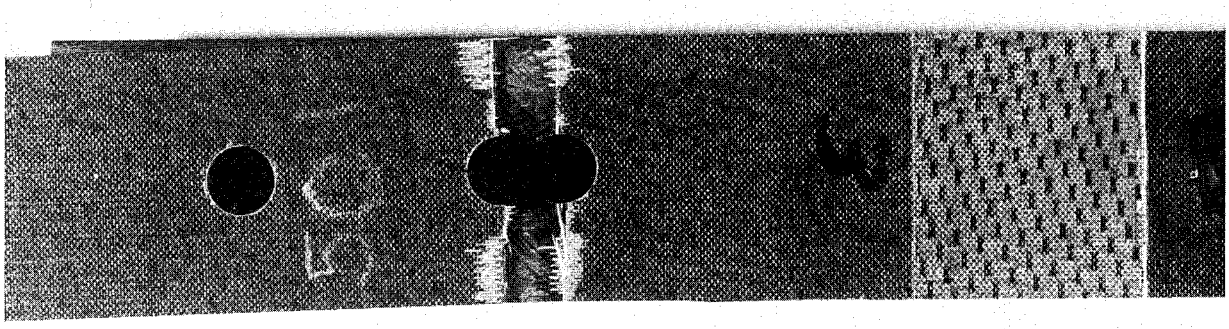

Figure 8. Tensile Failure at Inner Bolt Hole

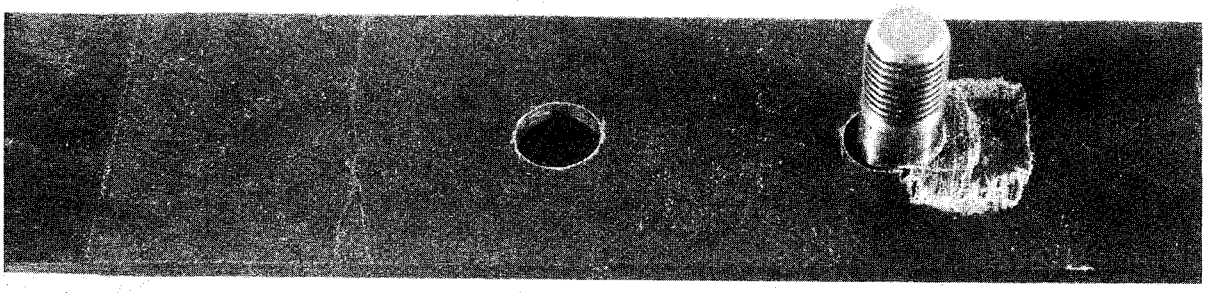

Figure 9. Bearing Failure at Bolt Hole

the bending tests, each segment being 0.61m (24 in.) long. Two hats were designed to a depth to provide the nominally required EI_R of 69.7 N-m^2 (2.43 x 10^4 lb-in^2). A third was designed to a depth computed to give a 55% increase in the EI_R value; the fourth section was computed to decrease the nominal EI_R value by 40%.

The hat portions of the ring-stiffener test samples were laid up and cured as a continuous sheet and then cut into separate stiffeners after being bonded to the separately made base plate. Bonding was accomplished with EA-9309 epoxy adhesive, the parts being held together under vacuum-bag pressure for 24 hours. Figure 10 shows the cured hat portions of the simulated stiffener segments after their removal from the male aluminum tool used for layup and cure. Figure 11 shows three of the simulated stiffeners ready for testing.

A four-point loading system was used to apply bending moments to each stiffener and deflections were measured as a function of load. The slope of the deflection versus load curve was then used to determine the effective EI_R

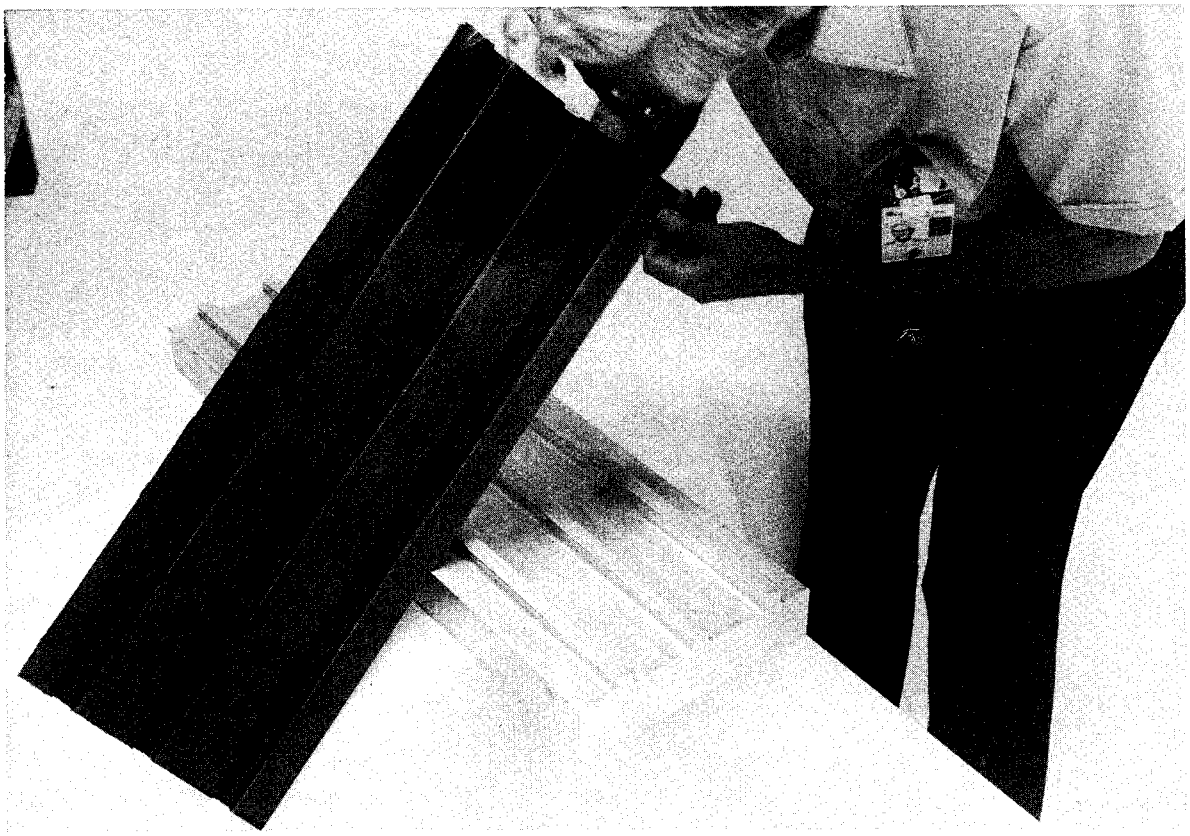

Figure 10. Ring-Stiffener Hat Test Samples Removed from Mold

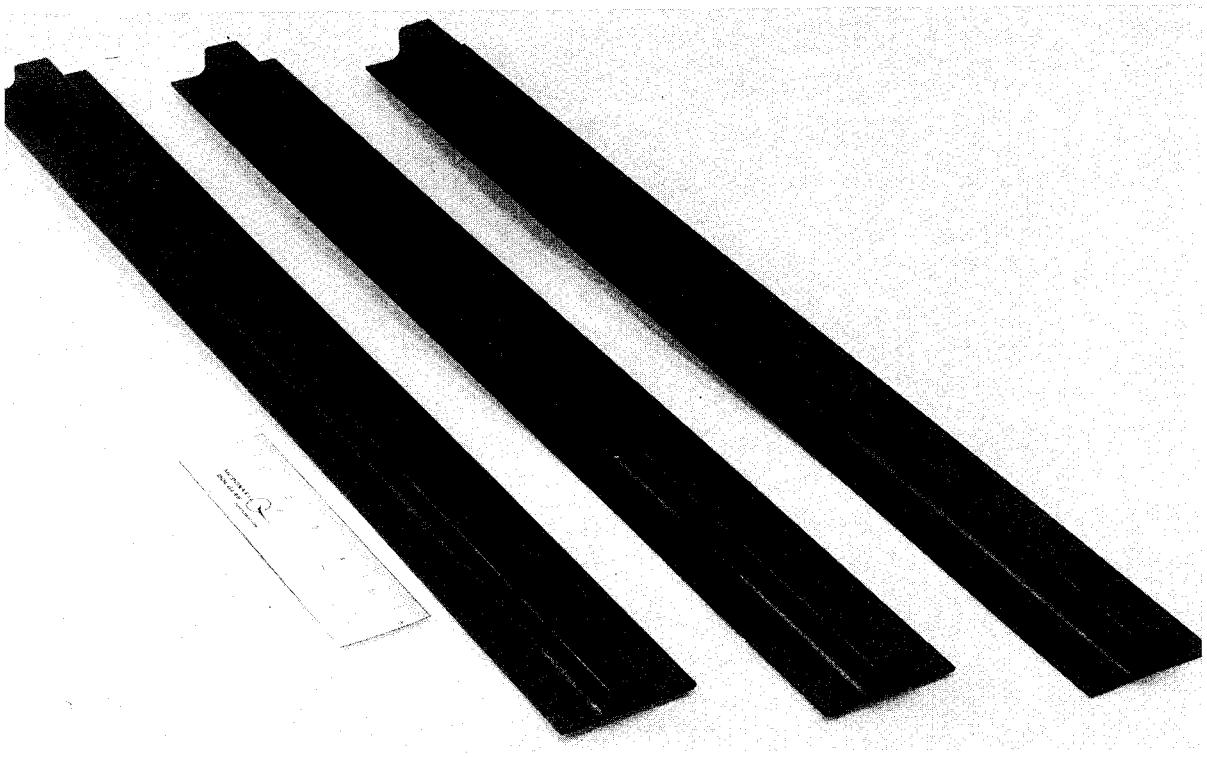

Figure 11. Ring-Stiffener Test Samples

for each test ring segment. Figure 12 shows results of the ring-stiffener bending tests and indicates satisfactory bending stiffness characteristics for stiffeners with a nominal design depth of 1.55 cm (0.612 in.)

2.4.3 Material Property Tests

Because initial design and analysis of the cylinder was based upon data obtained from monolayer (unidirectional) T300/5208 samples, tests of samples having the actual layup of the corrugation crown areas were conducted to provide coupon test data to supplement the panel test results. Tests were conducted to determine typical tensile strength and Young's modulus, flexural strength and modulus values, and elastic modulus under compressive loading. A portion of the samples were taken from extra crown areas at the sides of the 0.61m test panels, the mold for those panels having been made with sufficient width to accommodate an extra crown layup at both sides of the panel. A majority of the tensile and flexure specimens were obtained from panel trim material, with some being made from flat sheets laid up and cured using the same process as that used to fabricate the panels. Because of the

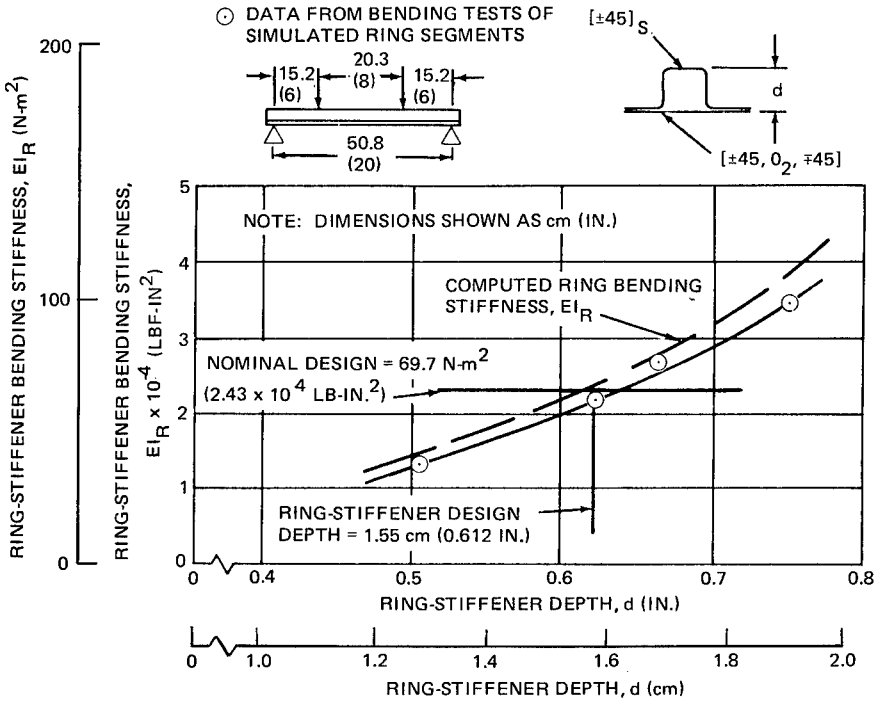

Figure 12. Ring-Stiffener Bending Stiffness as a Function of Stiffener Depth

change from four to five reinforcing plies in the crowns, tests were conducted with samples of each type of layup. A summary of the results is given in Table 6. Results from coupon tests added confirming data to the panel tests and helped verify the use of an additional zero-degree reinforcing ply in the corrugation crowns.

A majority of the compression tests were conducted with honeycomb samples to prevent premature buckling of the thin graphite-epoxy sheets that simulated the crown areas. Figure 13 shows a honeycomb compression sample with strain gage attached. A second type of sample, a short segment removed from a corrugated panel (Figure 14), was also used in compression tests. The ends of both types of samples were encapsulated in an epoxy compound and machined to provide flat, parallel ends.

Table 6

MATERIAL PROPERTY TESTS OF CORRUGATION CROWN AREAS

Ply Layup	Source of Test Samples	Average Tensile Properties		Average Flexural Properties		Compression Modulus, N/m^2 (psi)	Poisson's Ratio
		Strength, N/m^2 (psi)	Modulus, N/m^2 (psi)	Strength, N/m^2 (psi)	Modulus, N/m^2 (psi)		
$[\pm 45, 0_4, \mp 45]$	0.61m (24-in.) Test Panel No. 1	9.186×10^8 (133,240)	8.769×10^{10} (12.72×10^6)	8.304×10^8 (120,450)	3.812×10^{10} (5.53×10^6)	--	--
	0.61m (24-in.) Test Panel No. 2	9.549×10^8 (138,515)	8.128×10^{10} (11.79×10^6)	8.518×10^8 (123,560)	3.640×10^{10} (5.28×10^6)	7.163×10^{10} (10.39×10^6)	0.641
	Flat Sheets Simulating Panel Crown Areas	9.326×10^8 (135,280)	7.859×10^{10} (11.40×10^6)	7.821×10^8 (113,450)	3.668×10^{10} (5.32×10^6)	7.232×10^{10} (10.49×10^6)	0.662
$[\pm 45, 0_5, \mp 45]$	0.61m (24-in.) Test Panel No. 3	10.438×10^8 (151,410)	8.935×10^{10} (12.96×10^6)	8.323×10^8 (120,730)	3.675×10^{10} (5.33×10^6)	--	--
	0.61m (24-in.) Test Panel No. 4	10.017×10^8 (145,300)	9.031×10^{10} (12.10×10^6)	8.280×10^8 (118,200)	3.895×10^{10} (5.40×10^6)	--	--
	0.91m (36-in.) Test Panel No. 1	7.971×10^8 (115,620)	8.583×10^{10} (12.45×10^6)	8.149×10^8 (118,200)	3.723×10^{10} (5.40×10^6)	--	--
	0.91m (36-in.) Test Panel No. 2	9.004×10^8 (130,600)	9.321×10^{10} (13.52×10^6)	10.106×10^8 (146,590)	4.564×10^{10} (6.62×10^6)	--	--
	2.54m (100-in..) Test Panel No. 1	10.384×10^8 (150,620)	9.066×10^{10} (13.15×10^6)	9.863×10^8 (143,070)	4.653×10^{10} (6.75×10^6)	--	--
	2.54m (100-in.) Test Panel No. 2	10.451×10^8 (151,600)	7.694×10^{10} (11.16×10^6)	8.391×10^8 (121,720)	3.861×10^{10} (5.60×10^6)	--	--

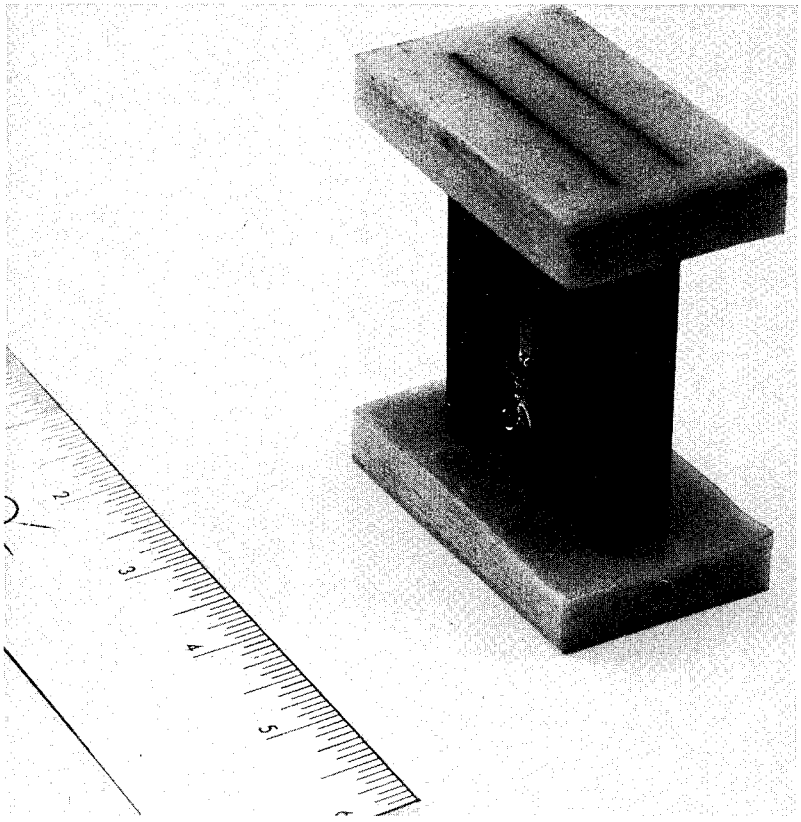

Figure 13. Honeycomb Compression Sample

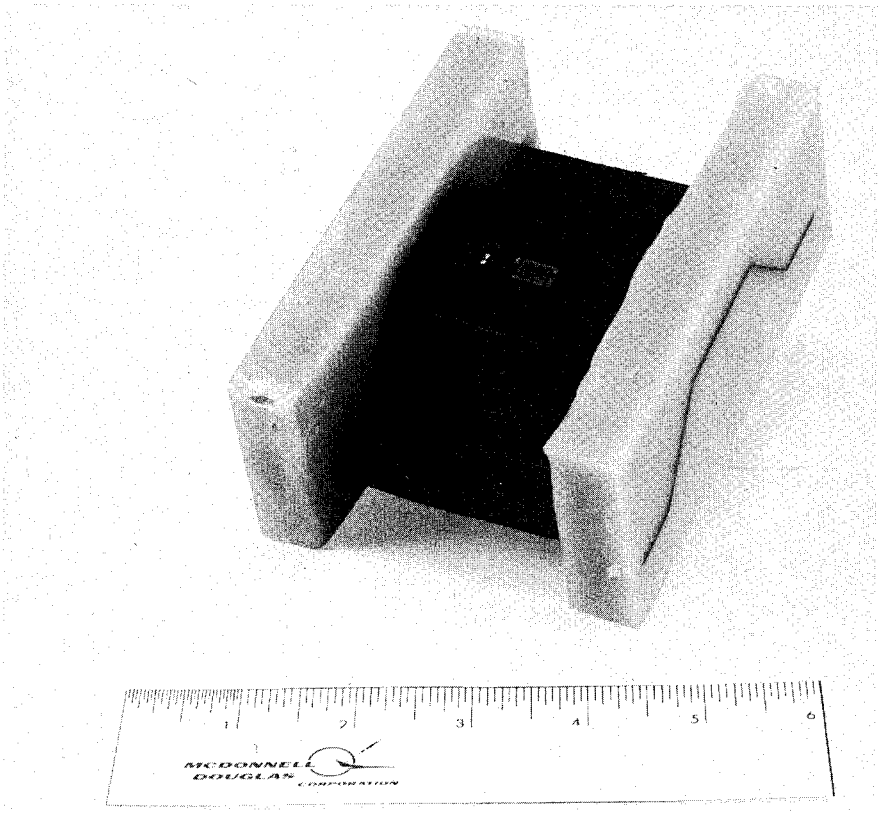

Figure 14. Graphite-Epoxy Corrugated Compression Test Sample

Section 3

SUBELEMENT TEST PANELS

3.1 PANEL DESIGNS

Three types of flat, subsize panels were fabricated and tested prior to initiation of cylinder fabrication, the designs being: (1) a 0.61m (24 in.) long by 0.46m (18 in.) wide panel without joints or stiffeners, (2) a 0.91m (36 in.) long by 0.46m (18 in.) wide panel with a longitudinal joint and end attachment angles, and (3) a 2.54m (100 in.) long by 0.94m (37 in.) wide panel with four simulated ring-stiffener segments attached. All of the panels contained the basic full-size corrugation design shown in Figure 2. Designs for the three types of panels are shown in Figures 15, 16, and 17.

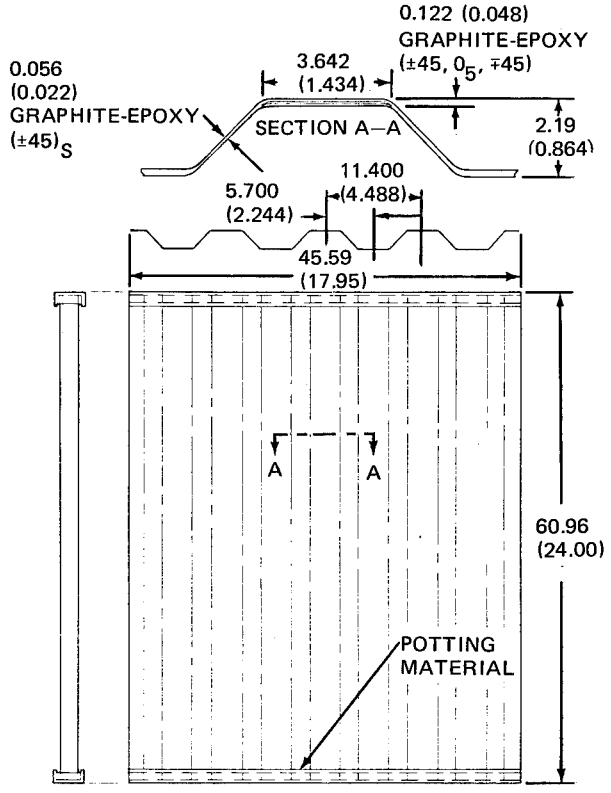

NOTE: DIMENSIONS SHOWN AS cm (IN.)

Figure 15. Graphite-Epoxy 0.61m (24 In.) Corrugated Test Panel

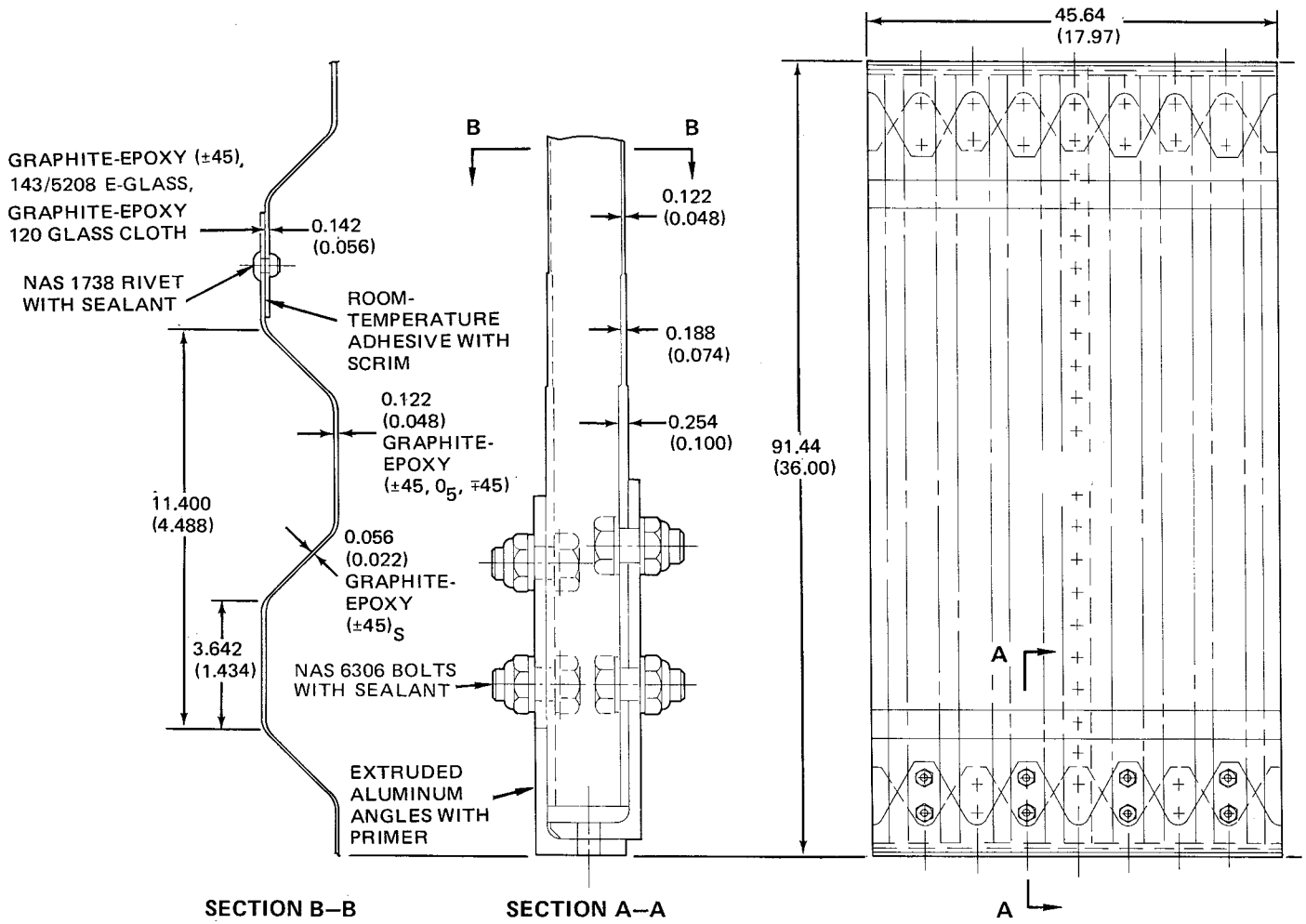

NOTE: DIMENSIONS SHOWN AS CM (IN.)

Figure 16. Graphite-Epoxy 0.91m (36-In.) Test Panel

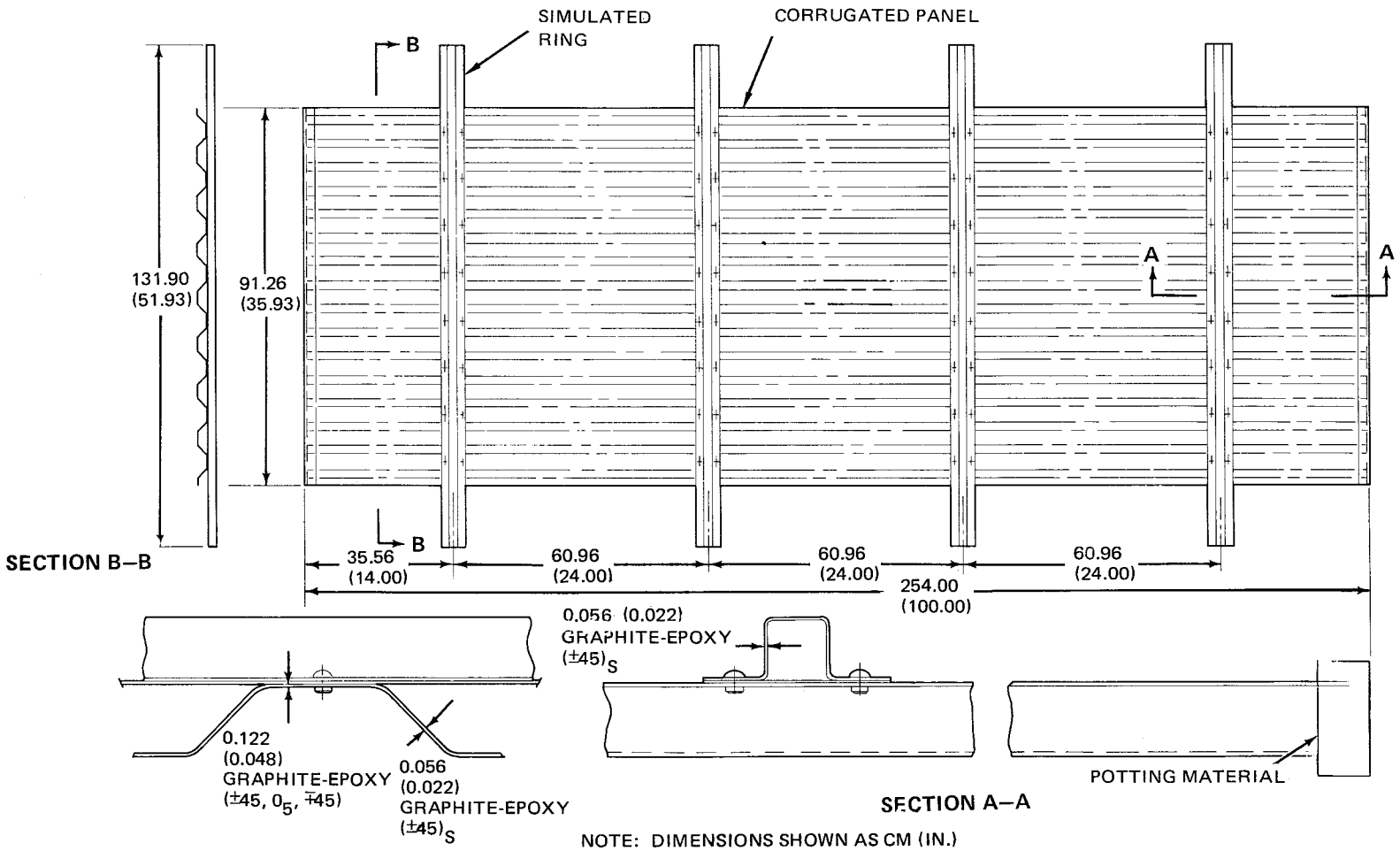

Figure 17. Graphite-Epoxy 2.54m (100-In.) Long Test Panel

The smallest type of test panel (Figure 15) was 0.61m long with a width of 0.46m. The panel was designed to provide an assessment of the local buckling capability of the basic shell wall corrugation configuration.

The second type of test panel (Figure 16), 0.91m by 0.46m, was designed to evaluate the longitudinal joint areas where the three corrugated panels are spliced to form the cylinder and to test the end attach areas where the bending moment is introduced into the shell wall.

A third type of test panel, shown in Figure 17, was 2.54m (100 in.) long and 0.94m (37 in.) wide. It was designed to evaluate the ring-stiffener attachment to the corrugated wall and to determine buckling characteristics of a panel approximating the full length of the cylinder.

3.2 PANEL FABRICATION AND NONDESTRUCTIVE TESTS

All test panels, as well as the full-size cylinder panels, were laid up and cured on flat aluminum molds machined to the proper corrugated cross-sectional configuration. All of the subsize test panels were sufficiently small in panel width that allowance for tool expansion was not required in designing the molds. However, the full-size cylinder panels with a nominal width of 3.23m (127 in.) required allowance for thermal expansion of the aluminum mold at the cure temperature of 177°C (350°F), and the corrugated cross section was therefore adjusted to a slightly smaller corrugation pitch dimension than the finished part. All panels were made with excess length and then trimmed to size after cure, a procedure that eliminated the necessity of tool dimension changes for expansion along the length of the corrugations. To reduce costs, a single mold was used to fabricate both the 0.61m panels and the 0.91m test panels. The mold for those two panels was machined from 6061 aluminum plate. However, the mold for the 2.54m (100 in.) long test panels and the mold for the full-size panels were machined from cast aluminum plates. This approach was taken to avoid welded seams in the full-size mold or, alternately, the possible expense of a special run of overwidth 6061 aluminum plate material.

Test panel fabrication was started with the 0.61m panels which provided trials for determining the best approach in layup and cure processes for the wall design. The panel fabrication was initiated by laying the lower two ±45-deg plies on a flat caul plate to form a preplied sheet. Strips of T 300/5208 prepreg 12 in. wide were layed up adjacent to one another in a ±45-deg orientation and trimmed diagonally at their ends to form a rectangular sheet of the proper size required to cover the corrugated mold. A second set of tape strips was then placed at right angles on top of the first, trimmed to the required rectangular size, and the two sets of tapes were then tacked together by applying vacuum pressure at room temperature for approximately an hour. The resulting rectangular sheet was then handled as a single sheet when it was applied to the mold. A second set of ±45-deg tapes was then laid up to form a second sheet in the same manner as the first, the only difference being a reversal in the order of layup to provide a symmetric arrangement of all four ±45-deg plies in the completed panel.

Concurrently with the layup of the ±45-deg sheets, the zero-degree reinforcements for the crown areas were prepared by laying up on a separate caul plate a set of five sheets of zero-degree tapes to form a rectangular sheet slightly longer than the full length of the panel corrugations and with sufficient width to provide a reinforcing strip at each crown position. The sheet of zero-degree plies was then staged at 107°C (225°F) for one hour and subsequently cut into 3.68-cm (1.45 in.) wide strips in preparation for the layup on the mold.

Prior to panel layup, the mold was prepared in a normal manner by cleaning it and baking on a mold release. Several trial 0.61m panels were then laid up and cured to determine the best process for producing satisfactory corrugated panels. The first panel was made by laying the lower sheet of ±45-deg plies directly on the aluminum mold with the mold at room temperature. The stiffness of the two-ply sheet required use of a heating iron to soften the material sufficiently to give good conformity with the corrugated mold. After the lower set of ±45-deg plies was laid up, the precut zero-degree reinforcements were placed on top of the preplied sheet at each corrugation crown position, tacked in position with the use of a heating iron, and then followed by placement of the upper two-ply sheet on the mold. Thus, the two sets of

±45-deg sheets provided continuity throughout the corrugated panel and sandwiched the zero-degree reinforcements at the crown areas. The internal location of the zero plies provided a superior design arrangement compared to externally located reinforcements since the latter arrangement often leads to separation of the zero plies under compression loads. After the graphite-epoxy material was in place, a layer of porous Armalon was used as a separator and one layer of Mochburg was used as a bleeder. For the 0.61m panels, nylon film bagging was used and the parts were autoclave-cured at 177°C (350°F) for 3 hours at 6.894×10^5 N/m^2 (100 psi) pressure.

The initial process was generally satisfactory but produced resin-rich areas at the corners of the lower corrugation crowns located in the "valleys" on the mold. Subsequent tests of a panel with resin-rich areas indicated that structural performance was not impaired by such areas; however, a process change was made to reduce the excess resin in local areas. The resin-rich areas were largely eliminated by using thinner bleeder material and placing one layer of bleeder between the mold and the graphite-epoxy plies as well as one layer on top of the layup. To provide satisfactory adherence of the bleeder to the mold, a volatile noncontaminating light adhesive was sprayed on the mold surface. The same procedure was used to tack the Armalon separator to the bleeder.

The basic panel layup that was developed during fabrication trials with the 0.61m panels and used throughout the remainder of the program consisted of (1) a thin layer of bleeder placed on the mold, (2) a sheet of porous Armalon on top of the bleeder, (3) a lower sheet of ±45-deg plies, (4) strips of zero-degree reinforcing plies at each corrugation crown, (5) a top sheet of ±45-deg plies, (6) a second sheet of porous Armalon, and (7) an upper layer of bleeder. A cured 0.61m panel is shown in Figure 18 with the aluminum mold.

The cured 0.61m panels were trimmed to the proper width and each end was then potted in an aluminum-filled epoxy compound to stabilize the ends and prevent local failure when the panels were tested in axial compression. The potted ends of the panels were then machined to provide flat, parallel surfaces that were perpendicular to the longitudinal axis of the panels to be mated with the loading surfaces of the test machine.

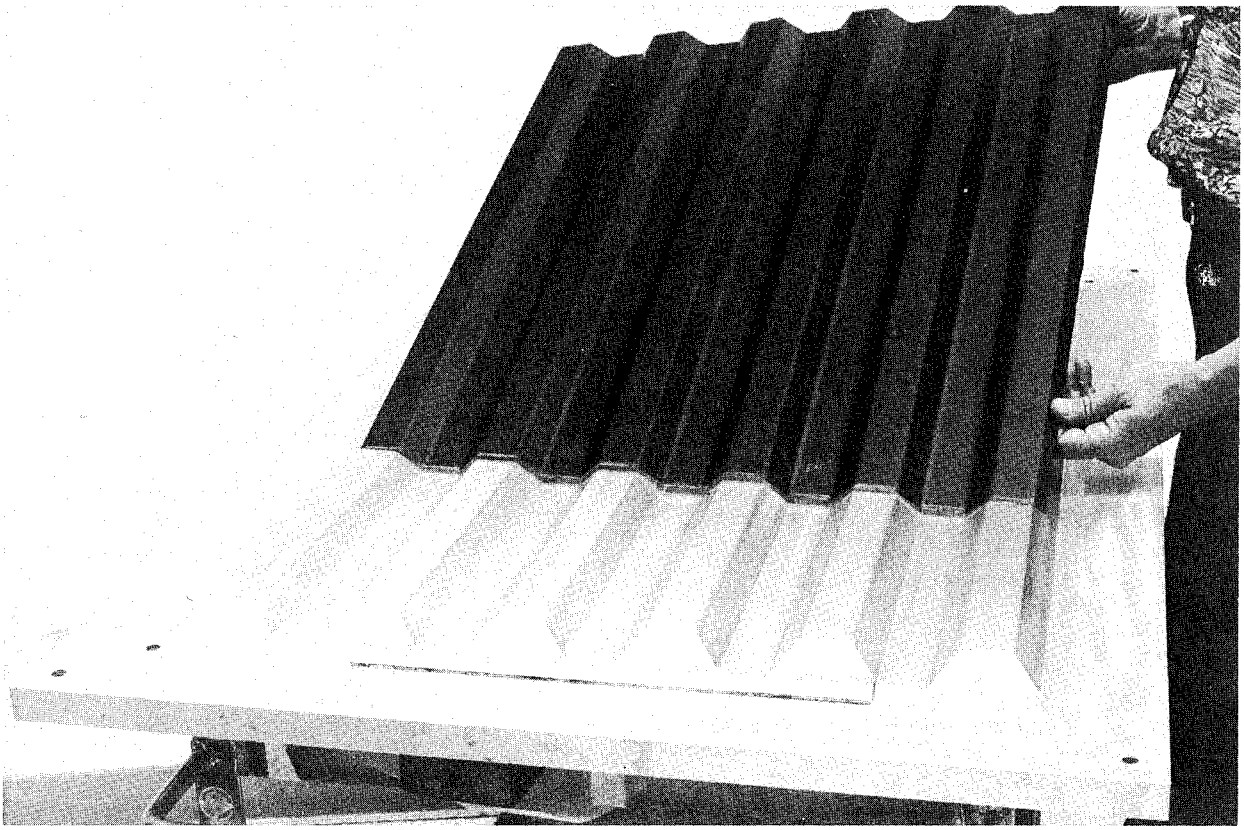

Figure 18. Corrugated Test Panel and Aluminum Mold

Prior to layup and cure of the 0.91m long panels, the aluminum mold was reworked to incorporate local cavities for panel end doublers and one crown area of the mold was remilled to provide for an overlap type panel-to-panel joint which was planned for the full size cylinder. Also, a reusable silicone rubber autoclave bag was prepared to evaluate such a concept for the full-size cylinder. The cured bag is shown in Figures 19 and 20. Use of the silicone rubber bag was entirely successful in fabricating the 0.91m panels, and that type of bag was therefore selected for use in making the full-size panels.

The 0.91m long panels were laid up and cured using the same basic technique as developed with the 0.61m panels. To provide evaluation of the end attachment areas, doublers made from T300/5208 bidirectional woven cloth were placed at the ends of each corrugation crown and cocured with the basic panels. Two thicknesses of cloth were used on both sides of each corrugation crown at the panel ends (Figure 16). In addition, the cured panel was cut longitudinally into two pieces and then rejoined with a riveted and adhe-

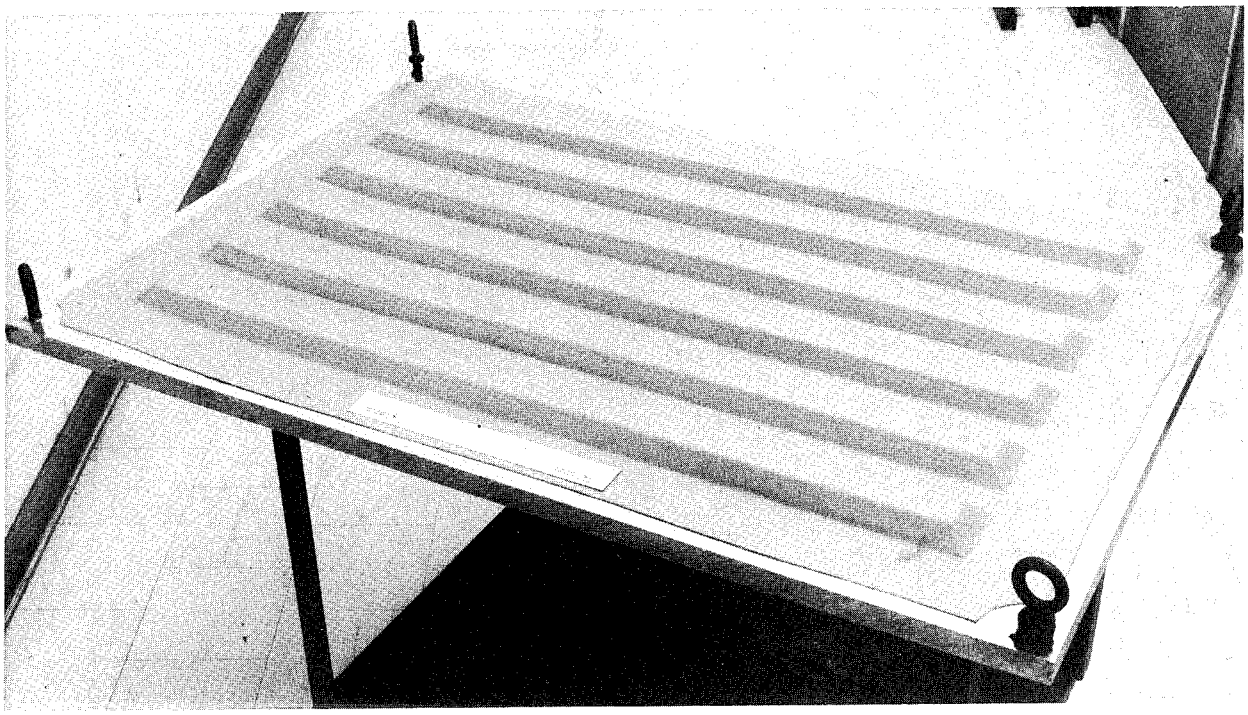

Figure 19. Silicone Rubber Bag on Corrugated Mold

Figure 20. Rubber Bag Being Removed from Mold

sively bonded joint at the panel's center. Scalloped aluminum angles were bolted to the ends to simulate the end attachment rings used in the full-size cylinder. A finished 0.91m panel is shown in Figure 21.

The riveted and adhesively bonded joint developed for the 0.91m panels used a room-temperature curing epoxy adhesive (EA 9309) combined with blind aluminum rivets. Carbide spade drills were used to drill the rivet holes, after which the holes were cleaned with MEK and inspected for chips or delaminations. Masonite was used as a backup material during drilling operations, and the use of sharp carbide drill bits, combined with masonite backup material, produced sharp, clean holes with the graphite-epoxy parts. The clamping action of the blind rivets, spaced at 5.08-cm (2 in.) intervals, proved to be sufficient for good adhesive bonds. Figure 22 shows a sample part used in developing the joints.

The 2.54m compression test panels were also fabricated in the same basic manner as that used for the 0.61m panels. Four transverse stiffeners were riveted and adhesively bonded to the panels to simulate the external ring

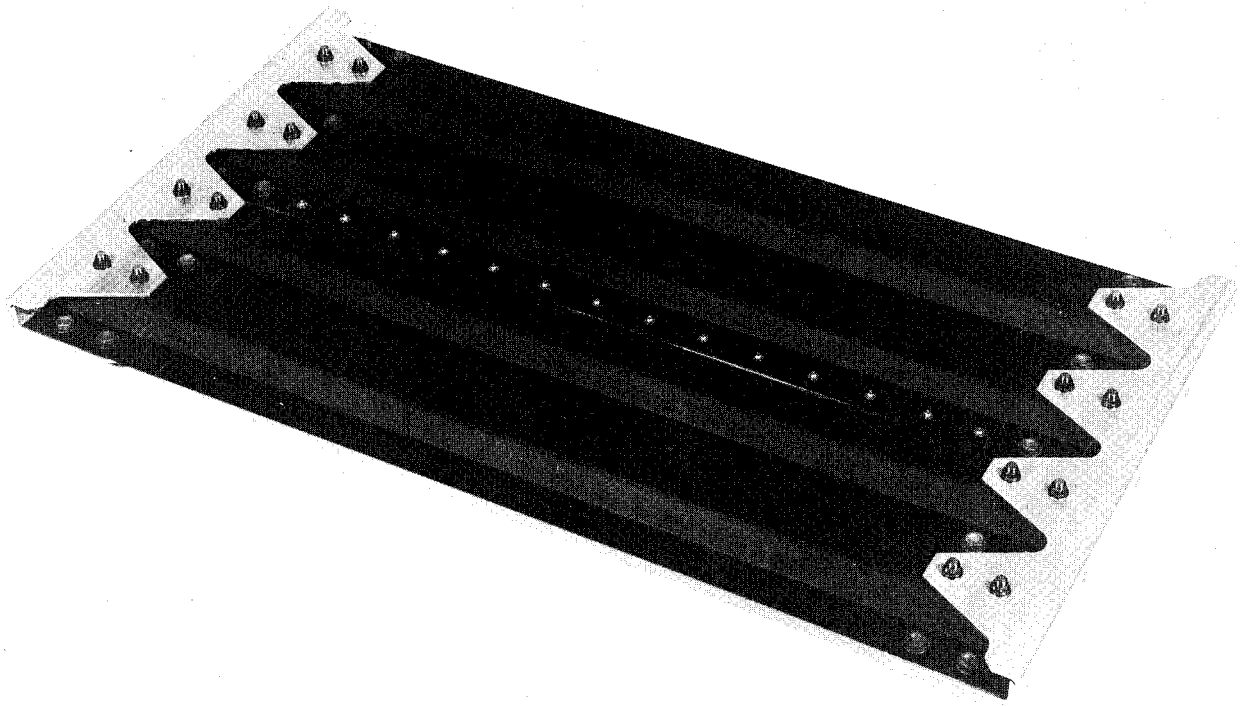

Figure 21. Corrugated Test Panel Simulating Longitudinal Joints and End Attachment Areas

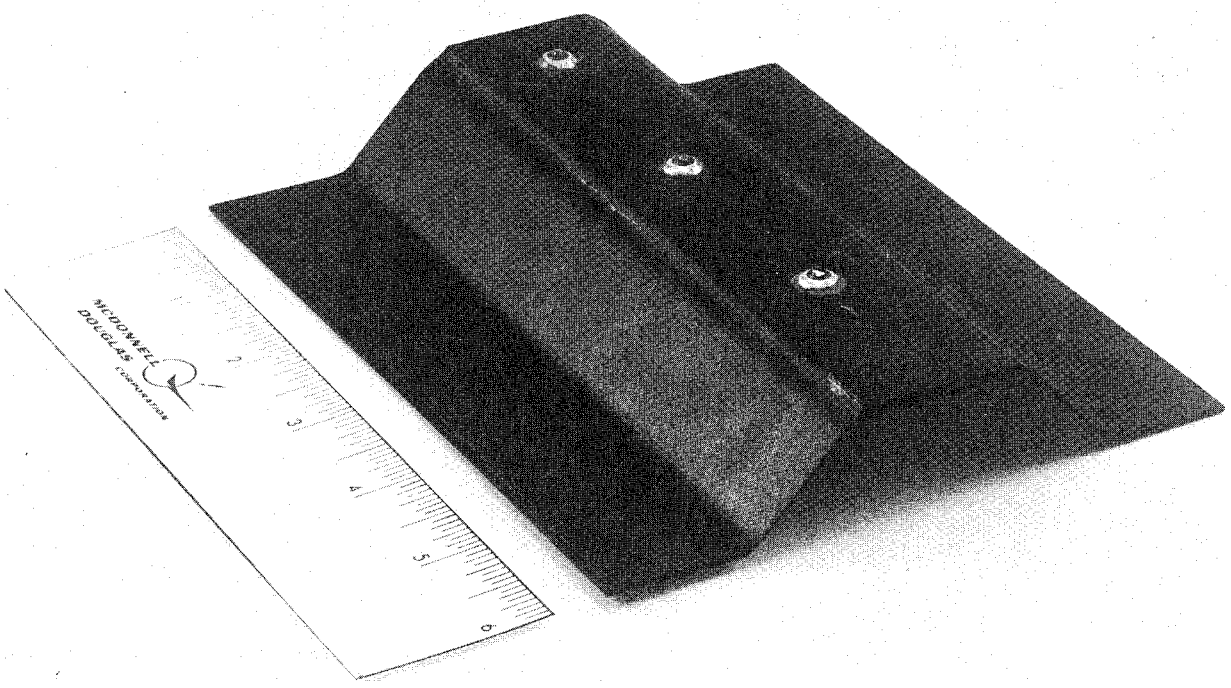

Figure 22. Segment of Bonded and Riveted Longitudinal Joint Sample

stiffeners attached to the full-size cylinder. As with the 0.61m panels, the ends of the 2.54m panels were encased with an aluminum-filled epoxy compound and machined to provide flat surfaces that mated with the loading heads in the test machine. Figure 23 shows a completed 2.54m test panel.

The basic process developed in fabricating the 0.61m panels was used for layup and cure of all subsequent test panels and the full-size cylinder panels. Because of their substantial masses and consequent large heat sink effects, the molds for the 2.54m test panels and the full-size cylinder panels prevented effective use of small heating irons to warm the ±45-deg preplied sheets of graphite-epoxy. To provide the necessary heat and the resulting pliability in the graphite-epoxy sheets, the larger molds were heated directly with hot air to approximately 37.8°C (100°F). That procedure proved successful in heating the graphite-epoxy plies sufficiently to permit good conformity of the ±45-deg sheets to the mold contour. Also, the bleeder material was changed to a 120-style fabric for the larger panels in order to obtain better conformity to the molds.

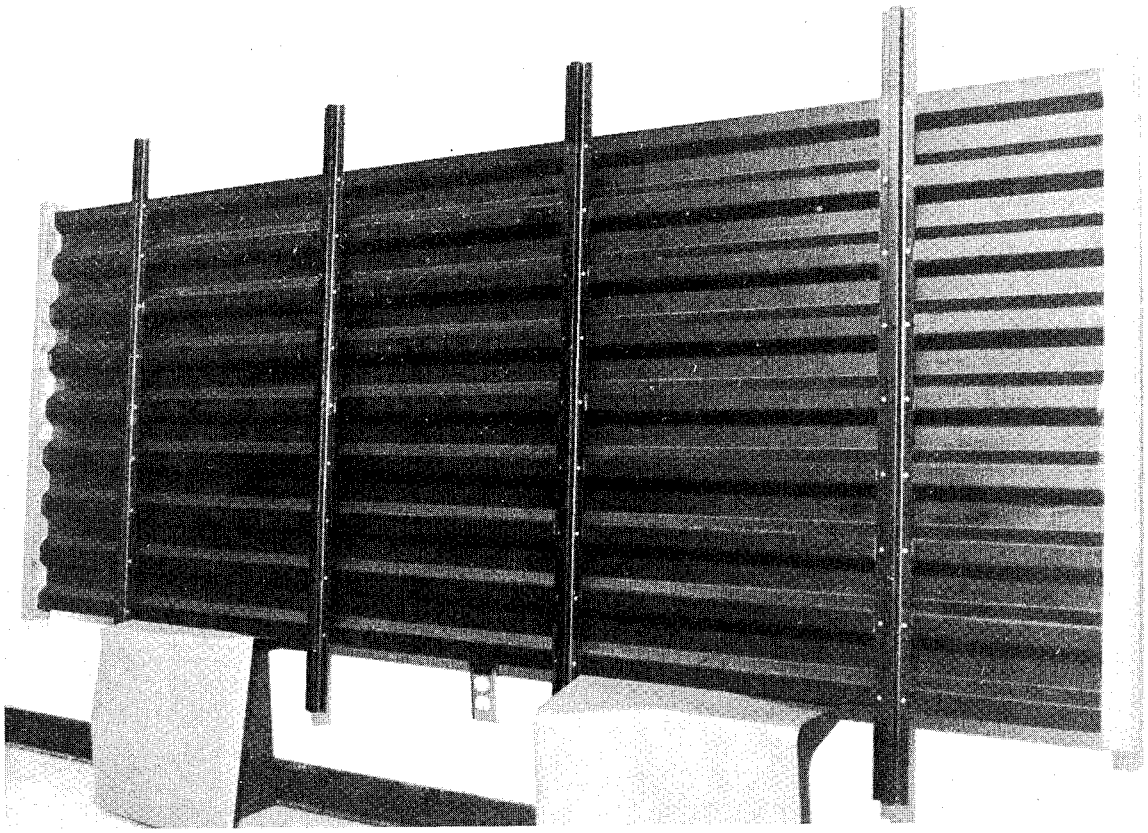

Figure 23. Subelement Test Panel 2.54m (100 In.) Long

Nondestructive tests using ultrasonic C-scan techniques were conducted to evaluate the subelement panels for internal defects. A sample corrugation 10.26 cm (4 in.) long was constructed and scanned ultrasonically initially to detect flaws. None were detected and the sample was purposely defected to provide a baseline C-scan chart to compare with those generated by scanning the corrugated test panels. The test setup is shown in Figure 24, in which the part was placed on a clear plastic reflector plate immersed in a tank of water. Crown areas were inspected by passing sound waves at 5 MHz through the panel crowns with the waves being reflected from the plastic plate back through the crown. A flat 5-MHz Automation Industries type SIL transducer 0.953 cm (0.375 in.) in diameter was used. After scanning the panel in one position, it was inverted to check the remaining crown areas. C-scan traces of the small, purposely defected panel are shown in Figure 25, and the defective area is noted.

A typical chart from scanning the crown areas of a 0.61m panel is shown in Figure 26. All of the panels tested by ultrasonic C-scan techniques were

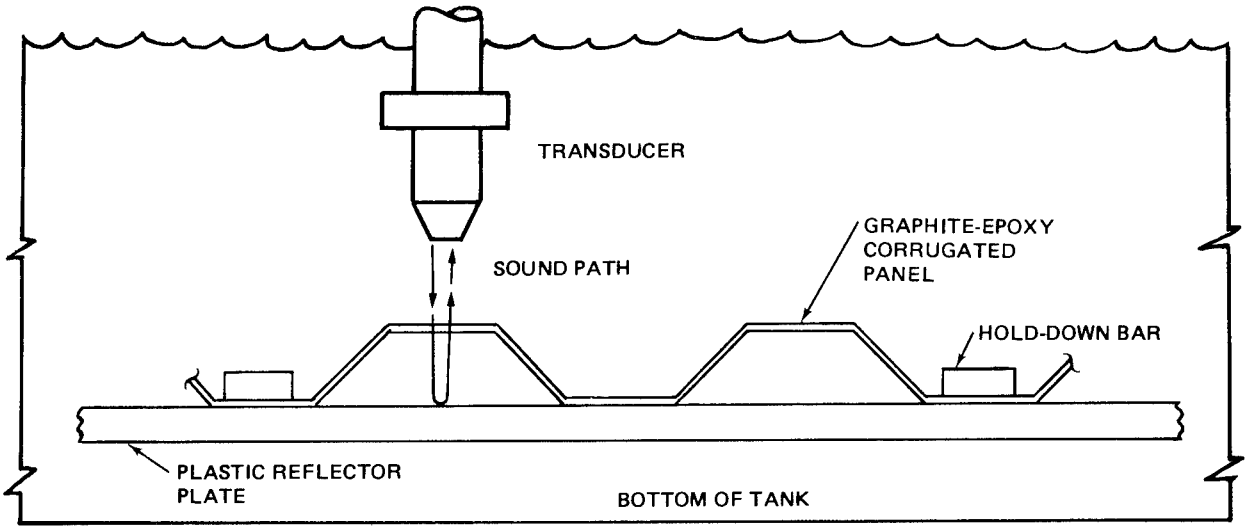

Figure 24. Ultrasonic C-Scan Test Arrangement

judged to have no delaminations or significant internal defects. Small anomalies in the C-scan charts were judged from experience with similar composite parts to be caused by local variations in fiber spacing or resin content within the panel layup. The latter estimate was substantiated by photomicrographs made of samples taken from a panel trim area. The photomicrographs, shown in Figure 27, showed a minimum void content and indicated no delaminations in resin areas between the ±45-deg plies and between the inner 45-deg ply and the zero-degree plies. No distinct separation of the zero-degree plies could be detected because of the nesting effect that occurs when they are laid up. Some areas between the ±45-deg plies had higher resin content than others, and thus tended to confirm the assessment from C-scan tests that small anomalies were caused by some non-uniformity in resin throughout the layup. The differences in resin content observed in the photomicrographs of the samples examined were normal for the type of laminate construction used.

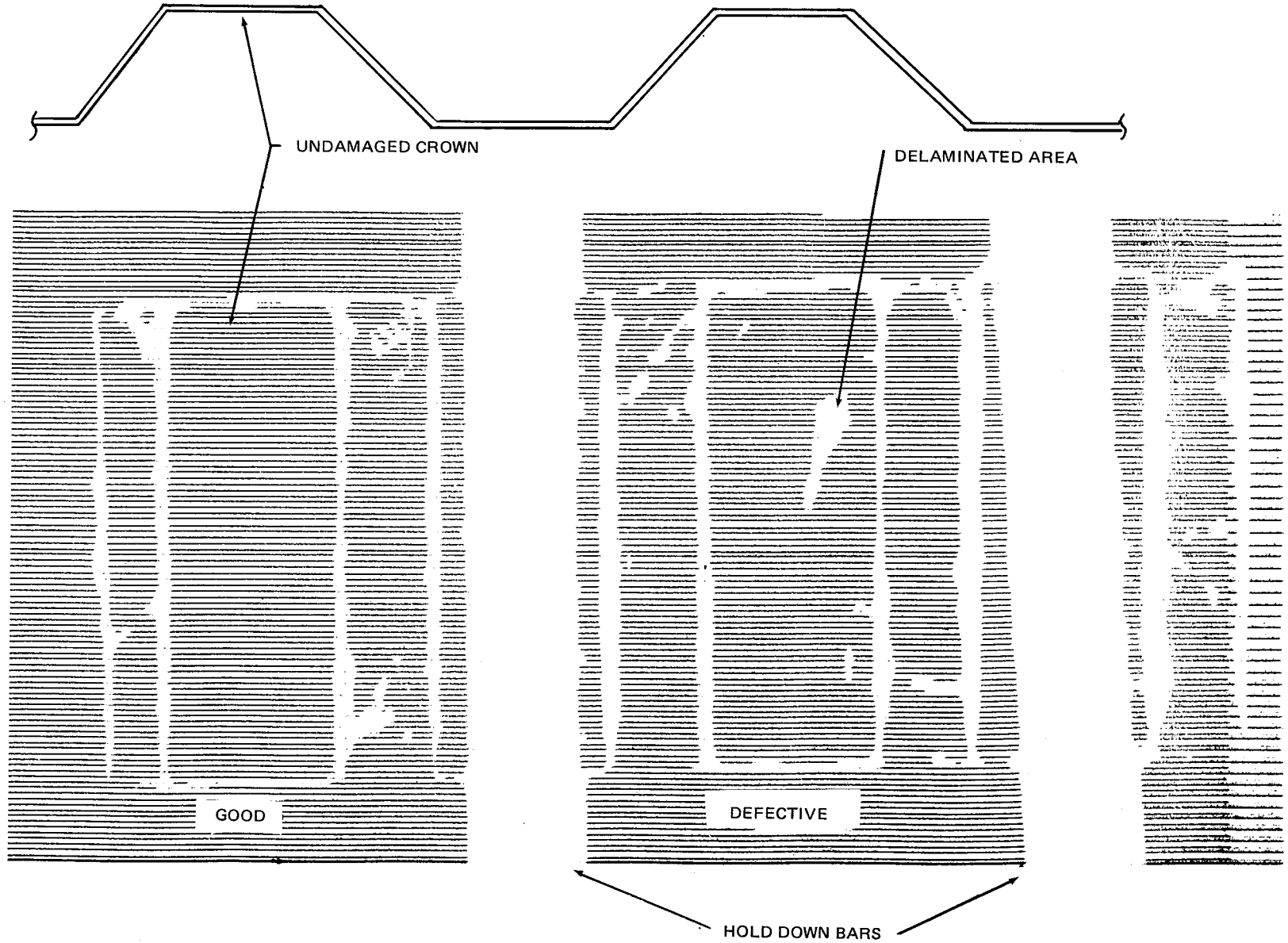

Figure 25. Ultrasonic C-Scan Trace of Purposely Damaged Corrugated Sample

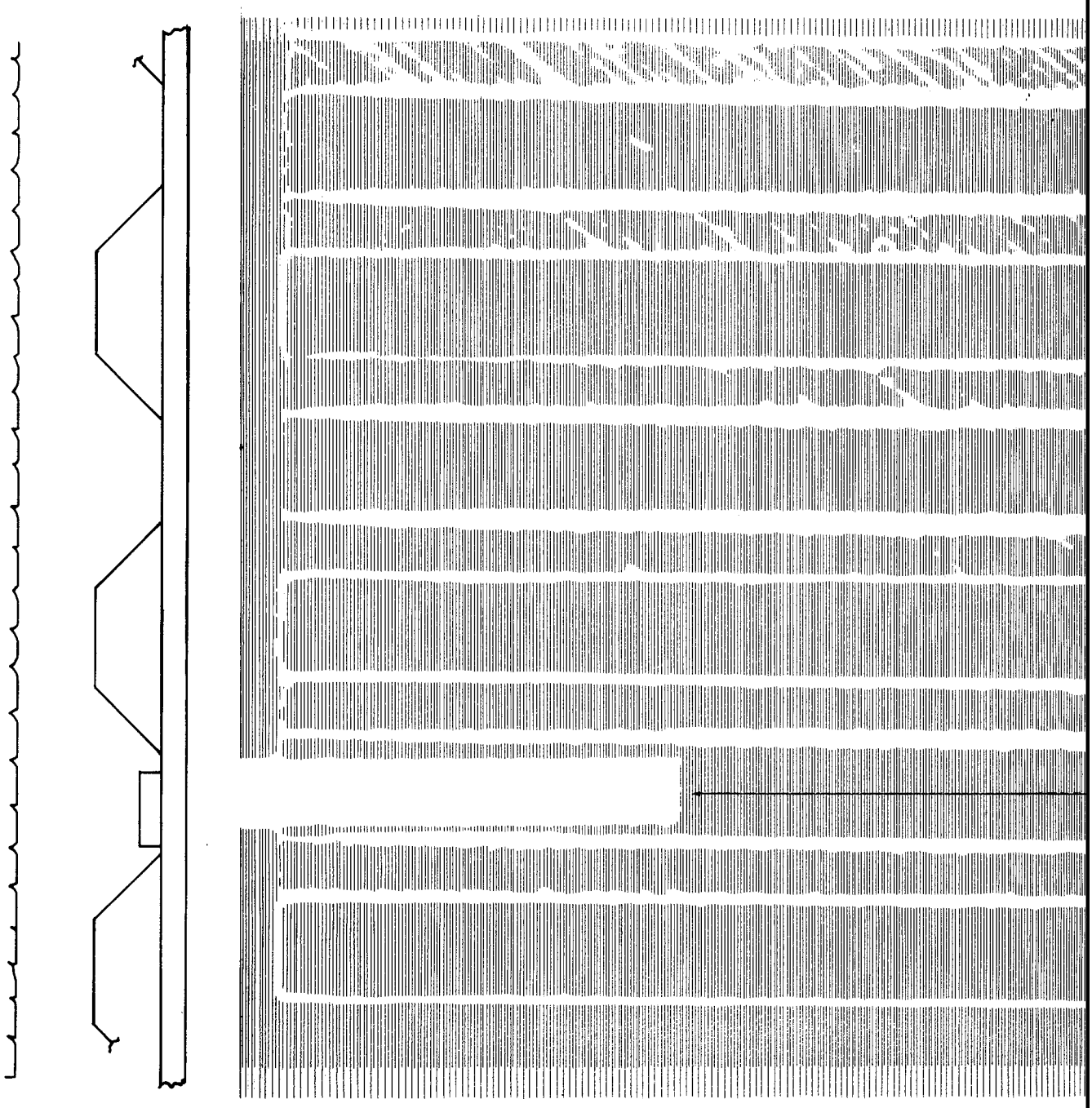

Figure 26. Typical Ultrasonic C-Scan of Graphite/Epoxy Corrugated Test Panel

(7)

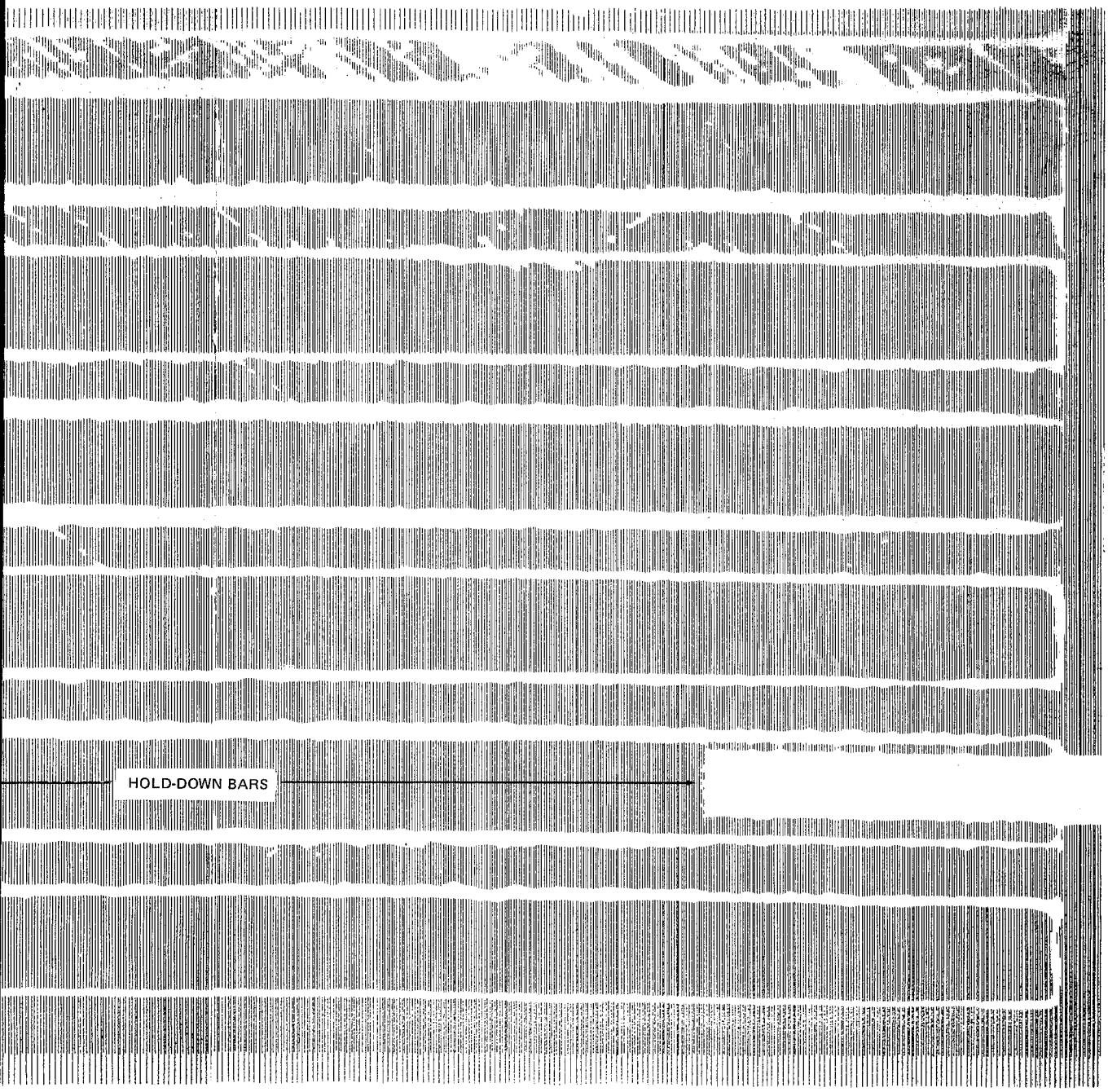

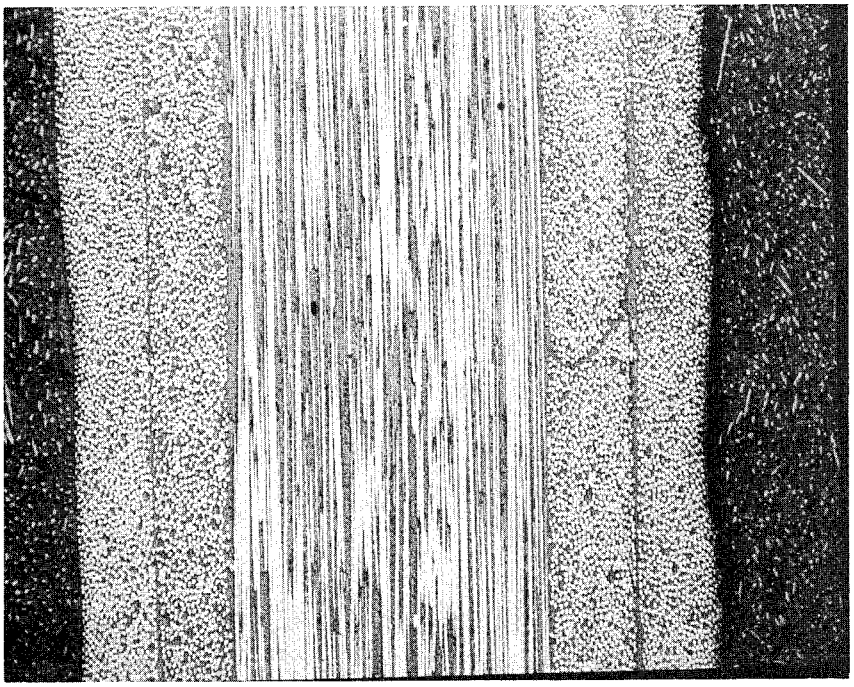

A. VIEW OF SECTION PARALLEL TO ZERO-DEGREE FIBERS

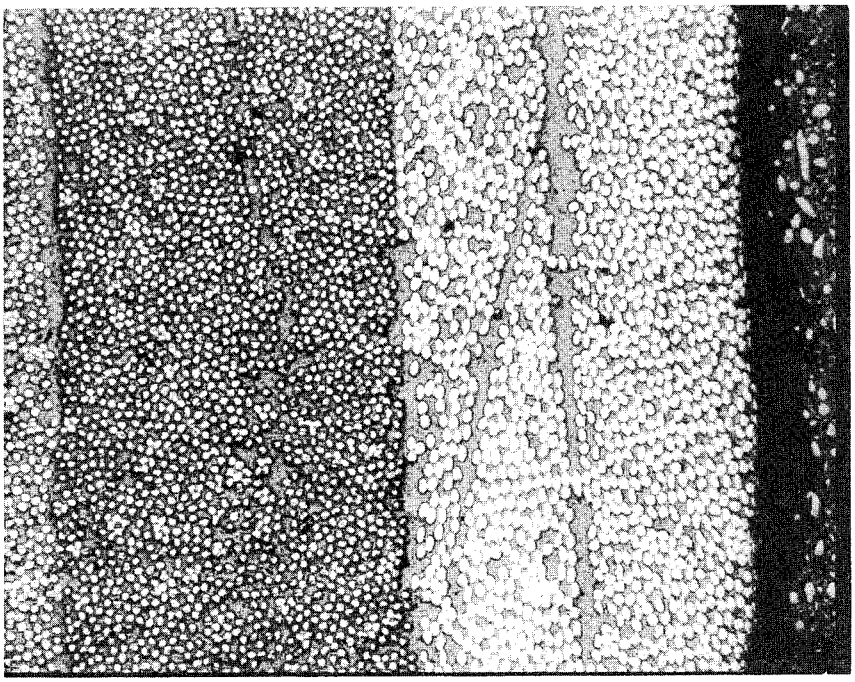

B. VIEW OF SECTION NORMAL TO ZERO-DEGREE FIBERS

Figure 27. Photomicrographs Showing Local Variations in Fiber Spacing and Resin

Both the ultasonic C-scan tests and the photomicrographic evaluations indicated that no significant imperfections were evident in the test panels.

Thickness measurements were also made at a number of points on the test panels, and such measurements were used in correlating results from local buckling tests with analytical predictions. Panel test results are described in the following subsection, and Figures 28 through 35 present thicknesses of the subelement test panels.

3.3 PANEL TEST RESULTS

Compression tests were conducted with four 0.61m panels to evaluate local buckling characteristics of the corrugation and correlate test results with the preliminary analysis. Initial tests, conducted with two panels using four zero-degree reinforcement plies in the corrugation crowns, indicated local buckling occurred in the crowns at load intensities approximately 20% lower than the design value of 1,576 N/cm (900 lb/in.). Evaluation of the initial test results showed that a reduction in the cured laminate minimum thickness was the primary cause for reduced buckling values observed in initial tests.

Measurements of the eight-ply crown thicknesses in a number of areas indicated values in the actual panel below the nominal 0.112-cm (0.044 in.) thickness used in preliminary analyses. The low thicknesses at the crowns proved to be critical in local buckling because those areas support approximately 90% of the axial compression load as a result of having the zero-degree reinforcements located there. The effect of corrugation crown minimum thickness on local buckling loads is shown in Figure 36, from which it can be seen that a 7% decrease in minimum crown wall thickness from the nominal design of 0.112 cm (0.044 in.) to 0.104 cm (0.041 in.) can produce approximately a 20% change in the predicted critical local buckling load. A contributing cause for the lower-than-expected thicknesses in the crown areas was the apparent nesting effect that occurred when the four plies of tape were laid together and staged in a unidirectional layup. Photomicrographs of sections cut from sample panels revealed this effect. The photomicrographs showed no distinct resin boundaries between layers of zero plies in contrast to easily distinguished resin layers between the ±45-deg plies that were oriented perpendic-

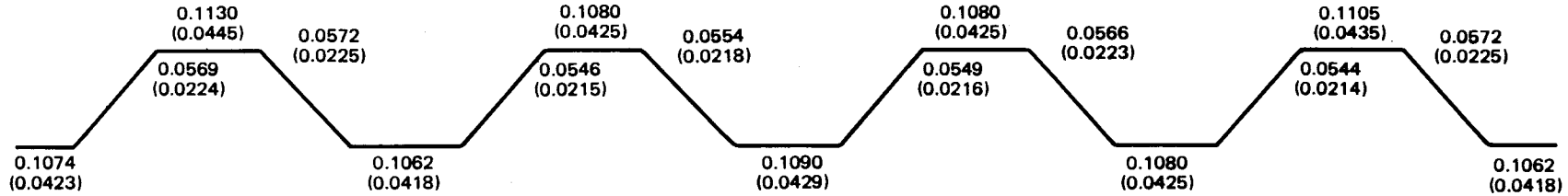

END A

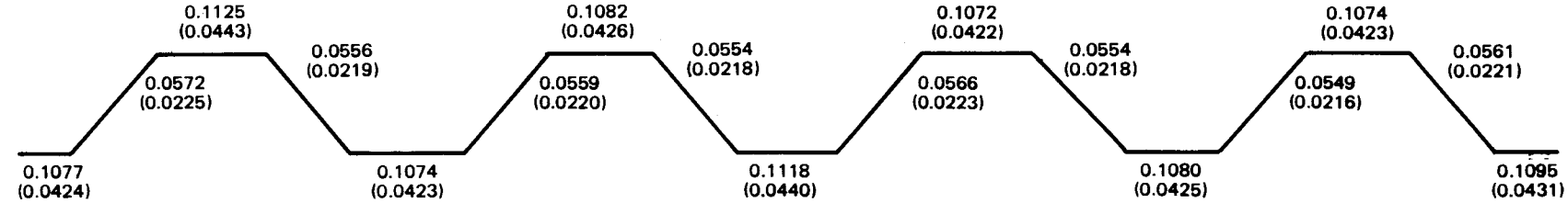

END B

NOTES:
1. MEASUREMENTS TAKEN 2.54 CM (1.0 IN) FROM EACH END
2. DIMENSIONS SHOWN AS CM (IN)
3. FOUR PLIES OF ZERO-DEGREE REINFORCEMENTS USED IN CROWN AREAS

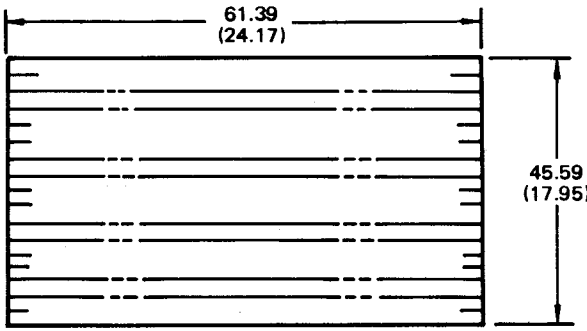

Figure 28. Thicknesses Measured on the First 0.61m Test Panel

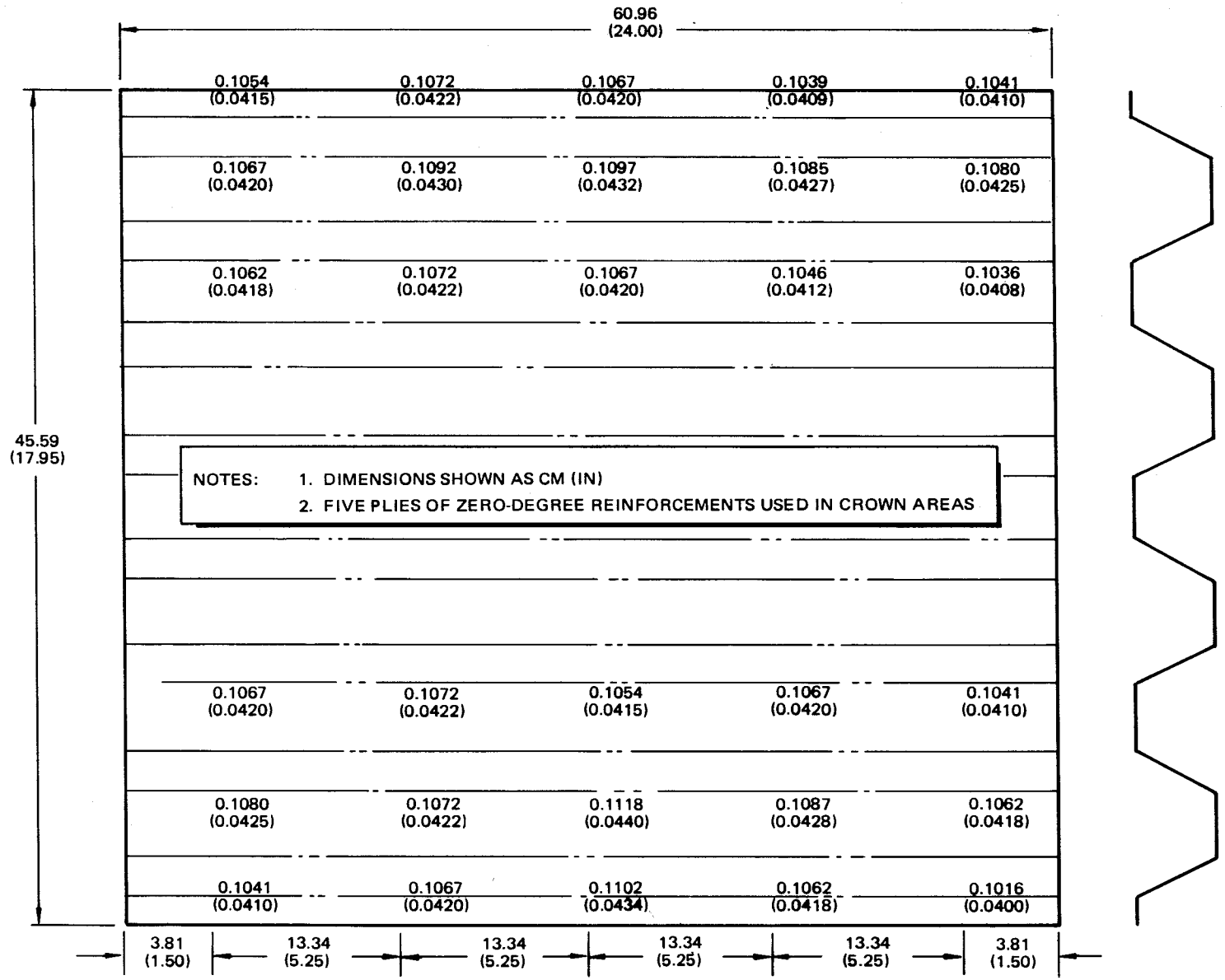

Figure 29. Thicknesses Measured on the Second 0.61m Test Panel

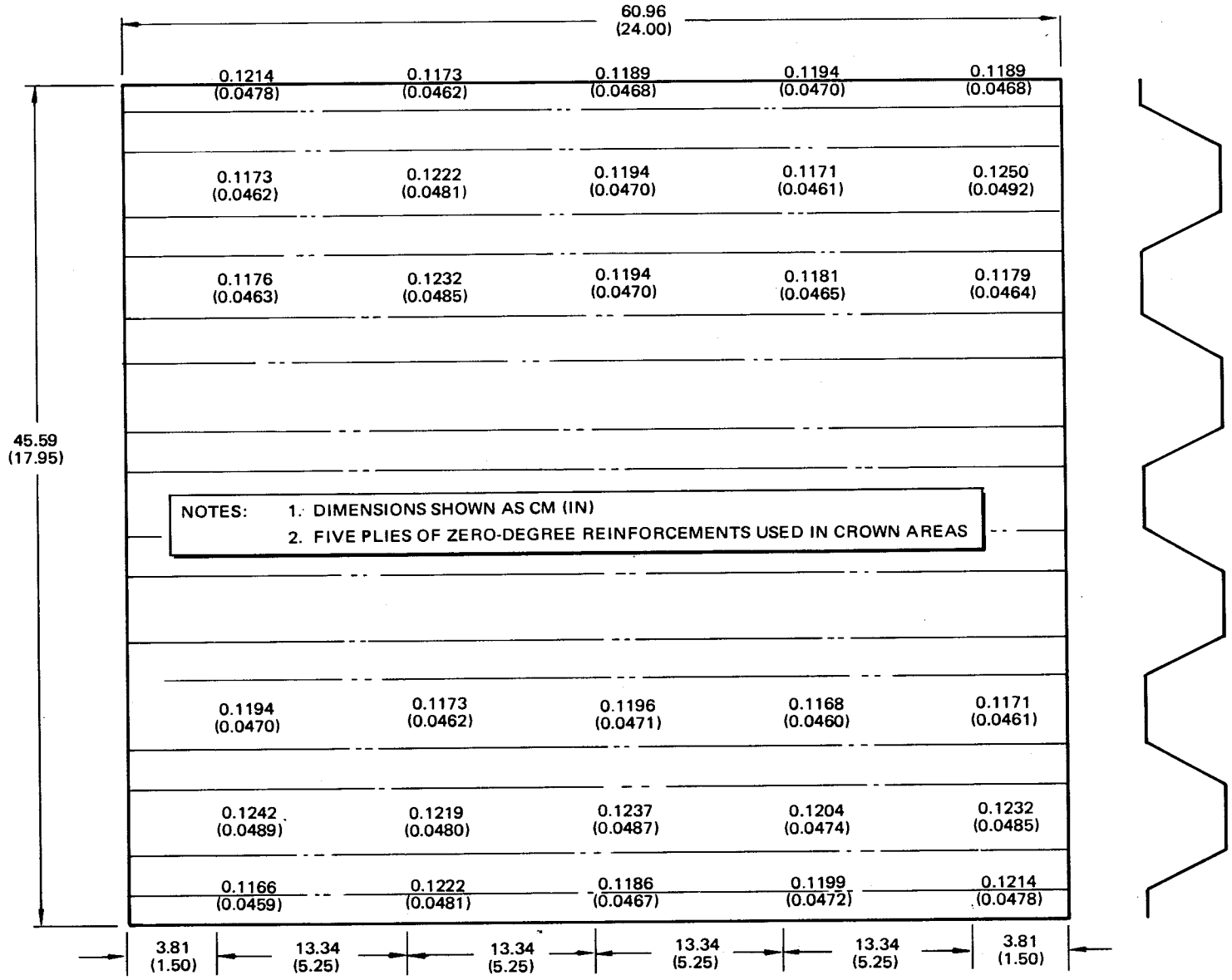

Figure 30. Thicknesses Measured on the Third 0.61m Test Panel

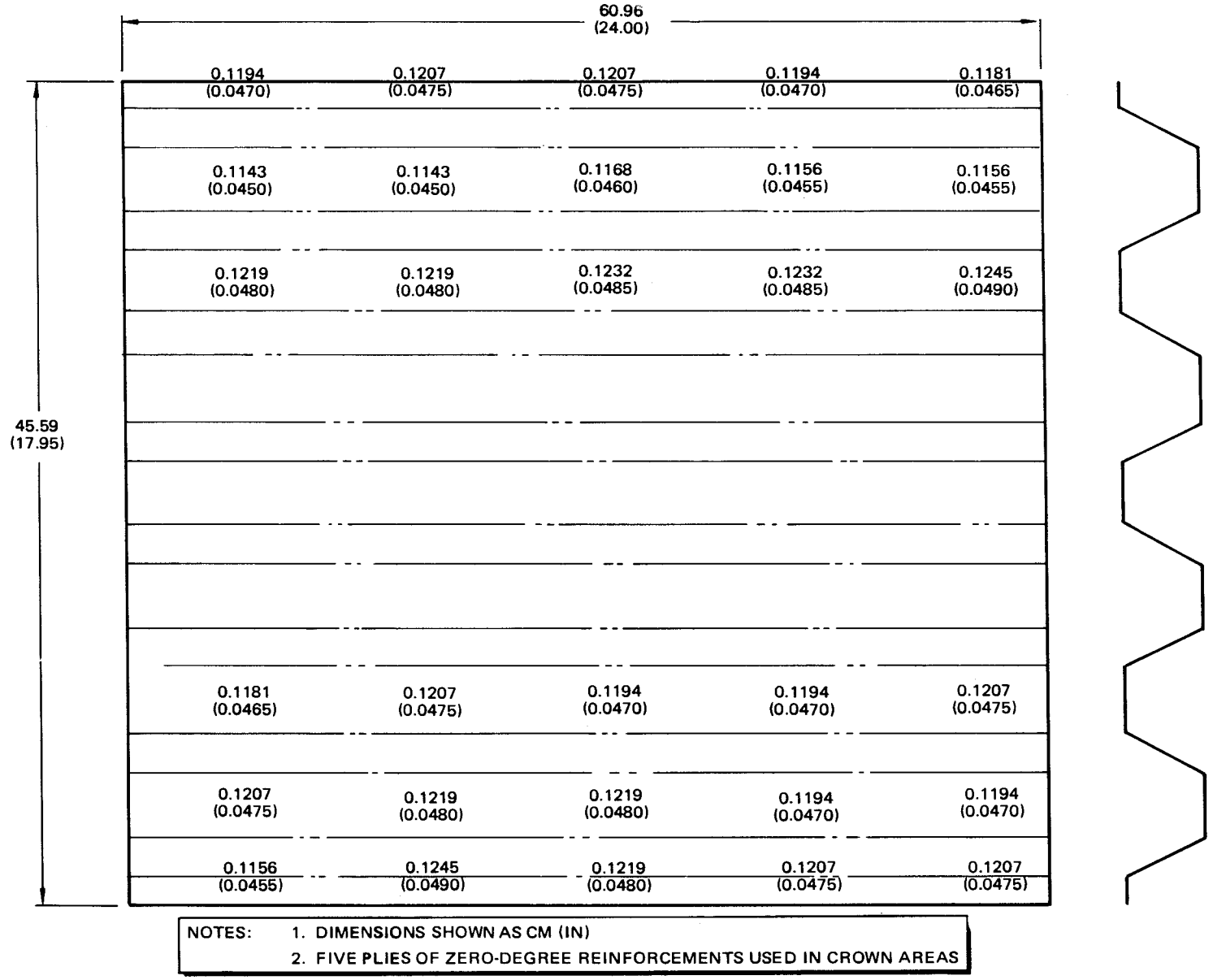

NOTES: 1. DIMENSIONS SHOWN AS CM (IN)
2. FIVE PLIES OF ZERO-DEGREE REINFORCEMENTS USED IN CROWN AREAS

Figure 31. Thicknesses Measured on the Fourth 0.61m Test Panel

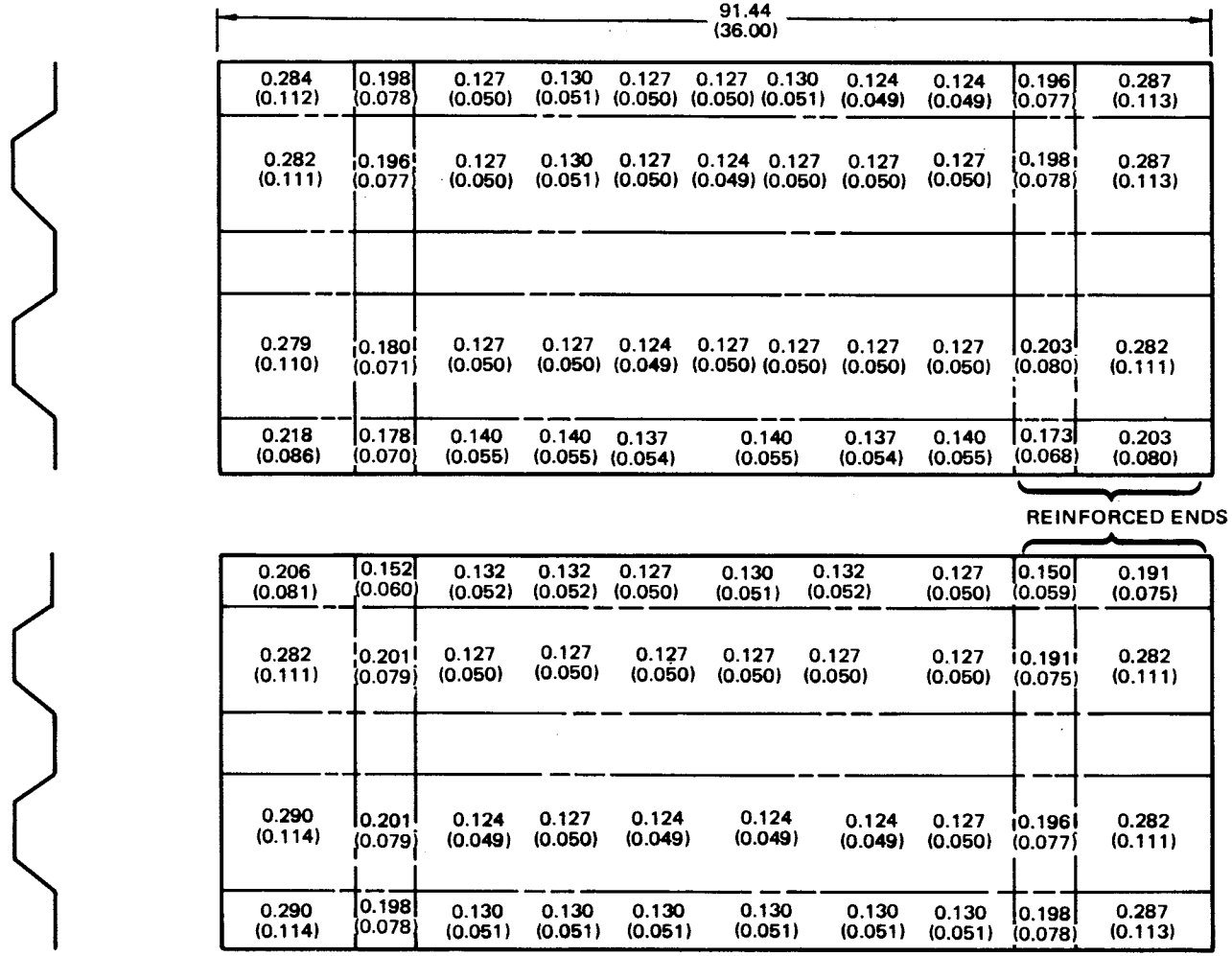

NOTES:
1. DIMENSIONS SHOWN AS CM.(IN)
2. FIVE PLIES OF ZERO-DEGREE REINFORCEMENTS USED IN CROWN AREAS

Figure 32. Thicknesses Measured on the First 0.91m Test Panel

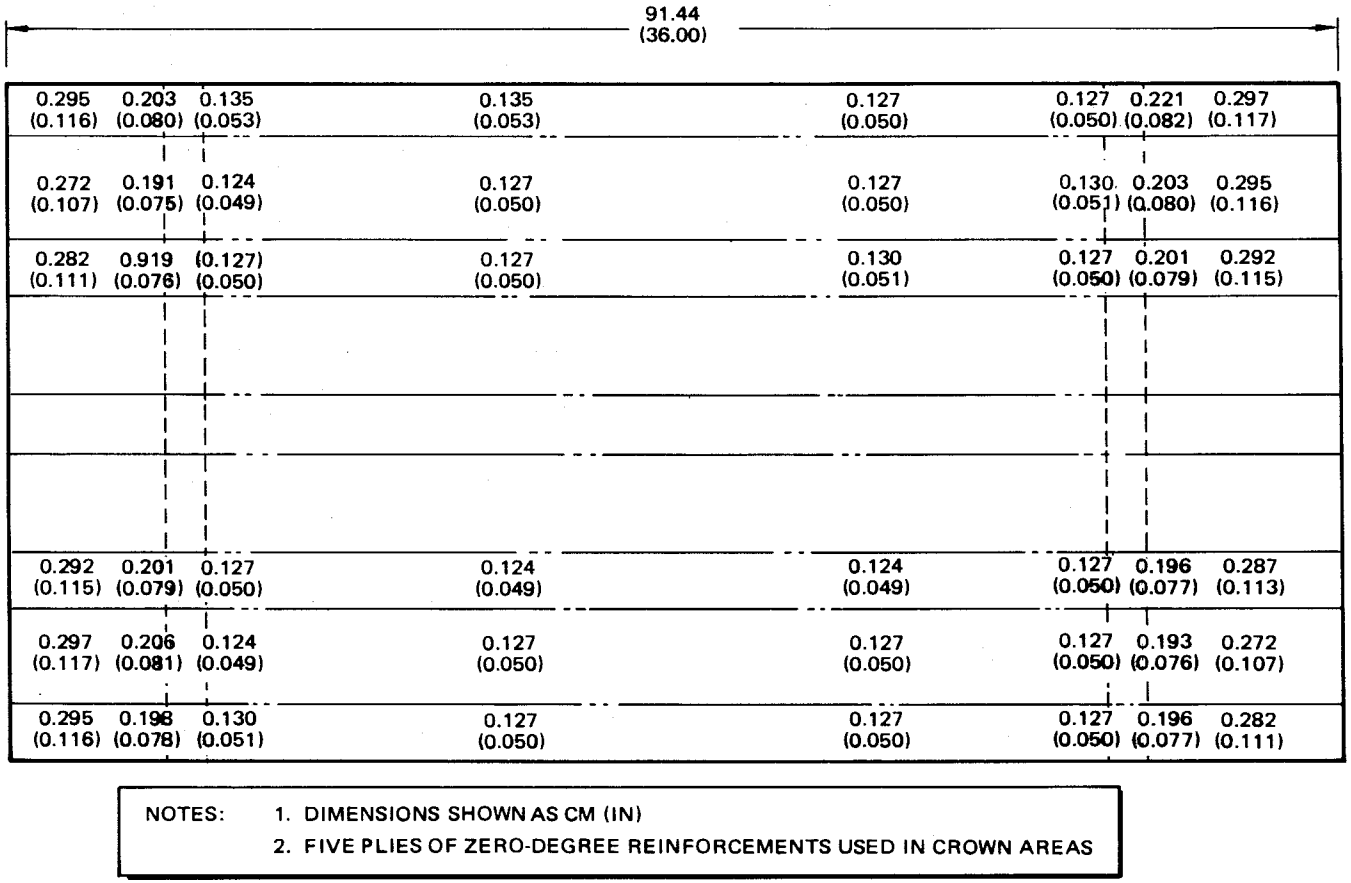

Figure 33. Thicknesses Measured on the Second 0.91m Test Panel

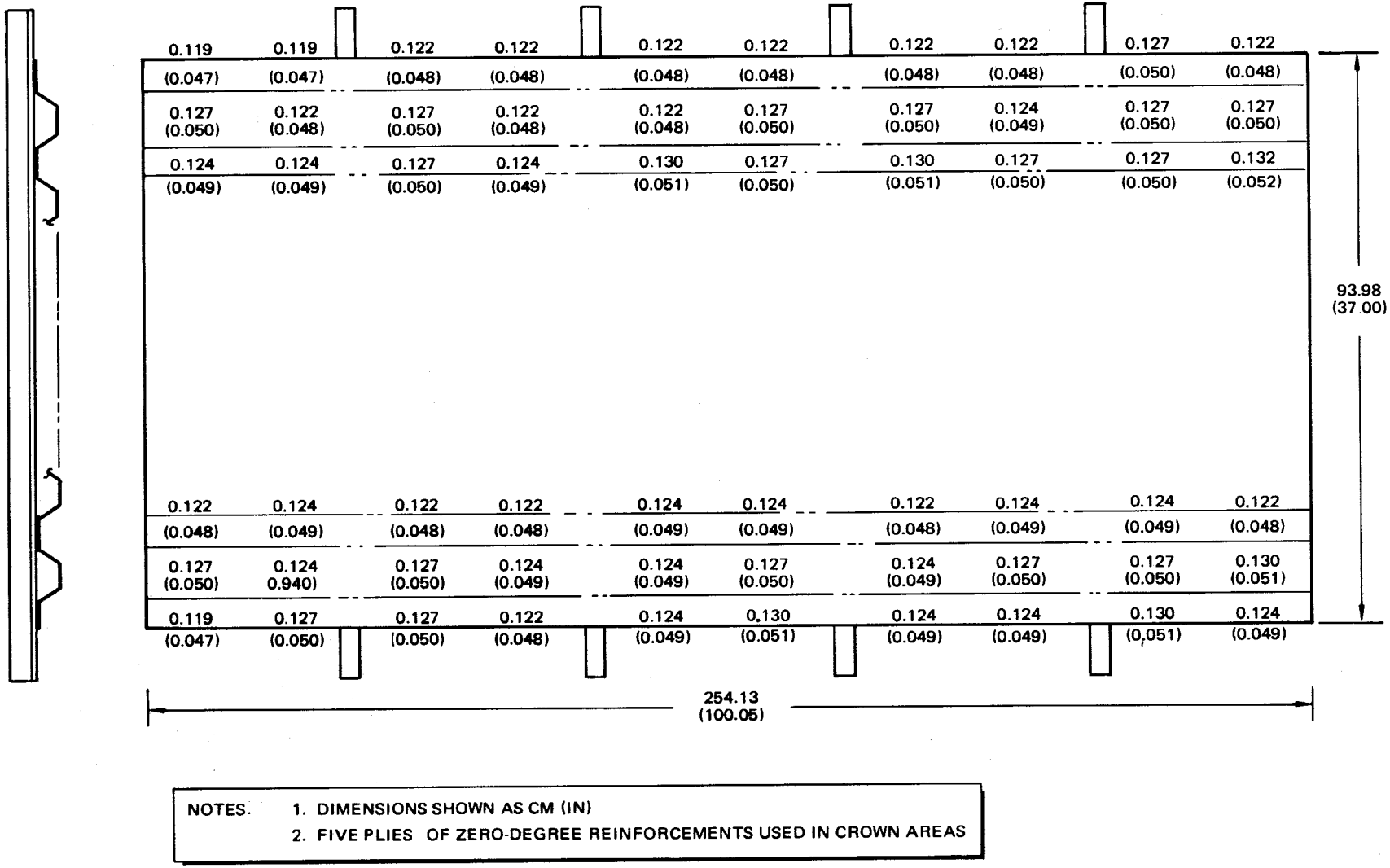

Figure 34. Thicknesses Measured on the First 2.54m Test Panel

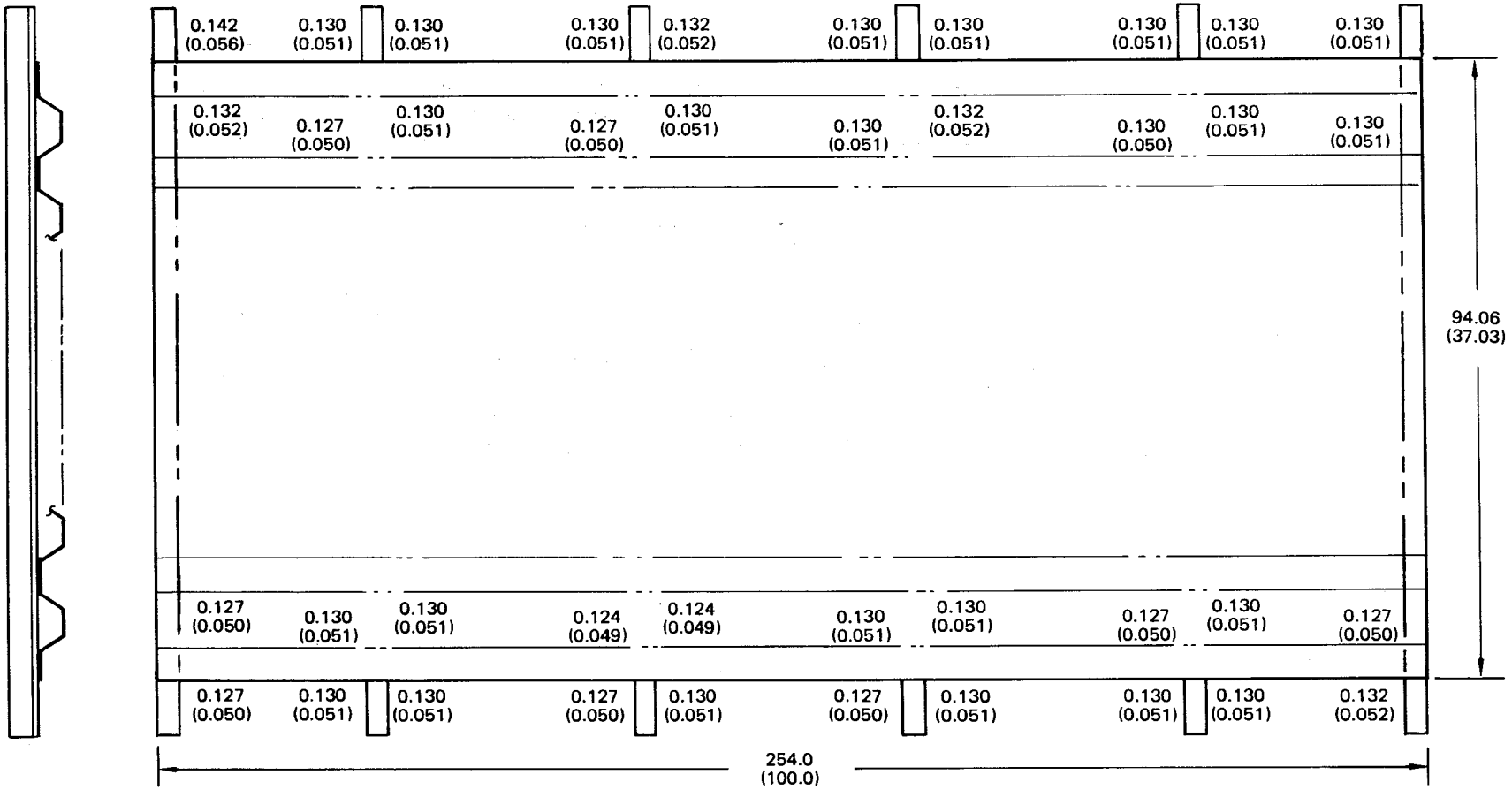

NOTES:
1. DIMENSIONS SHOWN AS CM (IN)
2. FIVE PLIES OF ZERO-DEGREE REINFORCEMENTS USED IN CROWN AREAS

Figure 35. Thicknesses Measured on the Second 2.54m Test Panel

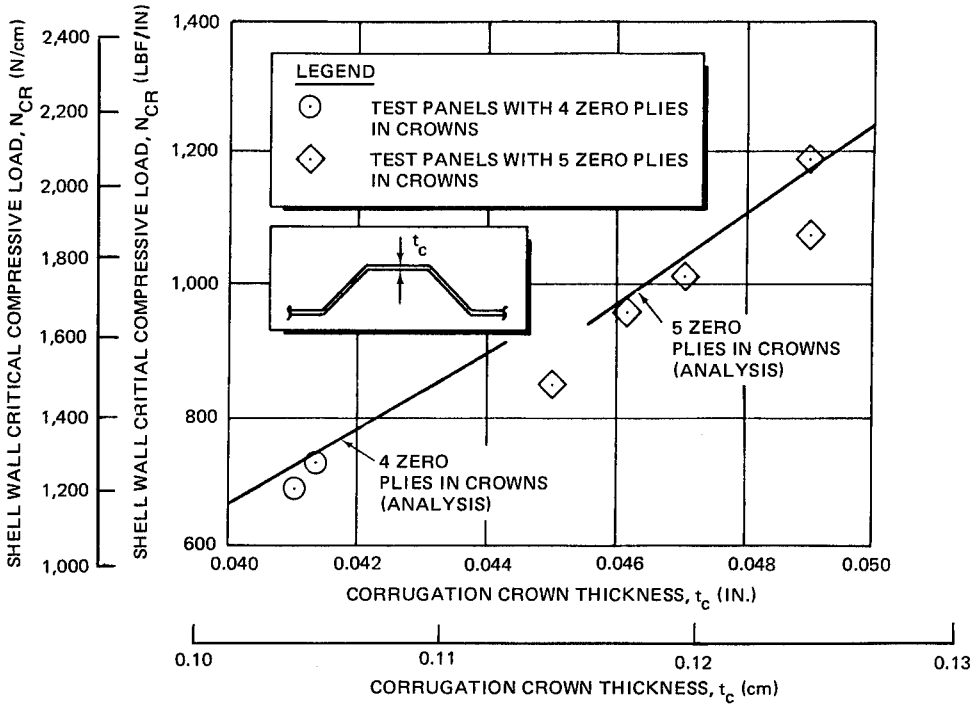

Figure 36. Critical Local Buckling Load As a Function of Corrugation Crown Thickness

ularly to one another. Figure 37 shows a sample photomicrograph of a section cut normal to the longitudinal axis of the panel.

As a result of the initial tests with the 0.61m panels, the corrugation crown layup was modified to include five zero-degree plies for reinforcement in place of the original four plies. Other steps taken to provide sufficient thickness in the crown areas included a reduction in staging time for the zero-degree plies from 1 hour to 30 minutes and an increase in width of the reinforcing plies from 3.68 cm (1.45 in.) to 3.73 cm (1.47 in.). The total accompanying cylinder weight increase was approximately 5%.

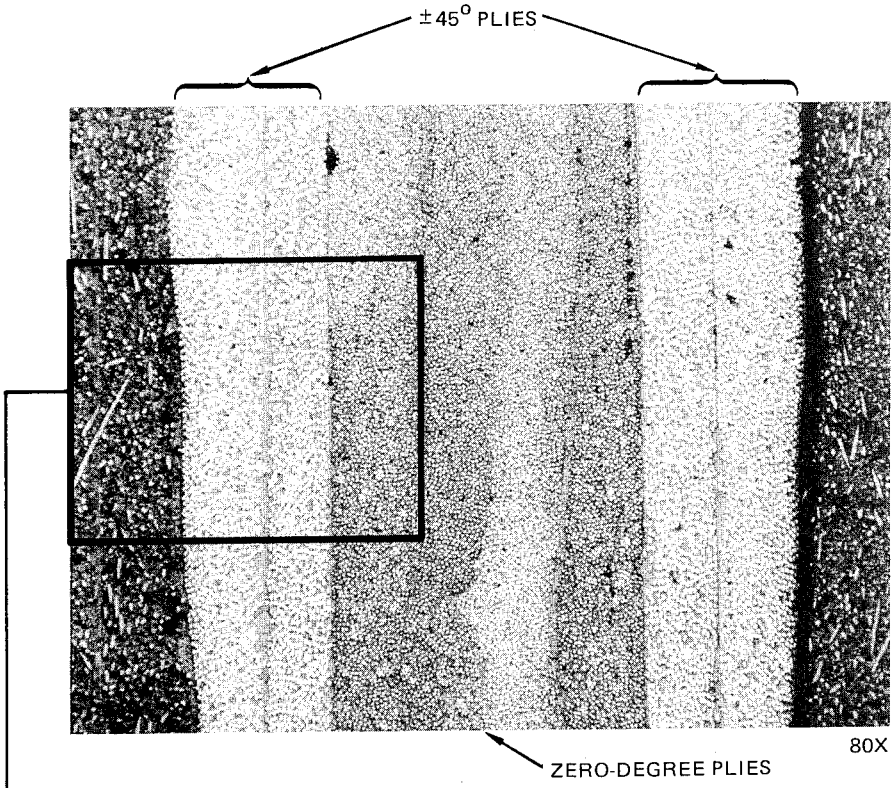

A. LOOKING INTO ENDS OF ZERO-DEGREE PLIES

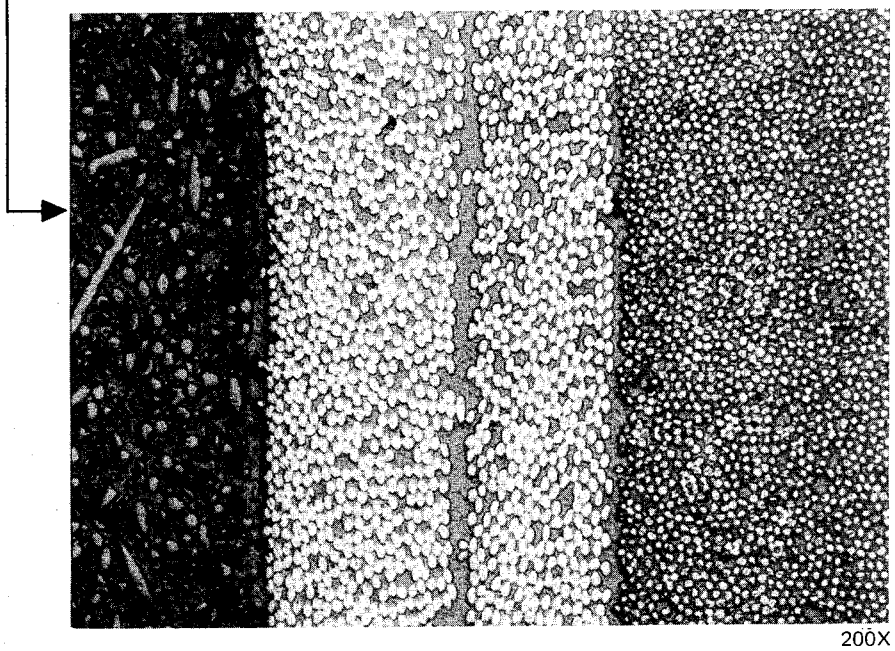

B. HIGHER MAGNIFICATION OF ±45° PLIES AND PORTION OF ZERO-DEGREE PLIES; LOOKING INTO ENDS OF ZERO-DEGREE PLIES

Figure 37. Photomicrographs of Trim Sample Taken from 0.61-m (24-Inch) Test Panel Showing Nesting of Zero-Degree Plies.

Section 4
CYLINDER TOOLING AND FABRICATION

Fabrication of the cylinder was divided into two basic areas of work: (1) fabrication of the graphite-epoxy corrugated wall panels and ring stiffeners, and (2) construction of the assembly jig, including the aluminum adapter angles.

4.1 FULL-SIZE PANEL FABRICATION

Full-size panels for the cylinder were fabricated on a large aluminum mold with overall dimensions of 3.35 by 3.56m (132 by 140 in.). A solid cast aluminum slab, 7.62 cm (3 in.) thick was machined to provide the corrugated shape with allowance being made in the corrugation pitch spacing for thermal expansion during cure. A welded aluminum reinforcing frame was bolted to the rear of the mold to provide stiffness for handling during panel fabrication. To provide access during panel layup, the mold was provided with a pivot support at its center and mounted on trunnions that permitted rotation of the mold. Figure 38 shows the rear side of the mold with the reinforcing frame and pivot. Layout of the ±45-deg preplied sheets was accomplished on an aluminum caul sheet using 0.305m (12 in.) wide tape as shown in Figure 39, the overall size of the graphite-epoxy sheets being 3.30 by 3.94m (130 by 155 in.). The sheets were vacuum-consolidated at room temperature prior to layup. For the zero-degree reinforcement, a five-ply panel was laid up 3.30m (130 in.) in length and 2.54m (100 in.) wide. The layup was consolidated under vacuum at a temperature of 107°C (225°F) for 30 min. Strips 3.73 cm (1.47 in.) wide were trimmed from the preform. Two preform strips, each consisting of 3 plies of Style 143 glass epoxy, were prepared for the panel edges in the same manner as the zero-degree preform strips. Orientation of the warp yarns in this cloth was in the 3.30m (130 in.) dimension. Graphite-epoxy doublers were cut from bidirectional cloth using dinking dies for layup at the panel ends at each crown position.

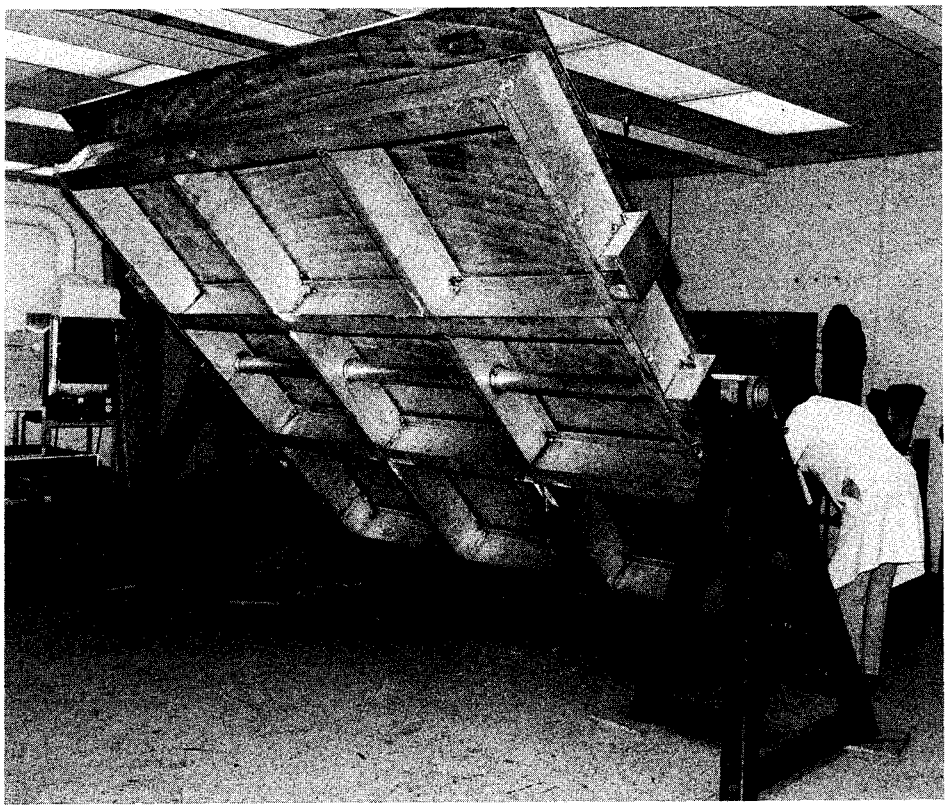

Figure 38. Rear Side of Full-Size Panel Mold Showing Reinforcing Frame, Pivot Tube, and Support Trunnions

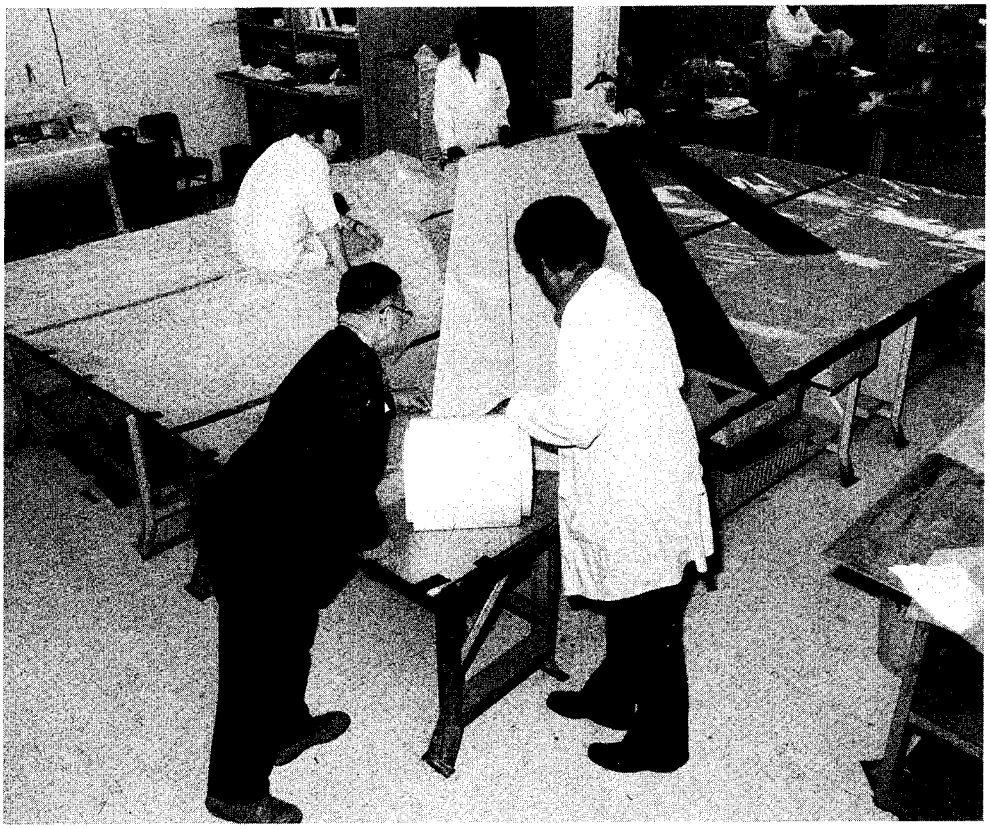

Figure 39. Preplying a ±45-Deg Sheet

After the layup surface of the mold had been treated with Frecote 33 mold release, a single ply of 120 glass bleeder and a ply of TX-1040 (Armalon) permeable release cloth were installed as described in Section 3. Stepped, two-ply graphite-epoxy cloth doublers were then pressed into all crown areas at the panel ends which required doublers. The capability to rotate the mold at its center, combined with the provision for raised stands, provided the technicians with good access to the entire mold surface and facilitated the layup operation. When the preplied sheet was ready for layup on the mold, the mold was heated to approximately 37.8°C (100°F) by the application of heated air against the rear of the mold. Layup of the preplied ±45-deg sheet is shown in Figure 40, where use of teflon-coated aluminum bars assisted in holding the sheet to the mold contour as layup progressed across the mold. After contouring the lower sheet of ±45-deg plies to the mold, precut strips of zero-degree reinforcements 3.73 cm (1.47 in.) wide were placed at each crown position and the glass-epoxy strips were laid up at the panel edges. Following that operation, the second ±45-deg sheet was contoured to the mold. Reinforcing end doublers were positioned on the upper surface at each crown position, and a single ply of Armalon release film and one ply of 120 glass cloth bleeder were contoured and tacked to the layup. Figure 41 shows the panel after placement of the 120 glass bleeder cloth on top of the layup; Figure 42 shows the layup with the rubber vacuum bag in place. Curing of the panels was done at the Rohr Aircraft Co. facility at Riverside, California. The steps in the cure schedule were: (1) drawing a minimum of 63.5 cm (25 in.) Hg vacuum, (2) applying 1.034×10^5 N/m^2 (15 lbf/in.^{2}) autoclave pressure, (3) heating the part to 87.7°C (190°F), (4) increasing autoclave pressure to 6.894×10^5 N/m^2 (100 lbf/in.^{2}) and venting the bag, (5) heating the part to 177°C (350°F) and holding for 3 hr at that temperature, and (6) cooling under pressure. After curing operations, each panel was trimmed and prepared for installation in the assembly jig. A completed panel is shown in Figure 43. A summary of the average thicknesses measured on the completed full size panels is presented in Table 7. Strength values obtained from samples removed from the edges of the full size panels are shown in Table 8.

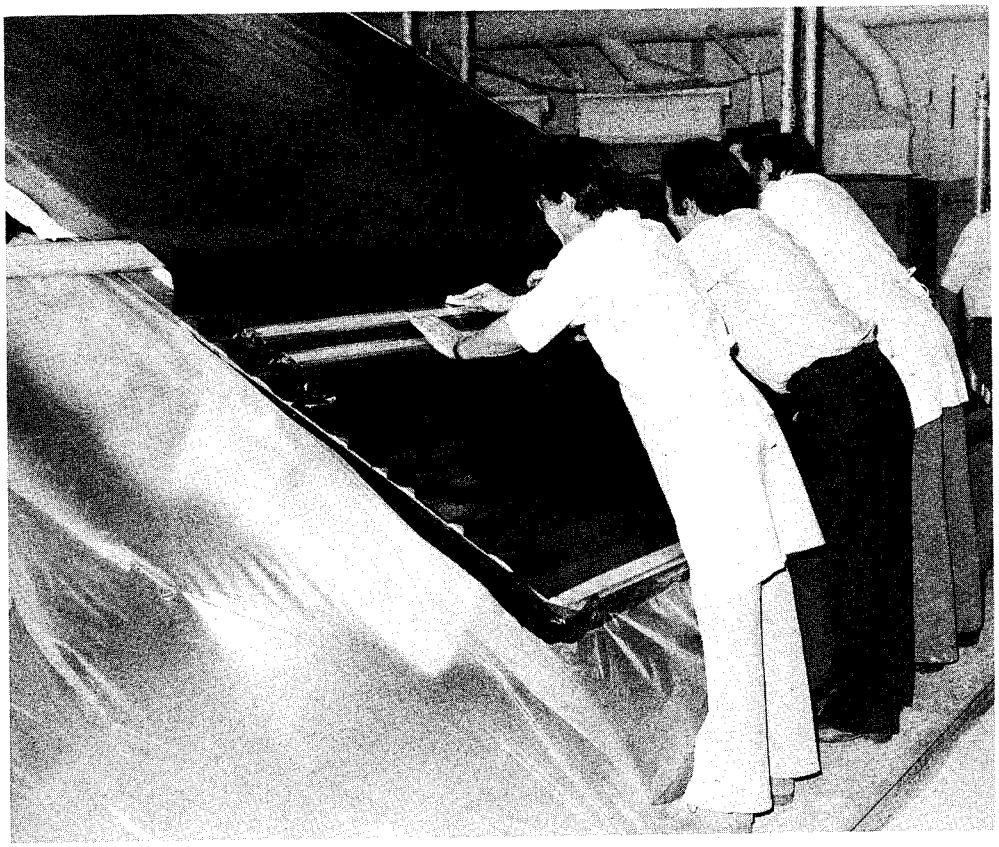

Figure 40. Contouring the Bottom ±45-Deg Preplied Sheet to the Mold

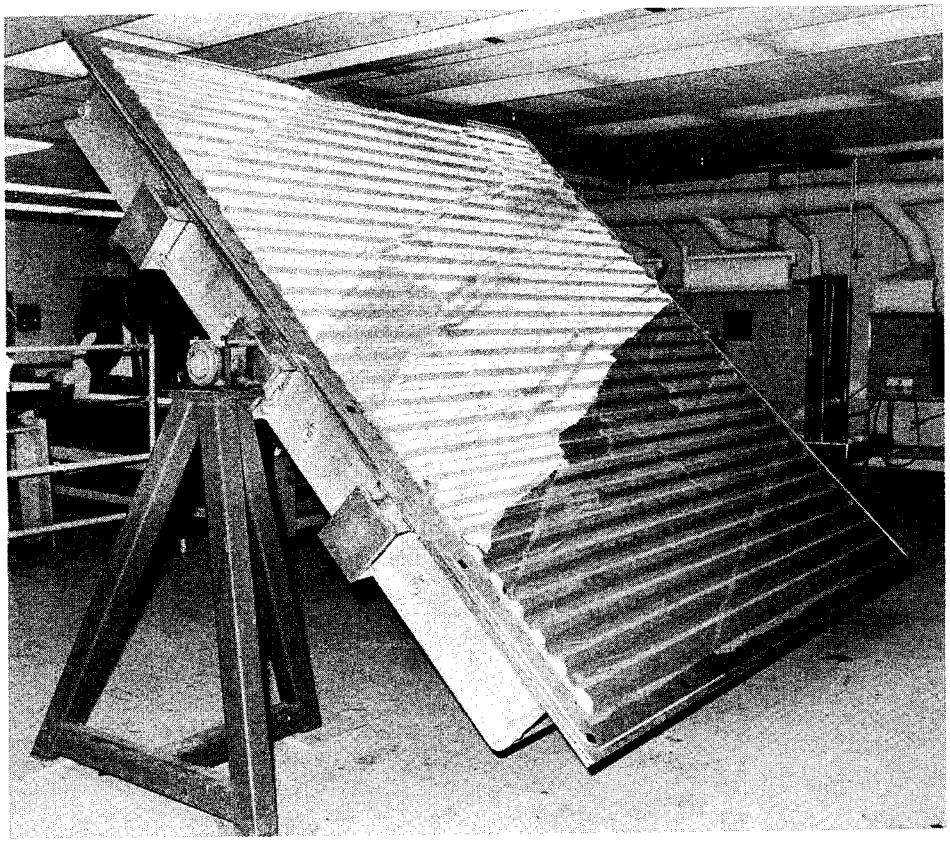

Figure 41. Full-Size Corrugated Panel Layup

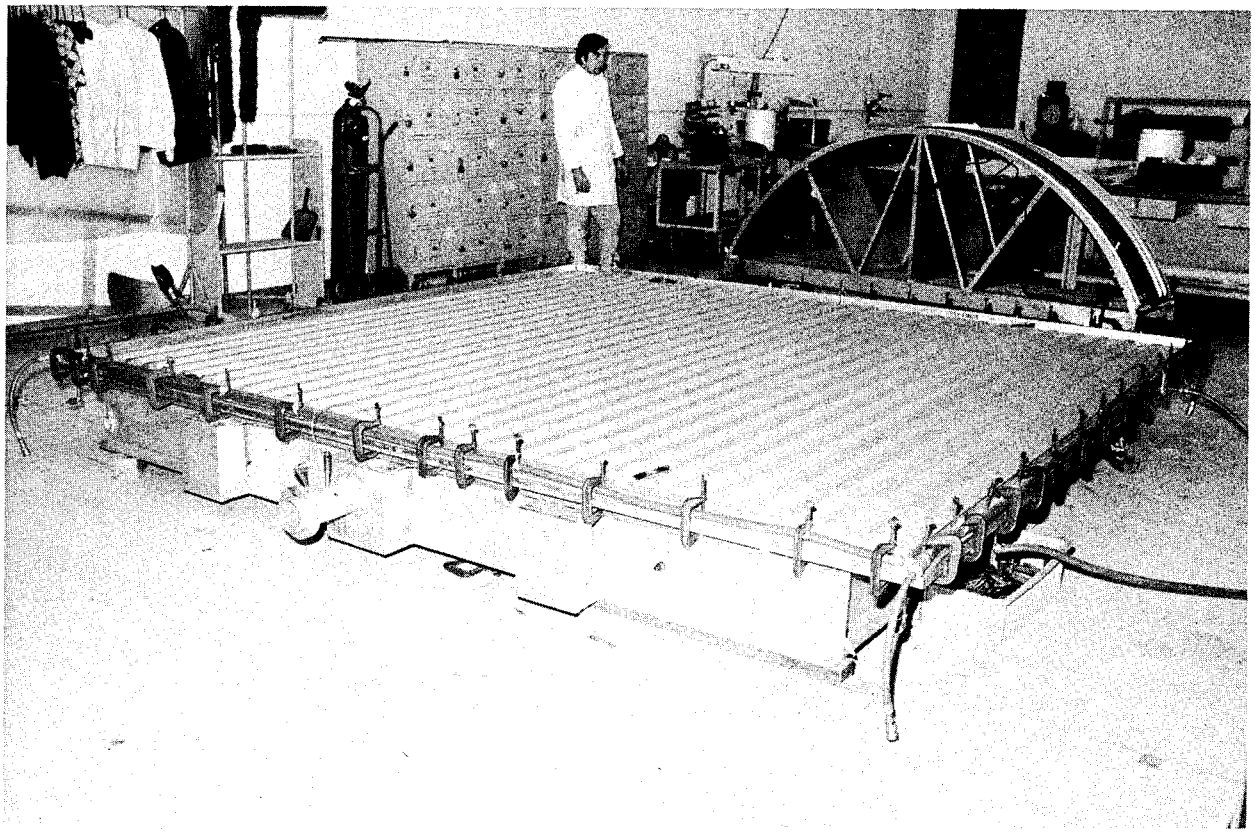

Figure 42. Completed Panel Layup with Silicone Rubber Bag in Place

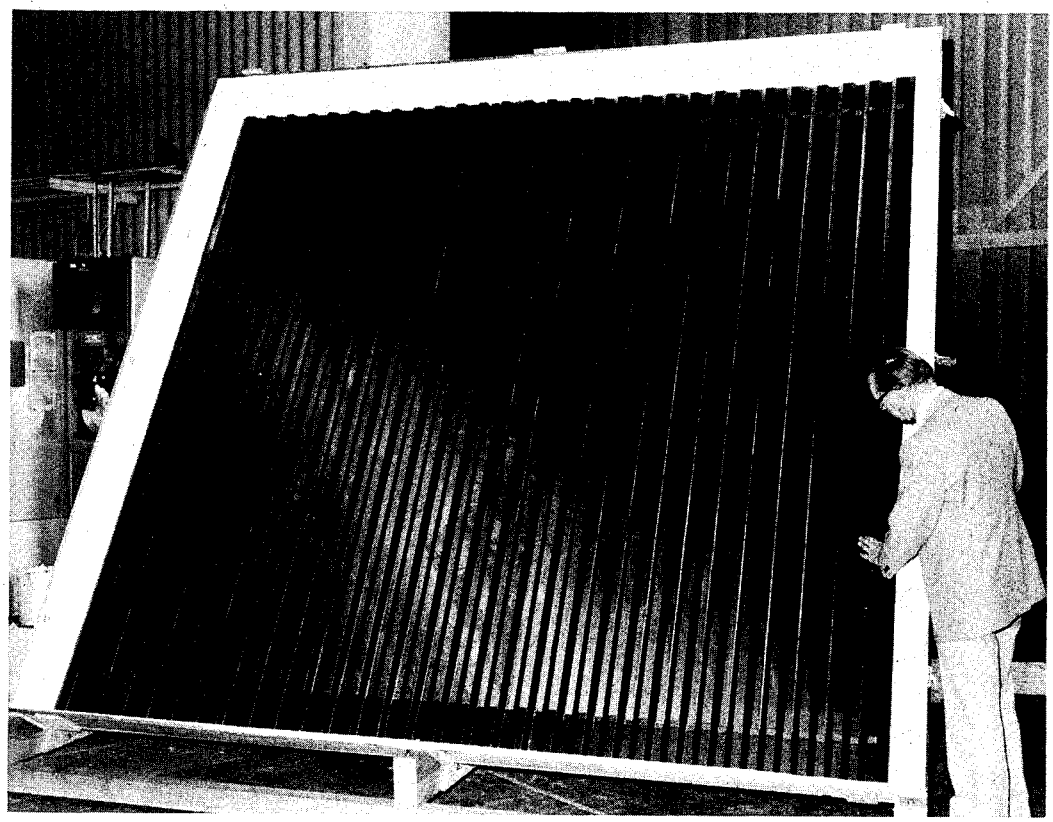

Figure 43. Completed Full-Size Panel

Table 7

SUMMARY OF AVERAGE THICKNESSES
OF FULL-SIZE CYLINDER PANELS

Panel Number	Average Crown Thickness, cm (in)	Average Thickness of Reinforced Ends, cm (in)
1	0.116 (0.0458)	0.246 (0.0970)
2	0.114 (0.0447)	0.243 (0.0958)
3	0.116 (0.0455)	0.243 (0.0958)

Table 8

SUMMARY OF MATERIAL PROPERTY TESTS
FOR FULL-SIZE CORRUGATED PANELS

	Average Tensile Properties		Average Flexural Properties	
Source of Test Samples	Strength N/m^2 (psi)	Elastic Modulus N/m^2 (psi)	Strength N/m^2 (psi)	Elastic Modulus N/m^2 (psi)
Panel No. 1	9.785×10^8 (141,930)	10.203×10^{10} (14.8×10^6)	8.054×10^8 (116,820)	4.102×10^{10} (5.95×10^6)
Panel No. 2	10.869×10^8 (157,660)	8.775×10^{10} (12.7×10^6)	7.479×10^8 (108,490)	3.619×10^{10} (5.25×10^6)
Panel No. 3	9.865×10^8 (143,090)	9.307×10^{10} (13.5×10^6)	8.241×10^8 (119,540)	4.219×10^{10} (6.12×10^6)

4.2 RING-STIFFENER FABRICATION

Fabrication of the ring stiffeners followed the basic process developed early in the program with the 0.61m panels. A single male mold was used to layup and cure two 120-deg ring stiffener segments. Two hat sections and two base strips were laid up and cured in each cycle, six layup and cure cycles being needed to complete the required twelve ring segments. Typical layup operations are shown in Figure 44. Allowance for thermal expansion at the cure temperature of 177°C (350°F) was made in machining the areas on the mold where the hats and base strips were laid up and cured. A separate area on the mold was used to adhesively bond the hats and base strips

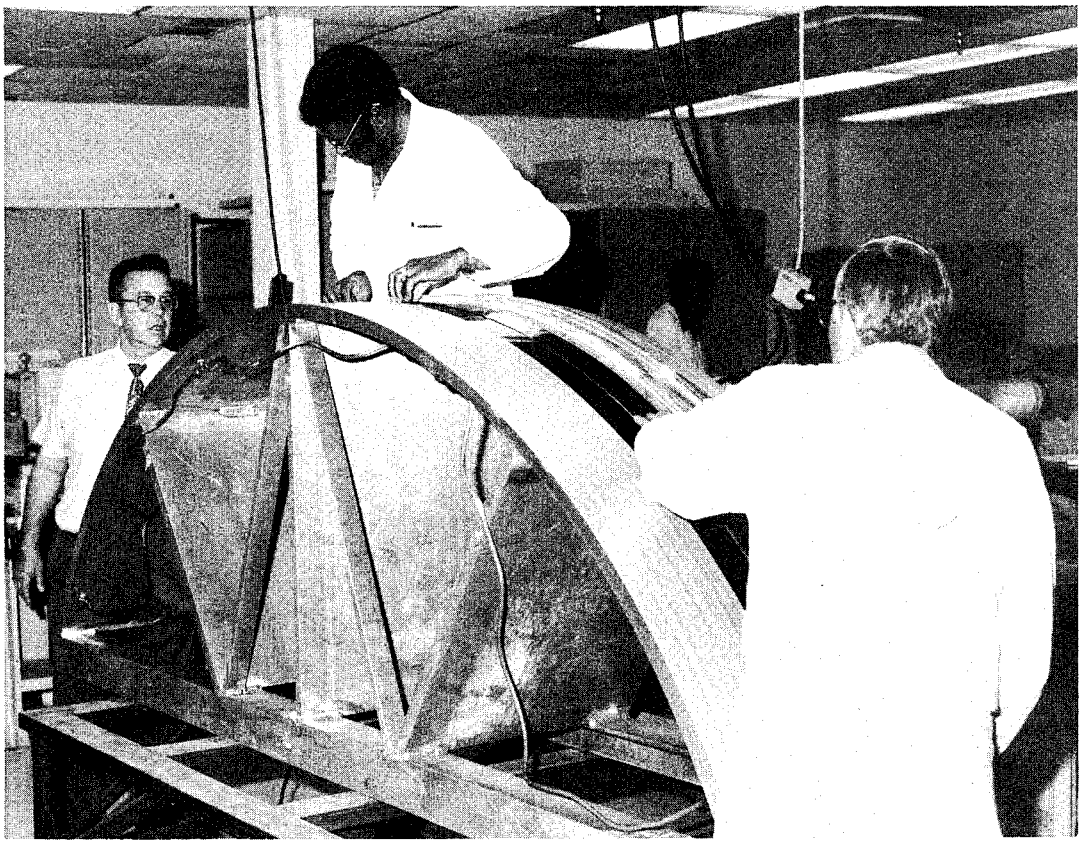

Figure 44. Layup of Ring-Stiffener Segments

together, that area being machined to the required finish radius for the ring stiffeners. The separate area was used because bonding was accomplished at room temperature in contrast to the individual part cure at 177°C (350°F). As a final step in completing the ring segments, the bonded parts were trimmed to size. Hat-section splice segments were laid up and cured on a separate small mold.

4.3 ASSEMBLY JIG

The NASA-furnished steel test rings were made an integral part of the assembly jig so that the graphite-epoxy cylinder was constructed between the two test rings. Three vertical steel I-beams with projecting angles formed supports for the steel end rings (Figure 45). The jig was thus arranged to assemble the corrugated panels vertically between the test rings with the longitudinal axis of the cylinder in a vertical position. Vertical aluminum posts were located on the inside of the cylindrical shell to provide backup for the wall panel joints, and internal frames were located at each

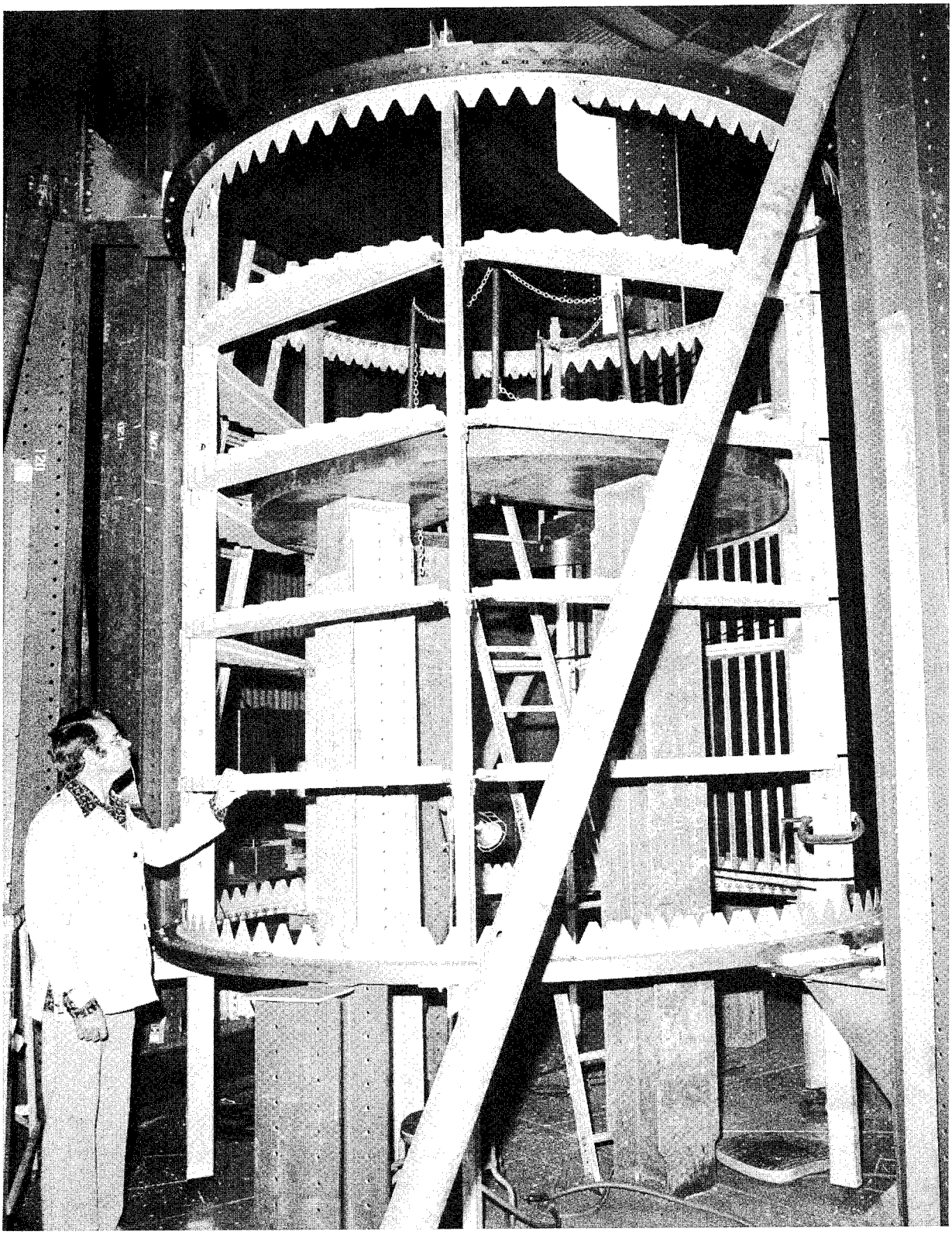

Figure 45. View of Assembly Jig Showing Vertical Support Posts, Steel Test Rings, and Internal Frames

ring stiffener position to provide forms for the corrugated panels and backup when assembling the ring stiffeners to the shell wall.

4.4 CYLINDER ASSEMBLY

The cylinder was assembled by fitting the three corrugated panels in position, making a final trim at the edges of each panel, and attaching the panels to the inner aluminum attachment ring. During this phase of assembly, the outer aluminum attachment ring segments were removed to allow direct access to the inner ring in placing the panels in position. The panels were bolted to the inner rings and the longitudinal panels were completed by riveting and bonding the panel edges together. The outer aluminum attachment ring segments at the cylinder ends were then placed in position and the panel ends were bolted to them. The external stiffening ring segments were then fitted to the cylinder, riveted and bonded to the corrugated wall, and spliced at the ring segment joints. Figure 46 shows the overall assembly of the cylinder. Figure 47 shows the initial fitting of the first full-size panel

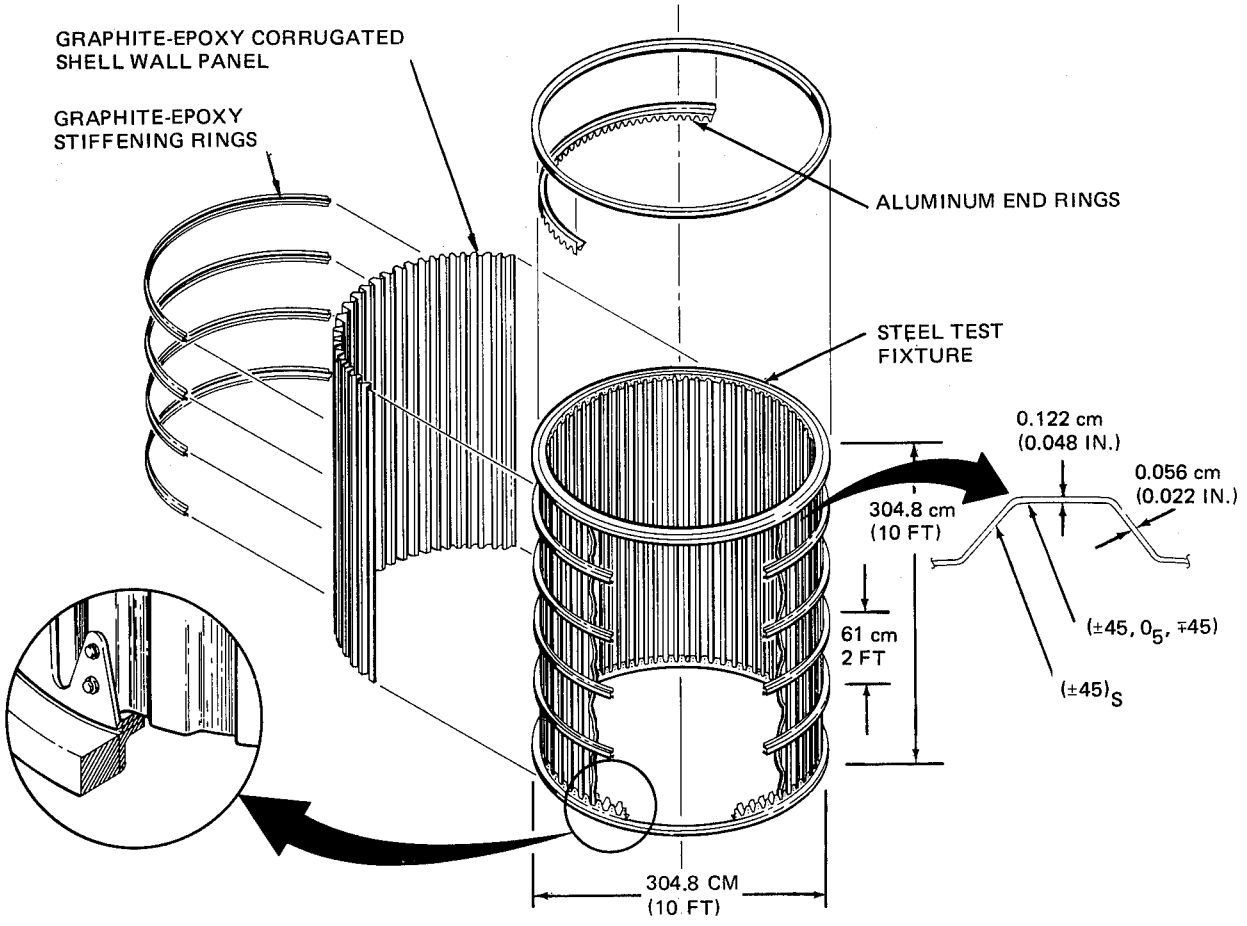

Figure 46. Graphite-Epoxy Ring-Stiffened Corrugated Cylindrical Shell Assembly

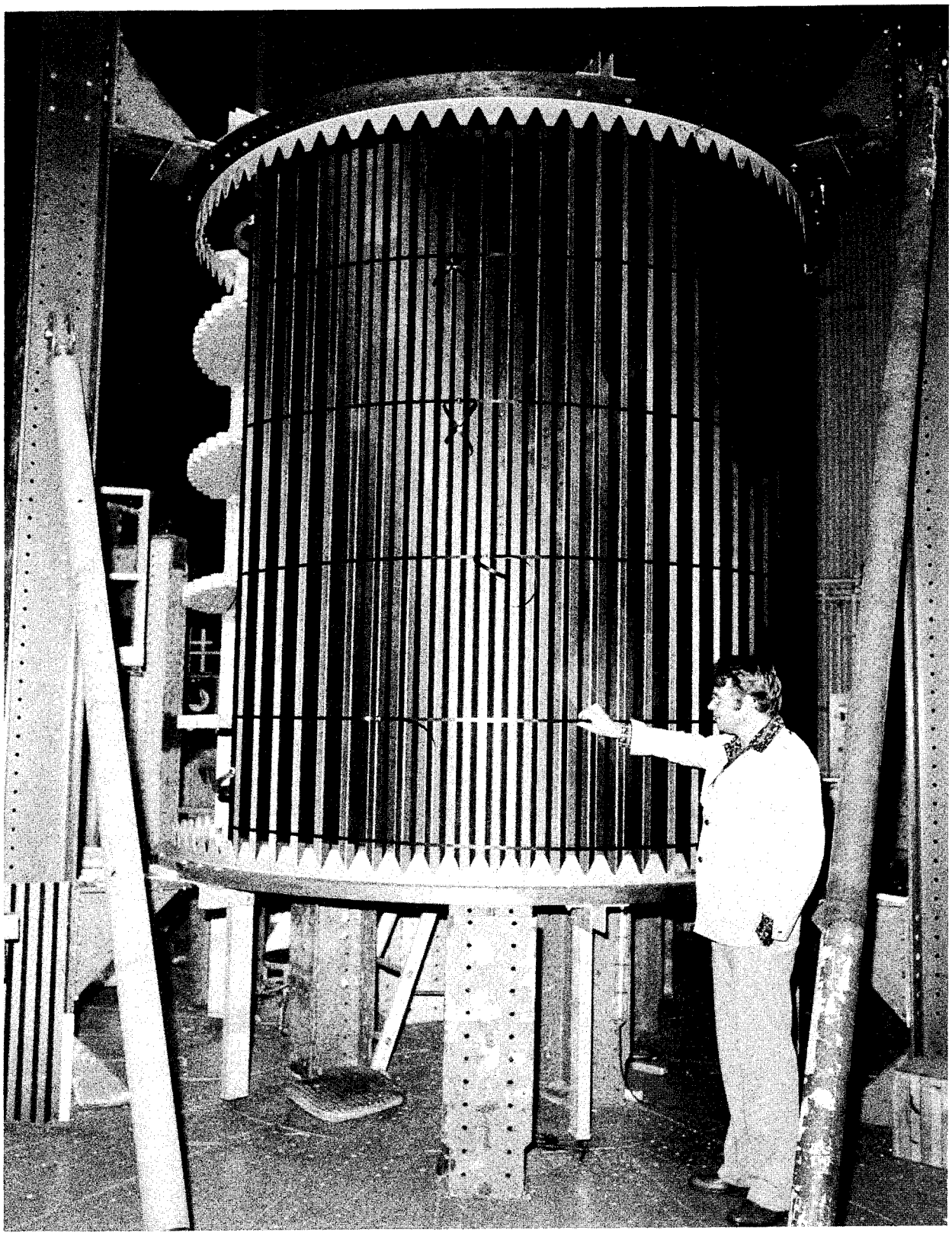

Figure 47. Initial Corrugated Panel Positioned in Assembly Jig

in the assembly jig. Plastic straps were used to hold the panel in position while it was being adjusted to match the end rings and determination of final edge trim requirements was being made.

The flexibility of the corrugated panels in a radial direction is easily seen in Figure 48, in which a full-size panel is being removed from a storage unit in preparation for placement in the assembly jig. The thin-walled corrugations were easily flexed with no damage to the panels. Figure 49 shows a view of the internal side of the cylinder wall with the corrugated forms providing a backup for the panels at each ring-stiffener position. Detailed views of the internal and external attachment rings and one of the steel test rings are presented in Figures 50 and 51. The completed cylinder is shown in Figure 52.

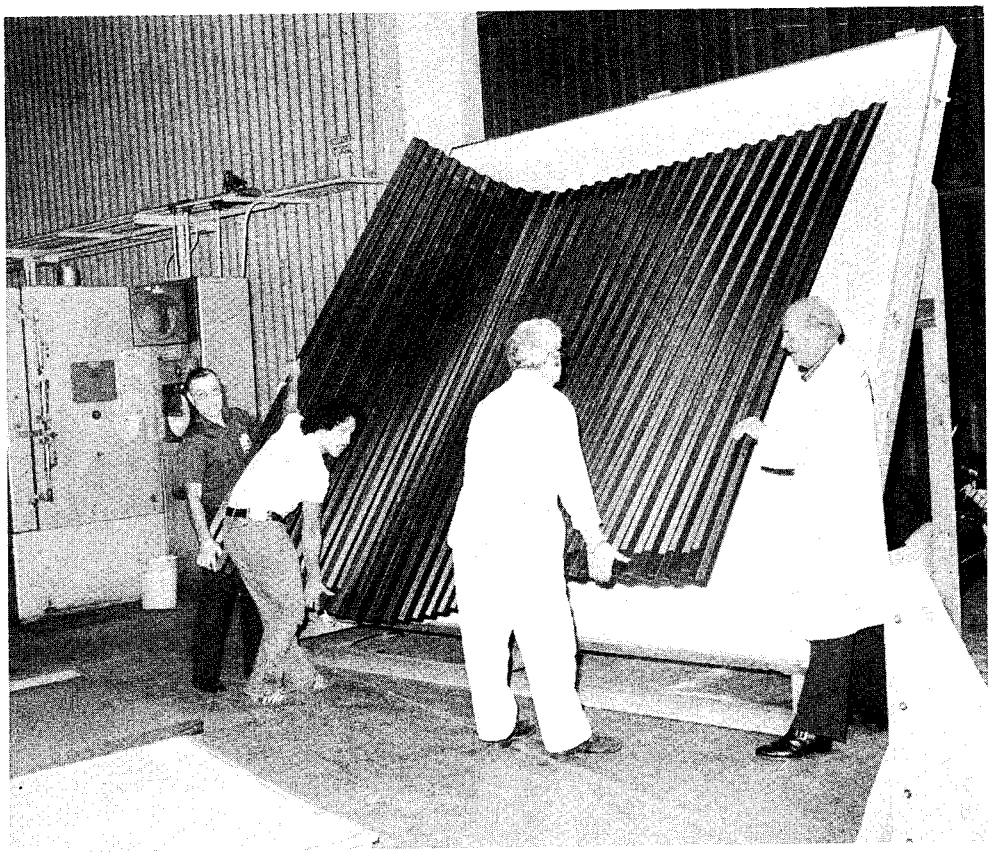

Figure 48. Corrugated Panel Flexibility During Removal from Storage Unit

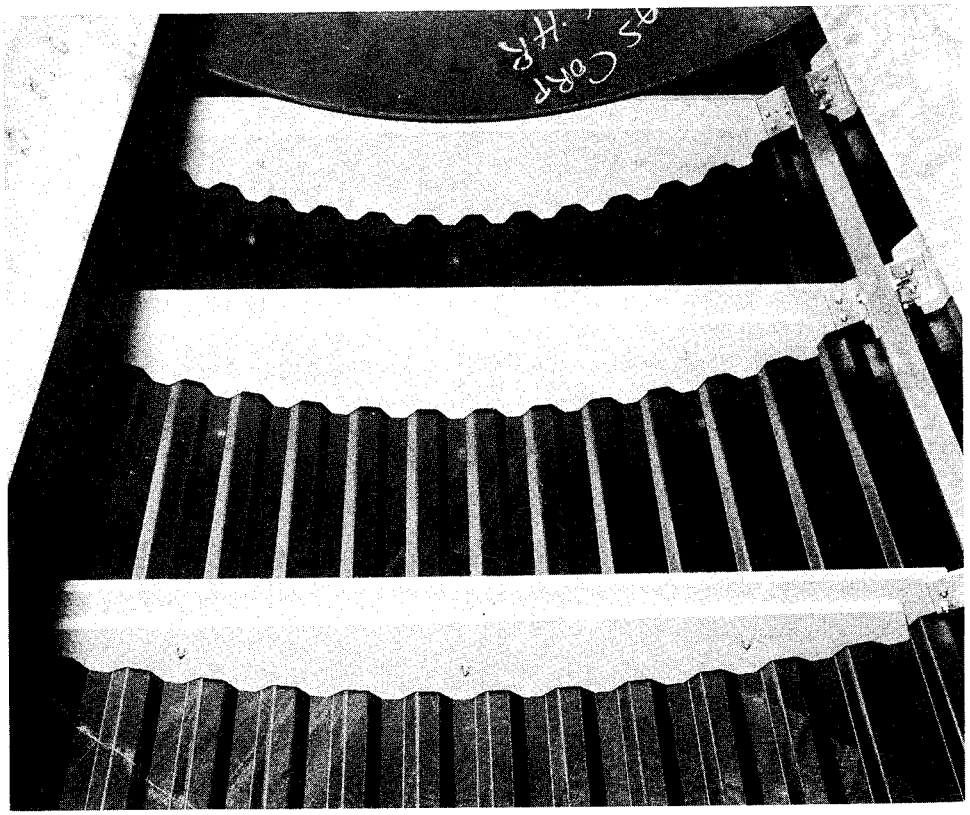

Figure 49. View of Internal Side of Cyclinder Wall

Figure 50. Internal View of Cylinder End, Showing Aluminum Attachment Rings and Steel Test Ring

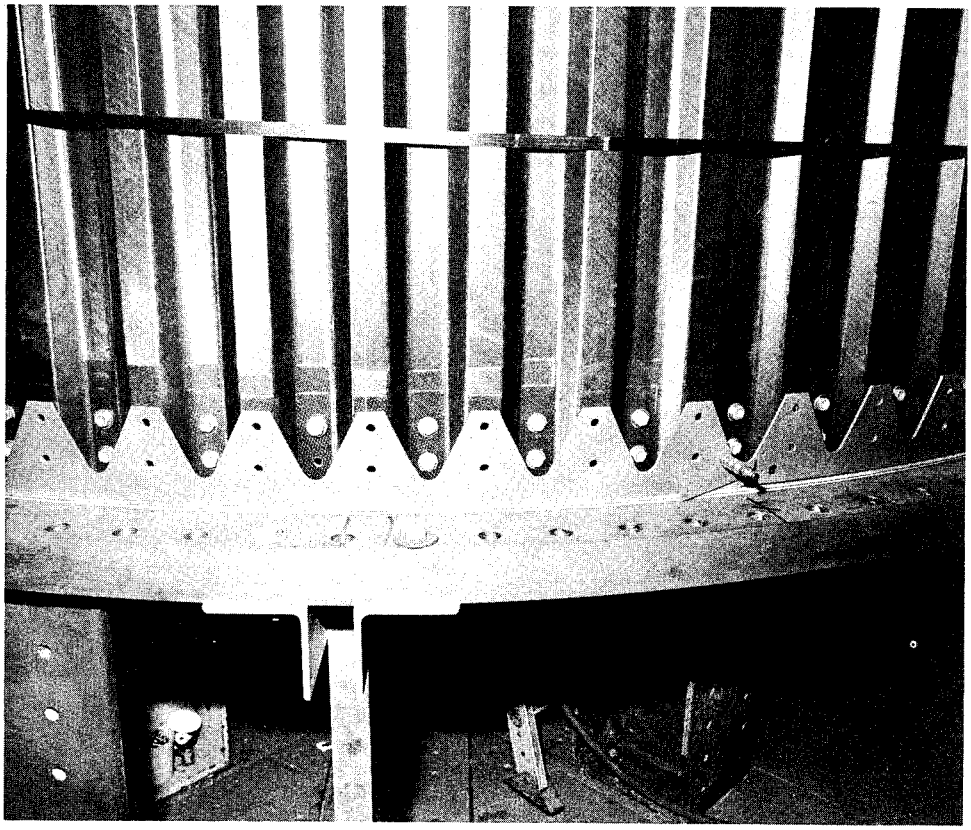

Figure 51. External View of Cylinder End, Showing Aluminum Attachment Ring Segments and Steel Test Ring

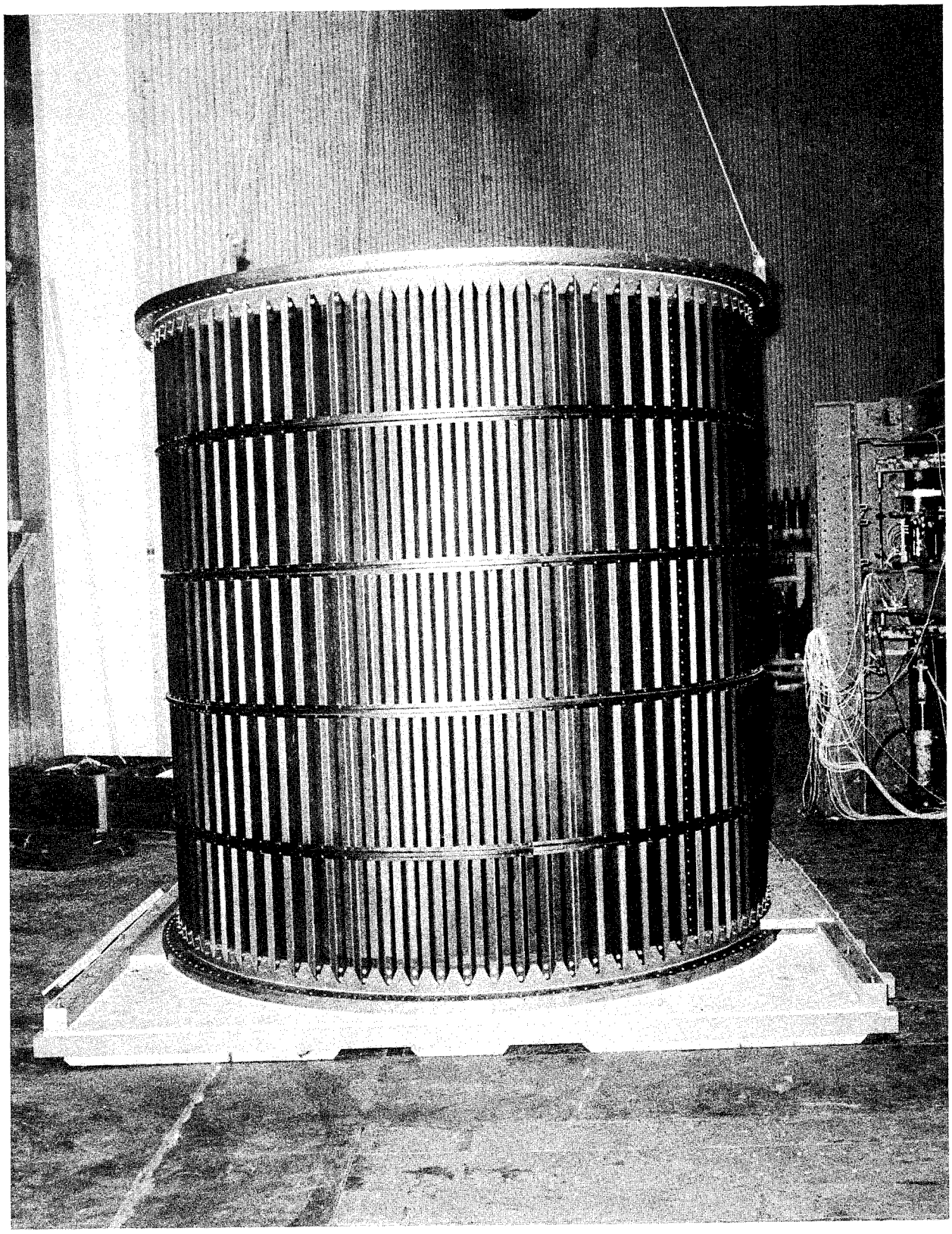

Figure 52. Completed Ring-Stiffened Graphite-Epoxy Corrugated Cylindrical Shell

Section 5

CYLINDER COST AND WEIGHT ANALYSIS

Cost and weight analyses were conducted as a part of the program to assess those important aspects of the use of advanced composites in large, lightly loaded shell structures. Cost projections for producing 100 units were developed based upon fabrication efforts during the program. The projections were then modified to account for learning curve effects plus more sophisticated tooling as appropriate for 100 units. Weight estimates were developed initially and updated as necessary. Actual weights of the finished components were obtained during and after assembly of the cylinder for comparison with computed weights.

5.1 COST ANALYSIS

A cost analysis for production of 100 units was conducted to determine the projected cost for production quantities of a graphite-epoxy cylindrical shell structure. The fabrication approach assumed for the cost study was basically the same as used in this program; however, tooling modifications were assumed as required for quantity production, and more extensive use of tooling aids was assumed for operations such as trimming the panel edges and ring stiffeners. A material cost of $44 per kg ($20/lb) was assumed for the T300/5208 graphite-epoxy prepreg tape.

Production of the 100 units was assumed to occur over a 5-year period with all costs based on January 1978 dollars and an assumed production rate of 20 units per year. Profit or fee was not included in the estimated cost of the 100 units. To account for improvement in production performance as the program progresses, a 90% learning curve was used for all recurring costs.

Tooling and manufacturing improvements assumed for large-scale production were:

1. Permanent tooling would be provided for manufacture of the aluminum adapter and load-introduction rings.

2. A second mold for panel layup and cure would be provided to sustain the production rate of 20 cylinders per year based on a 5-day, 2-shift work week.
3. The main assembly fixture would be a complete entity and include locating, positioning and holding attachments for the panels and hat sections. A permanent assembly fixture would be fabricated for the program.
4. The rubber vacuum bag used in panel curing operations would be a purchased item, carried in stock in sufficient quantity to accommodate the anticipated life span of each bag (12 units or 36 panels).
5. The main panel layup operation would be optimized by using fixtures to support the ±45-deg preplies and by providing platforms for improved access and reduced layup time.
6. Permanent trim fixtures would be provided for panel and ring-stiffener trimming.

Using the above assumptions, a total cost for production of 100 units was projected to be $6,217,000.

Past studies of cylindrical shells in which cost comparisons of aluminum and advanced composite structures of the same basic shell have been made show a moderate cost saving for the composite structure when the number of parts can be reduced significantly over the aluminum counterpart.

5.2 WEIGHT ANALYSIS

A summary of the computed weights of the ring-stiffened graphite-epoxy corrugated shell, the aluminum rings, and the steel test rings are presented in Table 9. Calculated weights for the graphite-epoxy components were based upon a material density of 152.5 kg/m^3 (0.055 lbm/$in.^3$) for the finished parts. Individual graphite-epoxy components were weighed prior to assembly of the shell for comparison with the computed weights shown in Table 9. Some elements, such as end reinforcing doublers on the corrugated panels, were cocured with the panels and thus could not be weighed separately. Consequently, comparisons were made where possible by summing computed weights of individual elements shown in Table 9 and comparing those sums with the actual part weights. Such comparisons are

Table 9

WEIGHT ESTIMATE OF THE TEST CYLINDER ASSEMBLY

Subassembly or Component	Individual Element	Material	Estimated Weight kg (lbm)	
			Element	Subassembly
Stiffened Corrugated Shell	• Basic Corrugated Shell (3 Panels)	T-300/5208	47.3 (104.2)	
	• Shell Splice Joint	T-300/5208 and E-Glass	0.8 (1.8)	
	• End Reinforcement	T-300/5208	5.1 (11.8)	60.4 (133.1)
	• Adhesive	EA-9309	0.2 (0.5)	
	• Ring Stiffeners	T-300/5208	6.2 (13.6)	
	• Ring Splices	T-300/5208	0.05 (0.1)	
	• Hardware	Cherry Rivets	0.50 (1.1)	
Load-Introduction (Adapter) Rings	• Inner End Rings (2)	7075-T6	15.5 (34.2)	
	• Outer End Rings (2)	7075-T6	15.6 (34.4)	79.9 (176.2)
	• Adapter Rings (2)	7075-T6	19.9 (43.8)	
	• Hardware	Bolts, Nuts, and Washers	28.9 (63.8)	
Mounting Rings	Government-Furnished (2 Required)			725.8 (1600)

Note: The load-introduction (adapter) rings were designed as test hardware without any attempt to optimize them for weight; proper introduction of the loads to the shell and minimum cost were the primary design objectives.

shown in Table 10. The lower actual weight of the shell wall panels is attributed to the decreased cured ply thickness experienced in fabricating all panels, including the subelement test panels. The computed panel weights were based on a ply thickness of 0.014 cm (0.0055 in.), whereas actual thickness per ply in the crown areas was measured as approximately 0.0132 cm (0.0052 in.).

Table 10

COMPARISONS OF COMPUTED AND ACTUAL WEIGHTS

Shell Components	Computed Weight kg (lbm)	Actual Weight kg (lbm)
Shell Wall Panels, Splice Joint, and End Reinforcements	53.4 (117.5)	50.6 (111.5)
Ring Stiffeners	6.2 (13.6)	6.3 (13.8)
Ring-Stiffener Splices	0.05 (0.10)	0.18 (0.4)
Subtotal	59.65 (131.2)	57.08 (125.7)

Section 6
CONCLUSIONS

A graphite-epoxy cylinder 3.05m (10 ft) in diameter and 3.05m (10 ft) long was designed and fabricated by using T300/5208 as the basic material for the corrugated wall and the external stiffening rings. To ease assembly and to maintain good dimensional control of the cylinder, the shell wall was made in three 120-deg segments, as were each of the four stiffening rings. Preliminary compression tests conducted with subsize test panels having the full-scale corrugation cross section provided design data required to refine the shell wall design.

The fabrication techniques developed in building the subsize corrugated test panels were successfully applied to the full-size cylinder wall panels, each of the three panels having dimensions of approximately 3.23 by 3.00m (127 by 118 in.). Fabrication of the 3.05m (10 ft) diameter graphite-epoxy cylinder demonstrated the feasibility of using lightweight advanced composites in lightly loaded full-size space vehicle structures. A 23% weight saving was achieved in the T300/5208 graphite-epoxy test cylinder when compared to an aluminum cylinder of the same basic design.

The following conclusions resulted from the work conducted in this program:

1. The flexibility of an open-corrugation design for a cylindrical shell wall permits a simplified manufacturing approach whereby flat corrugated panels may be laid up, cured, and subsequently wrapped to shape upon assembly.
2. Compression tests with flat panels of the open-corrugation configuration showed the ability to sustain the design load of 1576 N/cm (900 lb/in.) without local buckling when a layup of $[\pm 45, 0_5, \mp 45]$ was used in the crowns.
3. Aluminum tooling provided adequate dimensional stability for curing the T300/5208 tape prepreg parts at 177°C (350°F).
4. Actual weights of graphite-epoxy components were accurately predicted by preliminary analyses.

REFERENCES

1. Williams, Jerry G., and Mikulas, Martin M., Jr. Analytical and Experimental Study of Structurally Efficient Composite Hat-Stiffened Panels Loaded in Axial Compression. ASME/AIAA/SAE 16th Structures, Structural Dynamics, and Materials Conference, Denver, Colorado, May 1975, AIAA Paper No. 75-754.

2. Agarwall, B. L., and Davis, R. C. Minimum-Weight Designs for Hat-Stiffened Composite Panels Under Uniaxial Compression. NASA TN D-7779, 1974.

3. Bushnell, David. Stress, Stability, and Vibration of Complex Branched Shells of Revolution: Analyst's and User's Manual for BOSOR 4. NASA CR-2116, 1972.

4. Anderson, M. S., Hennesy, K. W., and Heard. W. L. Addendum to User's Guide to VIPASA. NASA TMX-73914, May 1976.

5. Viswanathan, A. V., Tamekuni, M., and Baker, L. L. Elastic Stability of Laminated, Flat and Curved, Long Rectangular Plates Subjected to Combined Inplane Loads. NASA CR-2330, June 1974.

6. Peterson, J. P., and Anderson, J. K. Bending Tests of Large-Diameter Ring-Stiffened Corrugated Cylinders. NASA TN D-3336, 1966.

1. Report No.	2. Government Accession No.	3. Recipient's Catalog No.
NASA CR-3026		

4. Title and Subtitle	5. Report Date
Design and Fabrication of a Ring-Stiffened Graphite-Epoxy Corrugated Cylindrical Shell	August 1978
	6. Performing Organization Code
7. Author(s)	8. Performing Organization Report No.
Read Johnson, Jr.	MDC.G7330
	10. Work Unit No.
9. Performing Organization Name and Address	11. Contract or Grant No.
McDonnell Douglas Astronautics Company 5301 Bolsa Avenue Huntington Beach, CA 92647	NAS1-14547
	13. Type of Report and Period Covered
12. Sponsoring Agency Name and Address	Contractor Report
National Aeronautics and Space Administration Washington, D. C. 20546	14. Sponsoring Agency Code

15. Supplementary Notes

Langley Technical Monitor: Randall C. Davis
Final Report

16. Abstract The work conducted from 30 July 1976 through 31 January 1978 in a program to design and fabricate a graphite-epoxy cylindrical shell 3.05m (10 ft) in diameter by 3.05 (10 ft) long is described. Design and fabrication of subelement test panels that represent key portions of the cylinder are also described, as are supporting tests of coupons, sample joints, and stiffening ring elements. The cylindrical shell is a ring-stiffened, open corrugation design that uses T300/5208 graphite-epoxy tape as the basic material for the shell wall and stiffening rings. The test cylinder, which is to be tested at the NASA Langley Research Center, is designed to withstand bending loads producing the relatively low maximum load intensity in the shell wall of 1,576 N/cm (900 lb/in). The resulting shell wall weight, including stiffening rings and fasteners, is 0.0156 kg/m^2 (0.37 lb/ft^2). The shell weight achieved in the graphite-epoxy cylinder represents a weight saving of approximately 23%, compared to a comparable aluminum shell. A unique fabrication approach was used in which the cylinder wall was built in three flat segments, which were then wrapped to the cylindrical shape. Such an approach, made possible by the flexibility of the thin corrugated wall in a radial direction, proved to be a simple approach to building the test cylinder. Based on tooling and fabrication methods in this program, the projected costs of a production run of 100 units are reported.

17. Key Words (Suggested by Author(s))	18. Distribution Statement
Cylinder, corrugation, graphite/epoxy, composite, stiffened, lightweight, rings, shell, fabrication.	Distribution is unlimited Subject Category 39

19. Security Classif. (of this report)	20. Security Classif. (of this page)	21. No. of Pages	22. Price*
Unclassified	Unclassified	76	$6.00

* For sale by the National Technical Information Service, Springfield, Virginia 22161

NASA-Langley, 1978